NORMAL AND ABNORMAL MITOSIS IN A MAMMALIAN CELL *IN VITRO*. A LIGHT AND ELECTRON MICROSCOPIC STUDY.

By

Urs-Peter Roos

A DISSERTATION PRESENTED TO THE GRADUATE COUNCIL OF
THE UNIVERSITY OF FLORIDA IN PARTIAL
FULFILLMENT OF THE REQUIREMENTS FOR THE DEGREE OF
DOCTOR OF PHILOSOPHY

UNIVERSITY OF FLORIDA
1971

Thus, the task is, not so much to see what nobody has seen yet; but to think what nobody has thought yet, about what everybody sees.

Schopenhauer

ACKNOWLEDGMENTS

I am grateful to Dr. Fred C. Johnson, Chairman of my Supervisory Committee, for his help in procedural matters.

Words cannot express my respect and gratitude for the liberal and stimulating guidance provided by Dr. Henry C. Aldrich, Co-chairman, throughout this study. His generosity regarding time and use of facilities was an important factor for the progress of my work.

I am much indebted to Dr. John W. Cramer and his staff, Department of Pharmacology, for instruction and use of facilities for tissue culture work.

Dr. Lynn H. Larkin and Dr. James L. Nation, members of my Supervisory Committee, deserve my thanks for their moral support and helpful advice. I appreciate the encouragement provided by Dr. John W. Brookbank, Dr. James H. Gregg, and Dr. Philip B. Morgan.

I am much obliged to Dr. Robert M. De Witt, Chairman of the Department of Zoology, for arranging financial assistance.

I also extend my thanks to Mrs. Rosemary Rumbaugh, and numerous unnamed persons with whom I was associated in the course of this study, for assistance and forbearance.

My wife, Loan, played a major part in this accomplishment. I am deeply grateful for her never faltering patience, her understanding, encouragement, and help.

PREFACE

Certainly, one cannot argue about the importance and significance of attempts to increase our knowledge of chromosomes and mitosis, both so basic to life in higher organisms. I was fortunate to have the liberty to choose a research project myself, and the study presented evolved mainly out of my curiosity to learn more about these two fundamental aspects of life.

At the time this project began, ultrastructural investigations of eukaryotic chromosomes had essentially reached a standstill. More new questions had been posed than old ones answered. On the other hand, electron microscopic techniques had not yet been applied to the study of chromosomal aberrations. Mitosis in animal cells was fairly well documented at the ultrastructural level, but many of its aspects were the subject of controversy. Like many other students at the beginning of a new road, I had only a limited knowledge of these problems; hence my idealistic assumption that an ultrastructural investigation of normal and abnormal mitosis could answer many of the questions remaining, or at least lead the way to significant experiments. It will become clear from the following presentation how far these hopes were fulfilled and justified.

TABLE OF CONTENTS

LIST OF TABLES

LIST OF FIGURES

KEY TO ABBREVIATIONS AND SYMBOLS

C	centriole(s)
CG	centromeric granules
Ch	chromosome(s)
Chd	chromatid(s)
Chr	chromatin
Ci	cisterna(e)
Co	corona of kinetochore
CV	intracentriolar vesicle
D	contamination of thin sections (dirt)
DC	daughter centriole(s)
EOC	8-ethoxycaffeine
F	fibrillar component of the nucleolus
G	Golgi complex
Gr	granular component of the nucleolus
H	achromatic hole(s) in chromatin or chromosomes
HChr	heterochromatin
IV	intranuclear vesicle(s)
K	kinetochore
K_1, K_2	sister kinetochores
KG	kinetochore granule
KI	inner layer of the kinetochore
KM	middle layer of the kinetochore
KO	outer layer of the kinetochore
MA	mitotic apparatus
MB	midbody
MF	microfibril(s)
Mi	mitochondrion
MI	mitotic index
MN	micronucleus
MT	microtubule(s)
N	nucleus
NE	nuclear envelope
NL	nuclear lobe
NO	nucleolus organizer
NP	pore-annulus complex(es) of the nuclear envelope
Nu	nucleolus
NV	membrane vesicle formed by fragmenting nuclear envelope
P, P_1, P_2	spindle pole(s)
Pa	particle(s) associated with centrioles
PC	parent centriole(s)
R	ribosomes (poly- or monosomes)
RER	rough endoplasmic reticulum
S	satellite(s), pericentriole body (bodies)
Sb	stem body
Sm	stem
SN	streptonigrin
V	cytoplasmic vesicle(s)
X	X chromosome; other chromosomes are numbered arbitrarily

Abstract of Dissertation Presented to the Graduate Council of the University of Florida in Partial Fulfillment of the Requirements for the Degree of Doctor of Philosophy

NORMAL AND ABNORMAL MITOSIS IN A MAMMALIAN CELL IN VITRO. A LIGHT AND ELECTRON MICROSCOPIC STUDY.

By

Urs-Peter Roos

December, 1971

Chairman: Dr. Fred C. Johnson
Co-Chairman: Dr. Henry C. Aldrich
Major Department: Zoology

Rat kangaroo cells (PtK_2 line), grown as monolayers, were fixed and embedded in situ. Cells in mitosis were examined and photographed under phase contrast. Serial sections were examined with the electron microscope.

Centrioles duplicate at the onset of prophase. Centriole migration, disintegration of the nucleolus, chromosome condensation, breakdown of the nuclear envelope (NE), and formation of the mitotic spindle are similar to these processes in other mammalian cells. Prophase kinetochores (Ks) appear as globular, fibrillar bodies in the primary constriction of chromosomes. Detailed observations on prometaphase chromosomes support the pulling theory of amphiorientation and metaphase stability. Amphiorientation is established by unipolar followed by bipolar attachment to spindle microtubules (MT), or by simultaneous bipolar attachment, depending on the position of a chromosome relative to the poles at the time of attachment. In the former case, bipolar attachment is presumably followed by congression. Concomitantly, Ks mature to trilaminar, flat, undulated, concave, or convex discs, 4,000-6,000 A in diameter. All the Ks reach maturity at metaphase. Inner and outer layers are 400 A, and the middle layer is 300 A thick. On the

average, 26 bundled MT are anchored in the outer layer. Staining characteristics and behavior in late mitosis suggest that the inner layer is chromatin, the outer layer possibly protein.

Daughter chromosomes are connected by strands of chromatin during very early anaphase. The strands rupture during early anaphase. In late anaphase, when chromosome movement has ceased, the K layers are fuzzy, and fewer, less organized MT are attached. In telophase the inner layer is a very opaque patch of dense material on the inner membrane of the NE; the outer layer is lost in the cytoplasm.

Reconstruction of the NE, cleavage, midbody formation, and reappearance of the nucleolus, are similar to these processes in other mammalian cells.

Mitotic stages in cells exposed to 0-4°C for 1 hr are similar to untreated cells. Prophase Ks are identical and mature metaphase Ks are typically triple-layered, though slightly fuzzy. Few MT, almost exclusively kinetochore MT, are preserved. They are coated by an amorphous or finely fibrillar substance.

No spindle MT are present in colcemid-arrested cells (0.05 µg/ml for 2 hr, 1 hr recovery; 0.25 µg/ml for 15 min, no recovery). Chromosomes are scattered in the central area of the cells. Centrioles have duplicated, but not migrated. The higher concentration of colcemid induced decondensation of chromosomes and dispersion of chromatin in all interphase cells. Kinetochores resemble immature prometaphase Ks in control cells. The inner layer is lacking. The outer layer is a convex or undulated, bilaminar plate, 400 Å thick and 5,000-9,000 Å in diameter, and embedded in a finely fibrillar matrix.

Streptonigrin (SN; 0.01 μg/ml and 0.05 μg/ml for 4 hr, 48 hr recovery) depressed the mitotic index (2.22 and 0.18, respectively, versus 2.59 in controls) and induced high frequencies of chromosomal and mitotic aberrations in meta- and anaphase cells (49.0% and 100%, respectively, versus 14% in controls). The most frequent aberrations in control cells were single dicentric anaphase bridges with a few acentric fragments. Multiple bridges and fragments were the most common aberrations in SN-treated cells. The higher concentration of SN produced very complex aberrations, including decondensation of chromosomes. Kinetochores of dicentrics are structurally normal. Micronuclei and very fine nuclear bridges connecting daughter cells in cytokinesis in SN-treated cultures are enveloped by normal NE.

REVIEW OF LITERATURE

Mitosis has been studied for nearly 100 years (Dietz 1969). Its fundamental importance as a mechanism for the orderly distribution of chromosomes has provoked numerous investigations and experiments. Accordingly, there is a vast amount of literature on both mitosis and chromosomes. I did not intend to compete with the much more knowledgeable and experienced authors of the many reviews that have appeared. Rather, I have tried to survey the literature on those aspects of eukaryotic mitosis and chromosomes which are most closely related to my own observations and results.

General Ultrastructural Features of Vertebrate Cells in Mitosis

Today, improved methods are available that allow correlated light and electron microscopic observation of single animal cells (e.g., Brinkley et al. 1967). It is a little surprising, therefore, that no detailed study combining the two approaches has been done on animal cells in mitosis. (For a good example of mitosis in plant cells see Bajer 1968, Bajer and Molè-Bajer 1969.) Ultrastructural features of mitosis have been described for a number of animal cells (see Luykx 1970 for references), but light micrographs are equally important for comparison with earlier light microscopic studies.

In the following description the emphasis is on the nucleus. Cytoplasmic organelles and components are considered only as far as they play a role directly related to the formation of the mitotic

apparatus (MA) and chromosome segregation. Mitosis in newt heart cultures (Barnicot and Huxley 1965), rat thymic lymphocytes (Murray et al. 1965), HeLa cells (Robbins and Gonatas 1964), L strain fibroblasts (Krishan and Buck 1965), and rat hepatoma cells (Chang and Gibley 1968) served as the basis for this summary.

Prophase

The chromatin, which is dispersed during interphase, begins to condense during early prophase. This process continues until, at the end of this stage, individual chromosomes are clearly recognizable and can be seen to consist of two sister chromatids. Kinetochores (centromeres) may become visible during prophase in some cell types. The centrioles may have duplicated during the previous interphase, or they do so during prophase. So-called procentrioles, or daughter centrioles arise at right angles to the separated parent centrioles. At this stage the centrioles often lie within a pocket of the nuclear envelope. A dense, osmiophilic mass can be seen associated with each parent-daughter pair. As prophase progresses, the pairs migrate to opposite poles. The timing of this event relative to the breakdown of the nuclear envelope varies. In any event, microtubules (MT), which radiate from the centrioles during early prophase, begin to invade the nucleus as the envelope breaks down. Fragments of the latter appear either as double stacks of membranes (Chang and Gibley 1968, Murray et al. 1965), or as vesicles (Barnicot and Huxley 1965). The fibrillar component of the nucleolus disappears (see also Hsu et al. 1965), the granular component disperses and breaks up into smaller masses which often remain attached to chromosomes during meta- and anaphase (Chang and Gibley 1968).

Prometaphase

This stage, which is characterized by metakinesis, i.e., chromosome movements that ultimately result in the alignment on the metaphase plate (Mazia 1961), has been neglected by investigators of the ultrastructure of mitosis in animal cells. This may be due partly to difficulties in recognizing and selecting cells in this stage.

Metaphase

The chromosomes are condensed and aligned on the metaphase plate. The mitotic spindle, made up of chromosomal and interpolar (continuous) microtubules, is fully formed between the two poles occupied by the two pairs of centrioles. Asters, consisting of MT radiating from the centrioles, may be more or less distinct. Larger cell organelles, such as mitochondria and endoplasmic reticulum (ER), are generally excluded from the spindle, but exceptions occur. Ribosomes are abundant within the spindle, mostly as monomers. Spindle MT converge at the poles, where they enter the osmiophilic zone around the centrioles. Bundles of MT connect to the chromosomes at the kinetochores. The latter are seen as straight or crescent-shaped, dark bands, separated from the chromosome by a lighter band. Remnants of the nuclear envelope may be present at the periphery of the spindle, often more concentrated near the poles. Nuclear pore complexes are absent from these fragments.

Anaphase

As the two sets of daughter chromosomes separate, the chromosomal (kinetochore) MT shorten, while the pole-to-pole distance increases (spindle elongation). Later, the chromosomes fuse to one large mass of dense chromatin. Concomitantly, pieces of double membrane, possibly

derived in part from the remnants of the nuclear envelope, appear at the periphery of the chromatin mass, first at the polar face. Ribosomes and nuclear pores are found on some of these pieces. It is not unusual for membranes to get caught between the coalescing chromosomes. The presence of restored nuclear envelope seems incompatible with the occurrence of MT within the chromatin mass. In the interzone, mitochondria and, in some cases, ER can be found, and dense material around the MT in the equatorial region indicates early stages of midbody formation.

Telophase

The nuclear envelope is completely reconstructed by fusion of membrane vesicles and cisternae. Nucleoli are reconstituted from material formed at the nucleolar organizer or by coalescence of small nucleolar bodies, but the process is poorly understood (see Busch and Smetana 1970). Concomitantly, the mass of chromatin disperses. The cytoplasm is divided either by a wedge-shaped constriction in the equatorial region (Robbins and Gonatas 1964), or by the formation of a vesiculated equatorial plate (Murray et al. 1965). In the latter case the vesicles fuse to form the cleavage furrow.

Cytokinesis

Cleavage progresses until the daughter cells are connected only by a cytoplasmic stem. Included in the stem are tightly bundled MT and the midbody, which has formed by fusion of the dense material in the equatorial region (see also Byers and Abramson 1968, Paweletz 1967, Schroeder 1970). The midbody is included in one of the daughter cells or lost. Decondensation of the chromatin may not be completed until late in interphase.

Centrioles

Occurrence

Centrioles occur in most or all animal cells (Brinkley and Stubblefield 1970), in some fungi (Aldrich 1967, Renaud and Swift 1964), and some algae (Ringo 1967a). They are absent in cells of higher plants, either before or during division (Pickett-Heaps 1969, Wilson 1970). The possibility that certain non-dividing, fully differentiated animal cells may also lack centrioles has been suggested by Bernhard and de Harven (1960; see also de Harven 1968), but the available evidence is inconclusive.

The apparent de novo origin of centrioles during certain stages of the life cycle in many lower plants is an intriguing problem. A detailed discussion, however, is beyond the scope of this survey. The reader is referred to reviews by de Harven (1968), Luykx (1970), Mazia (1961), and Pickett-Heaps (1969).

Ultrastructure

There is good agreement in the literature that centrioles of interphase cells do not differ structurally from centrioles of the mitotic apparatus (Brinkley and Stubblefield 1970, de Harven 1968, Stubblefield and Brinkley 1967). A centriole is a cylindrical body 1,500-2,500 A in diameter and 3,000-7,000 A long. Nine triplets of fused 240 A MT form its wall. Centriolar MT possibly have 13 subunits in cross section, as do flagellar MT (Ringo 1967b). The triplets are not arranged radially, but slanted, giving the image of a pinwheel. Centrioles are polarized bodies. The so-called distal end is capable of generating the shaft of a flagellum or cilium (Gibbons and

Grimstone 1960). The proximal end, where daughter centrioles are formed during duplication, exhibits a cartwheel structure with spokes radiating from a hub. This cartwheel is recognizable in ideal cross sections only, but it can also be reenforced photographically by the Markham technique (Markham et al. 1963; for an example see de Harven 1968, Figure 2). The spokes seem to connect the hub with the innermost MT of each triplet; other connections possibly occur between the outermost and innermost MT of neighboring triplets. Centrioles are often embedded in an amorphous, osmiophilic matrix (Murray et al. 1965, Robbins and Gonatas 1964, Stubblefield and Brinkley 1967), that may undergo periodic changes in preparation for, and during, cell division (Robbins et al. 1968).

In Chinese hamster fibroblasts the occurrence of a small, membrane-bound vesicle, termed nucleoid, approximately in the center of the centriole seems to be the rule (Brinkley and Stubblefield 1970, Stubblefield 1968, Stubblefield and Brinkley 1967). These investigators also claimed to have detected a helical filament, 60-70 A in diameter, that winds 8-10 turns just inside the triplets.

In many cells so-called satellites (pericentriole bodies) have been observed (Brinkley and Stubblefield 1970, de Harven 1968, Murray et al. 1965, Robbins et al. 1968). These are osmiophilic bodies in the vicinity of interphase centrioles, but in most cell types studied they seem to be absent or inconspicuous during mitosis (de Harven 1968). They possibly contain RNA (Brinkley and Stubblefield 1970). The existence of connections between satellites and centrioles, and the possibly regular number and arrangement of satellites around centrioles are controversial (see de Harven 1968 for a discussion). A few authors

have claimed that nine satellites form a symmetrical crown around the centrioles (Bessis et al. 1958, Gachet and Thiéry 1964).

Chemistry

It is obviously a difficult task to determine the elemental or molecular composition of centrioles. Cytochemical methods generally lack sufficient resolution and bulk isolation of reasonably purified centrioles seems virtually impossible. The important information concerning the chemical composition of centrioles is therefore derived from studies on basal bodies (kinetosomes) of cilia, and is based on the assumption that the close structural and developmental relationship between kinetosomes and centrioles (see de Harven 1968 for references) justifies extrapolation of chemical analyses. Seaman's early findings (1960) of 2% RNA and 3% DNA in kinetosomes of Tetrahymena did not remain uncontested (see de Harven 1968 for a detailed discussion). At best, it seems, the possibility that kinetosomes contain RNA and/or DNA cannot be ruled out, but the presence of these important macromolecules in centrioles remains hypothetical.

Duplication

As early as 1952 Inoué concluded from experiments with colchicine-treated Chaetopterus eggs that centrioles duplicate and mature in the absence of a mitotic spindle. In a now classical experiment Mazia et al. (1960) determined the time sequence and mode of duplication of mitotic centers in echinoderm embryos. Although the methods used by the investigators did not allow direct visualization of centrioles (hence the term "mitotic centers"), the results predicted what has since been confirmed by electron microscopy. The results can be summarized as follows: (1) At all times the center is at least a

duplex structure. (2) Duplication occurs in very early interphase or in late telophase of the preceding mitosis. (3) The splitting of the centers is a process distinct from duplication, although the two usually occur at about the same time during mitosis. As the two members of a pair of "old" centers split, each one gives rise to a new one with which it remains associated until the next cycle. (4) The primary duplication event involves only a part of the parent structure. (5) Mercaptoethanol (ME) inhibits duplication, but not splitting and separation of existing centers. If ME is applied prior to duplication, two daughter cells result from the first division after release from inhibition. Multipolar divisions ensue if ME is applied after duplication.

Went (1966) did a similar experiment with sand dollar eggs. Benzimidazone (BIA) inhibits cell division, but not duplication of mitotic centers. After release from BIA-inhibition the cells cleave into as many blastomeres as there had been mitotic centers. Comparing these results with those from ME-treatment, Went proposed there should be a pair of potential mitotic centers at each pole of a BIA-induced tetrapolar mitotic spindle, while in the case of ME-induced tetrapolar cells there should be a single center.

The formation of so-called daughter or procentrioles during duplication has been confirmed by electron microscopy (Bernhard and de Harven 1960, Brinkley and Stubblefield 1970, Erlandson and de Harven 1971, Murray et al. 1965, Stubblefield and Brinkley 1967). Procentrioles arise at the proximal end of the parent centriole and approximately at a right angle to the latter. They are structurally similar to the parent centrioles, but much shorter during the early stages of duplication.

Stubblefield (1968), using a technique that renders centrioles in fixed cells visible for light microscopy, studied centriole duplication and behavior in colcemid-treated Chinese hamster cells. His findings concerning duplication, maturation, and separation agree well with the above-mentioned inhibitor studies (Mazia et al. 1960, Went 1966). Further confirmation came from an ultrastructural study on colcemid-treated cells (Brinkley et al. 1967).

From the references and reviews mentioned the following picture of the centriole cycle emerges: (1) At some stage between divisions each of the two centrioles normally present in interphase cells produces a daughter centriole by an as yet unknown mechanism. (2) The daughter centrioles undergo maturation, which involves elongation and, possibly, formation of the intracentriolar structures. If we define "mature" as being capable of generating a procentriole and to participate in spindle formation (see the following paragraph for reservations about the latter), then the timing relative to the cell cycle under normal conditions is so that procentrioles are mature no sooner than the end of karyokinesis following duplication. (3) If spindle formation is inhibited by colcemid or ME, maturation of the procentrioles continues and they may act as mitotic centers after release from the block. As a consequence, multipolar spindles occur more frequently than under normal conditions, and the proportion of these increases with increasing time of exposure to the inhibitor.

Function

Only the role played by centrioles in animal mitosis will be discussed here. For the involvement of centrioles in the generation of

flagella and cilia see Dirksen and Crocker (1966), Renaud and Swift (1964).

Two principal functions have been assigned to centrioles in dividing animal cells: (1) Determination of the poles of the mitotic apparatus, and (2) assembly of spindle MT (for detailed reviews see Luykx 1970, Nicklas 1971, Pickett-Heaps 1969).

The axis of the mitotic spindle is not determined by the orientation of the centrioles at the poles, except, possibly, in special cases (de Harven 1968, Luykx 1970). A number of observations seem to indicate that centrioles are indispensable as pole-determinants. In normal bipolar mitosis there is one pair of centrioles at each pole (Krishan and Buck 1965, Murray et al. 1965, Robbins and Gonatas 1964, Robbins et al. 1968, Stubblefield 1968, Stubblefield and Brinkley 1967). Furthermore, cytasters produced in sea urchin eggs by artificial activation are centered around poles containing centrioles (Dirksen 1961). In contrast to this, the number of poles in hybrid somatic cells often does not correspond to the number of centriole pairs present (e.g., Yamanaka and Okada 1968), and in cranefly spermatocytes mitosis occurs without centrioles under certain conditions (Dietz 1959, 1966). Finally, mitosis in higher plants proceeds without centrioles and many lower animals and plants have pole-determinants other than typical centrioles (see Luykx 1970, Pickett-Heaps 1969).

The idea that centrioles might be active in the assembly of MT draws support from claims that spindle MT are directly connected to centriole walls (Brinkley and Stubblefield 1970, Gall 1961), and from the proposition that the poles may be an area where MT are assembled

and disassembled (Inoué 1964, Inoué and Sato 1967). It should be noted, however, that the direct connection of MT to centrioles has not been proven unequivocally (see de Harven 1968, Luykx 1970, Pickett-Heaps 1969). More often, MT seem to connect to pericentriolar bodies or the amorphous, osmiophilic mass surrounding the centrioles. Similar dense masses can be found at the poles of higher plant cells (Pickett-Heaps 1969, Wilson 1970). Most recent reviews, therefore, consider this material, or part of it, a more likely candidate for a pole-determinant and MT organizer, not only because it occurs almost universally, but it would also bridge the gap between centriolar and acentriolar mitosis (see Luykx 1970, Nicklas 1971, Pickett-Heaps 1969). In this scheme, centrioles are thought to play a much more passive role, being carried along and distributed mainly for use as basal bodies of cilia and flagella (see also Friedländer and Wahrman 1970).

Brinkley and Stubblefield (1970; see also Stubblefield and Brinkley 1967) have presented a different hypothesis. They maintain that centrioles do play a role as pole-determinants and in the assembly of MT. However, in the absence of solid evidence, their detailed mechanistic and molecular model of centriole-MT interaction in mitosis remains highly speculative.

Spindle Fibers

Under favorable conditions fibrillar elements are visible in the mitotic spindle of living cells with the phase contrast microscope (Ris 1955). In fixed and stained cells spindle fibers can be seen without difficulty in the light microscope (e.g., Heneen 1970). The Nomarski interference-phase contrast system also allows visualization of the

fibrous organization in some cells (Bajer and Allen 1966). The most convincing evidence concerning the reality of spindle fibers has come from polarization microscope studies (Inoué 1964, Inoué and Sato 1967).

Early electron microscopic observations by Harris (1962) and Roth and Daniels (1962) revealed numerous MT in the mitotic spindle of sea urchin eggs and amebae, respectively. That the mitotic spindle is a collection of prominent MT has since been substantiated by numerous other workers (e.g., Aldrich 1969, Krishan and Buck 1965, Robbins and Gonatas 1964, Roth et al. 1966). The distribution of spindle MT agrees well with that of spindle fibers as seen in the light microscope (see Luykx 1970, Table III). Further support for the contention that the spindle fibers of the light microscopists consist of bundles of MT came from birefringence and electron microscopic studies on the effect of colchicine, colcemid, vinblastine, cold, and ultraviolet light (UV) on spindle MT. All these agents cause loss of spindle birefringence and a reduction of the number of MT as seen in the electron microscope (Bajer 1969, Inoué 1952, Inoué and Sato 1967, Malawista et al. 1968, Roth 1967). On the other hand, treatment of mitotic cells with heavy water increases birefringence and the number of MT in the spindle (Inoué and Sato 1967). The observation by Rebhun and Sander (1967), that MT are not the only birefringent component of the mitotic spindle, imposes limits on the interpretation of such results, but the fact remains that MT are birefringent elements. The correlation between birefringence and MT is generally regarded as sufficient evidence for the occurrence of MT in living cells, particularly since improved fixatives for electron microscopy have made the demonstration of MT easy (but see Nicklas 1971 for a discussion of this point).

Following common usage in the literature, the term spindle fiber shall hereafter designate the structure seen in the light microscope. The term microtubule (MT) shall be reserved for the fibrils seen in the electron microscope. By this definition a kinetochore fiber consists of one or several MT.

Fine Structure

Spindle MT are slender cylinders 150-250 A in diameter and several microns long (de Harven 1968, DuPraw 1968, Luykx 1970, Nicklas 1971, Roth 1964). The tubules are hollow and have a wall 40-60 A thick. The substructure of the wall is best resolved by negative staining of isolated MT (Barnicot 1966, Kiefer et al. 1966), or by freeze-etching (Moor 1967). Globular subunits, 30-40 A in diameter, form linear filaments. Ten to thirteen such filaments form the tubule wall. The filaments are arranged in such a way that the subunits form a helix with a pitch of 10-20°. Spindle MT are thought to be as rigid as cytoplasmic MT (Luykx 1970), and therefore should run more or less straight over a certain distance, or only be slightly curved. Wavy MT can be a shrinkage artifact produced during dehydration (Jensen and Bajer 1969).

Kiefer et al. (1966), citing a number of studies on the extraction of proteins from mitotic apparatus, all of which seem to have yielded a protein particle sedimenting at approximately 2.5S (MW approximately 34,000), proposed that this particle corresponds to the 35 A globular subunit of the MT wall. Results from the various laboratories have, however, been interpreted in different ways and the correlation between visible subunits and isolated particles is not firmly established

(see Luykx 1970, Nicklas 1971, for detailed discussions). Inoué and his collaborators (Inoué 1964, Inoué and Sato 1967) have proposed that MT polymerize from a pool of subunits in a dissociation-association equilibrium, probably under control of "organizing centers" such as kinetochores and centrioles. Certainly, the rapid loss and reappearance of birefringence in mitotic cells subjected to rapid temperature shifts (Inoué et al. 1970) suggests self assembly of subunits to form MT (see Nicklas 1971).

Fine interconnections or "cross-bridges" between spindle MT, and "arms" on single MT have been reported for a number of plant and animal cells (Hepler and Jackson 1968, Krishan and Buck 1965, Wilson 1969). Hepler et al. (1970) devoted a more detailed and systematic study to these structures in cultured human cells and Haemanthus endosperm, but although they play a major role in the model of mitosis proposed by McIntosh et al. (1969), their reality is conjectural at best (see also Nicklas 1971).

Distribution and Classification

Spindle MT can be divided into two main categories: chromosomal and continuous (interpolar) MT (de Harven 1968, Luykx 1970, Nicklas 1971, Roth 1964). In the case of chromosomes with a well-defined kinetochore the chromosomal MT run between the latter and the corresponding spindle pole (Brinkley and Stubblefield 1966, 1970; Harris and Mazia 1962, Jokelainen 1967, Krishan and Buck 1965, Murray et al. 1965, Robbins and Gonatas 1964). Chromosomes with so-called diffuse kinetochores are connected with MT at various points along their length (Buck 1967). Luykx (1970) distinguished several

subcategories of spindle MT. Notable among them are the penetrating or transchromosomal MT (Nicklas 1971) observed in many animal cells (e.g., Behnke and Forer 1966, Buck 1967, Jokelainen 1967, Robbins and Gonatas 1964). They may actually be part of the population of continuous MT.

It is obviously difficult to demonstrate that continuous MT do run from one pole to the other, because they often pass into and out of sections. However, this has been demonstrated in two cases involving relatively short spindles (Aikawa and Beaudoin 1968, Manton et al. 1969b). On the other hand, studies on late stages of mitosis indicate most "continuous" MT overlap in, and terminate beyond, the midbody (Byers and Abramson 1968, Paweletz 1967). Understandably, this point, which is important for an explanation of the function and mechanics of the MA, is still controversial. More detailed studies, involving counts of MT in serial sections cut at a right angle to the spindle axis, have only recently been published (Brinkley and Cartwright 1970, Manton et al. 1969b, McIntosh and Landis 1971). It appears that relatively few MT [10% in the diatom Lithodesmium (Manton et al. 1969b, 1970); 30-40% of the interpolar MT which make up 40-50% of all the spindle MT in Chinese hamster and rat kangaroo cells (Brinkley and Cartwright 1970)] are truely interpolar. Most "continuous" MT project across and terminate beyond the equator.

It is generally agreed (see Luykx 1970) that there is no difference regarding structure and dimensions between the different classes of spindle MT. However, kinetochore MT differ from continuous and astral MT in their sensitivity to spindle poisons. Upon exposure of Chaetopterus eggs to colchicine, the continuous fibers lose their

birefringence more rapidly than the chromosomal fibers (Inoué 1952). Sauaia and Mazia (1961) found that in sea urchin eggs the asters, but not the kinetochore fibers, are disorganized by brief exposure to colcemid. Likewise, a low concentration of colcemid disorganizes continuous MT in Chinese hamster cells, but some kinetochore MT remain (Brinkley et al. 1967). Similar differences apply for cold treatment. Kinetochore fibers in lily pollen mother cells in anaphase regain birefringence first when the cells are brought to ambient temperature after chilling (Inoué 1964). In contrast to this, continuous fibers in Chaetopterus eggs are the first to regain birefringence lost during chilling (Inoué 1964). In mammalian cells in vitro Brinkley and Cartwright (1970) found cold shock completely disorganized interpolar MT, while the number of chromosomal MT was reduced by 30-40%.

Function

It has been proposed that continuous fibers, which form the so-called "central spindle" (Mazia 1961), function in the separation of the pole-determinants (centrioles where applicable. Brinkley et al. 1967, Brinkley and Stubblefield 1970, Friedländer and Wahrman 1970, Mazia 1961). In Chinese hamster cells exposed to colcemid, chromosomes arrange more or less radially around the two unseparated pairs of centrioles (Brinkley et al. 1967). The reformation of pole-to-pole MT after release from the inhibitor seems necessary for the separation and migration of the centrioles.

In cells with diffuse kinetochores, the penetrating or transchromosomal MT may play an important, if not exclusive, role in chromosome movement (Luykx 1970, Nicklas 1971). Whether they also

participate in the movement of chromosomes with a well-defined kinetochore is uncertain. The often cited observations by Carlson (1938) on apparent poleward movement at anaphase of X-ray-induced acentric fragments in grasshopper neuroblasts are not convincing. Bajer (1958) and Bajer and Molè-Bajer (1963) presented better evidence based on cinemicrography of β-irradiated Haemanthus endosperm cells. In the majority of cases, however, acentric fragments do not behave as normal chromosomes (Kihlman 1966, Lea 1962).

Finally, continuous MT are supposed to produce spindle elongation at anaphase in cells where this occurs (Mazia 1961, Roth et al. 1966). Spindle elongation is a process different from poleward movement of chromosomes, as demonstrated by Ris' (1949) observation that chloral hydrate prevents the former, but does not inhibit the latter.

The chromosomal fibers form the "chromosomal spindle" (Mazia 1961). Chromosomes with a distinct kinetochore are firmly attached to the kinetochore fibers. This can be inferred from the above-mentioned study by Ris (1949), and from observations by Inoué (1952) that in Chaetopterus eggs treated with colchicine the chromosomes disperse from the metaphase plate only after the birefringence of the chromosomal fibers has completely disappeared. Shimamura (1940) reported that chromosomes at the centripetal pole of centrifuged lily pollen mother cells are firmly anchored by their kinetochore fibers, although the centrifugal force is strong enough to cause uncoiling of the chromosomes themselves. Finally, the most direct evidence came from elegant micromanipulation experiments by Nicklas and Staehly (1967) on grasshopper spermatocytes. Chromosomes can be stretched with a microneedle without changing the kinetochore-to-pole distance

significantly from the beginning of prometaphase to the end of anaphase. Lateral displacement within the spindle is possible, however. The authors found no evidence for interzonal connections between separating chromosomes at anaphase.

There is a large body of evidence that kinetochore fibers play a major, if not exclusive, role during metakinesis, i.e., those movements of the chromosomes that begin with prometaphase and terminate with the alignment of the chromosomes on the equator of the spindle (congression), as well as in the poleward movement of chromosomes during anaphase. Bivalents of spermatocytes in prometaphase often have the shape of an arrowhead with the kinetochore at the tip (Dietz 1969). If one bivalent is stretched to a greater extent than its partner, the movement is always in the direction of the pole towards which the former is oriented. More direct evidence comes from UV microbeam irradiation experiments. In newt fibroblasts irradiation of the kinetochore, but not of other parts of a chromosome, stops prometaphase movement and the irradiated chromosome never reaches the metaphase plate (Bloom et al. 1955, Uretz et al. 1954). In Haemanthus endosperm cells, on the other hand, similarly treated chromosomes do reach the metaphase plate, although their paths of movement during prometaphase may be altered and become very complex (Bajer and Molè-Bajer 1961).

Chromosome motion at metaphase is very slow and minimal (Dietz 1969, Mazia 1961). The equatorial position of the chromosomes is very likely maintained by a balance of forces on opposed sister kinetochores. If one kinetochore pair of a bivalent in a grasshopper spermatocyte in metaphase is irradiated with a UV microbeam, the bivalent shifts towards the pole closest to the unirradiated

kinetochore (Izutsu 1961). An exception to this rule was reported by Forer (1966) for crane fly spermatocytes. Here, UV microbeam irradiation of the chromosomal fibers on the poleward side of the metaphase plate does not induce movement. A possible explanation for this behavior is the apparent absence of any kind of kinetochore on these chromosomes, as reported by Behnke and Forer (1966). Finally, the necessity of opposing poleward forces for stable metaphase alignment was clearly demonstrated in Nicklas' laboratory (Henderson and Koch 1970, Henderson et al. 1970, Nicklas and Koch 1969).

It is a well-supported conclusion that chromosomes move as individuals, although they may move synchronously (Luykx 1970, Mazia 1961, Nicklas 1971). Since Ris' study (1949) two types of anaphase movement are distinguished: (1) spindle elongation, and (2) shortening of the chromosome-to-pole distance. The two processes are based on different mechanisms, because the former, but not the latter, is inhibited by chloral hydrate (Ris 1949). In grasshopper spermatocytes the two processes act together (Ris 1949), but in other cells each of the two possible extremes can occur (see Mazia 1961 for references). Mazia (1961), who also discussed the various early hypotheses concerning anaphase movement, summarized the events as follows: "The central spindle is more or less rigid; it moves the poles apart and provides an anchor for the poles which must bear the load of the chromosomes."

The question whether chromosomes are pulled or pushed has engaged the mind of many a biologist. Most reviewers (Dietz 1969, Luykx 1970, Mazia 1961, Nicklas 1971) arrived at the conclusion that a pulling force must be involved in the movement of chromosomes, although a

pushing force (similar to the "Stemmkörper" proposed by Bělár 1929) may contribute to anaphase separation. Clearly, prometaphase movement cannot be explained on the basis of pushing forces only. The behavior of chromosomes that are pushed away from the spindle into the cytoplasm by micromanipulation also suggests a pulling force (Nicklas 1967). The results of Forer's (1966) UV microbeam irradiation experiments on crane fly spermatocytes seem to refute the idea that chromosomes are simply pulled by their kinetochore fibers. Nevertheless, the results can be interpreted as supporting a pulling hypothesis (Nicklas 1971).

Even if we accept the pulling hypothesis there remains the problem of how the MT accomplish this, a problem around which center all of the more recent models of mitosis (Dietz 1969, Luykx 1970, McIntosh et al. 1969). There is no change in diameter as MT shorten or lengthen (see Luykx 1970, Nicklas 1971, for references), and a simple contraction mechanism is not compatible with structural observations. Inoué and his collaborators (Inoué 1960, 1964, Inoué and Sato 1967) have consistently explained this phenomenon with their "dynamic equilibrium model," which proposes a pool of MT subunits in the spindle region. Free subunits are in a dynamic equilibrium with subunits bound in MT. Shifts in the equilibrium induce further polymerization or depolimerization. The former would produce lengthening, the latter shortening of MT. Orienting centers are thought to determine the direction of the "growing" MT during polymerization.

Chromosomes

Three basic questions must be considered here: (1) What is the unit fiber of the mitotic (and interphase) chromosome? (2) What is the

relationship between the DNA double helix and the unit fiber? (3) How is the unit fiber arranged in the highly condensed metaphase chromosome? Data and observations bearing on these questions come from a number of fields of study and so far it has not been possible to reconcile them in one comprehensive model of the eukaryotic chromosome.

In thin sections of interphase nuclei and mitotic chromosomes fibrils approximately 100 A in diameter are visible (Wolfe 1969). Because the fibers are cut at various angles, little can be concluded regarding their three-dimensional organization. Whole-mount preparations of isolated chromosomes seemed initially much more promising (for references see Wolfe 1969). In isolated chromosomes the diameter of the fibers varies from approximately 20 A to 500 A or more, depending on the quality of the preparation, but most investigators agree that the mean diameter is approximately 250 A (DuPraw 1968, Wolfe 1969). However, Ris has demonstrated (1961, 1967; Ris and Kubai 1970) that 100 A fibers can consistently be obtained. Understandably, a lively controversy revolves around these differing results and their interpretation. DuPraw (1968) considers the 250 A fiber as the unit fiber (type B fibril). On the other hand, Wolfe (1969; see also Zirkin and Wolfe 1970) considers this to be an artifact produced by the deposition on a 100 A fiber of contaminating material during preparation. A third view is held by Ris (Ris 1967; Ris and Kubai 1970): after certain chemical treatments the 250 A fibers can be shown to consist of two 100 A fibrils, more or less twisted around each other. Both Ris (Ris and Kubai 1970) and Wolfe (1969) present arguments and evidence supporting their respective hypothesis. At the center of the dispute are the many possible artifacts produced by

differences in the method of preparation. A discussion of these is beyond the scope of this summary. Perhaps Ris and Kubai (1970) are closer to the truth in their conclusion that the 250 A fiber is the structure present in the intact nucleus, but that its relationship to the 100 A fiber is not yet clear.

The second question can be divided into two parts: (a) Does the unit fiber contain a single DNA double helix or several in lateral association? The DNA-histone complex is expected to have a diameter of approximately 30 A (Zubay and Doty 1959). Many investigators have claimed to have observed a fibrillar substructure within the 100 A fiber (see Wolfe 1969, for references). However, enzyme digestion and other treatments that are assumed to remove all or most of the histones from the chromosomal fiber leave a strand 20 A thick, which most probably represents a single DNA double helix (DuPraw 1968, Ris and Kubai 1970, Wolfe 1969). It is thus generally accepted that the unit fiber contains a single DNA double helix. However, there is ample evidence that this helix is highly compacted in the unit fiber (DuPraw 1968, Ris and Kubai 1970). The major role in folding of the DNA has been assigned to the histones, but the molecular basis is not yet clear (see Ris and Kubai 1970, for discussion).

(b) Is the DNA double helix in the unit fiber continuous or does it consist of subunits of variable length, perhaps connected by so-called linkers? Sedimentation coefficients and direct electron microscopic measurements of purified DNA from isolated chromosomes or chromatin yield fragments of variable length (see Ris and Kubai 1970). Similar results are obtained with autoradiography of DNA labeled during replication. Both methods, however, have their limitations and do not

unequivocally support the idea that the DNA is discontinuous. Similarly, the observation of multiple replication points in eukaryotic nuclei is no definite evidence (see DuPraw 1968), and the accepted conclusion is that the DNA molecule in the unit fiber is continuous (DuPraw 1968, Ris and Kubai 1970).

The third question, concerning the organization of the unit fiber in metaphase chromosomes, is at the center of the uninemy-polynemy controversy. The answer is very simple: the problem is not resolved (DuPraw 1968, Ris and Kubai 1970, Wolfe 1969). Bajer (1965) observed the half-chromatid structure of chromosomes in living Haemanthus endosperm cells. When fixed metaphase chromosomes from Vicia cells pretreated with 5-amino uracil are digested with trypsin, each chromatid appears to consist of two subunits (Wolfe and Martin 1968). In whole-mounted, isolated chromosomes, each chromatid contains many fibers (e.g., Abuelo and Moore 1969, DuPraw 1968, Lampert 1969, Stubblefield and Wray 1971, Wolfe 1965), which can be interpreted to form longitudinal subunits of chromatids, although it is virtually impossible to follow individual strands over a greater distance. Cells exposed to X-ray or certain chromosome-breaking chemicals during G_2 exhibit, at the following metaphase, bridges between sister chromatids that involve apparent subunits of chromatids (subchromatid aberrations or "side-arm bridges"; Brinkley and Humphrey 1969, Heddle 1969, Kihlman 1966). Kihlman, who formerly supported polynemy based on his experiments with chromosome-breaking chemicals (e.g., Kihlman 1966), has recently questioned the occurrence of true subchromatid aberrations (Kihlman 1970), and favors the single-stranded "folded fiber" model of DuPraw (1965, 1968).

Isolabeling of chromatids (e.g., Peacock 1963) has always been a strong argument in favor of polynemy, but it can be accommodated in a single-stranded chromosome model (Comings 1971, Ris and Kubai 1970). On the other hand, the observation that chromosomes replicate semi-conservatively (Taylor et al. 1957) is in favor of uninemy. As Ris and Kubai (1970) pointed out, the most compelling evidence against multi-strandedness comes from studies on the uniqueness or redundancy of DNA sequences (e.g., Britten and Kohne 1968). In Drosophila and the mouse the majority of DNA sequences are unique. This would exclude the presence of two or more identical DNA strands per chromatid, which is, of course, a prerequisite for multi-strandedness dictated by the orderly segregation of genes at mitosis.

In view of these contradictory observations and results it seems premature to propose a detailed model of the architecture of metaphase chromosomes. For examples of such models the reader is referred to the review by DuPraw (1968) and the paper by Stubblefield and Wray (1970).

Kinetochore Structure and Function

Light Microscopic Observations

Chromosomal granules, presumably corresponding to the centromere studied by many later cytologists, were first described by Metzner (1894), who called them "Leitkörperchen." By 1930 a number of different terms were in use (see Schrader 1936). Sharp (1934) introduced the term "kinetochore," which has been used as a synonym of "centromere" by many authors. For clarity I prefer to apply the term centromere to the structure seen with the light microscope in the primary constriction of chromosomes, and to reserve the term

kinetochore for the structure as it appears in the electron microscope. For this review, however, I use the terms in accordance with the authors cited.

For many years most cytologists described the centromere as a "gap" or non-staining constriction (for references see Schrader 1953). Schrader (1936, 1939) presented a detailed description of the kinetochores of meiotic chromosomes in two species of amphibia and in Tradescantia. He interpreted each tetrad to have two kinetochores, each of which consisted of two spherules lying in a commissural cup. Using various stains to enhance visibility of the spherules, he was able to follow the changes in appearance of the kinetochores during the different stages of meiosis.

Much of the early discussion about centromeres concerned the problem of the presence or absence of DNA in this chromosome region. Applying the Feulgen test to pachytene plant chromosomes, Lima-de-Faria (1950) demonstrated the presence of DNA in the centromere, which he described as consisting of fibrils and chromomeres. Gall (1954) documented that kinetochores of newt lampbrush chromosomes are also Feulgen-positive. He noticed that the kinetochores resemble chromomeres in general appearance, except for the lack of lateral loops. Lima-de-Faria (1956, 1958) furnished additional evidence for his view of kinetochores of plant chromosomes as a specialized region showing Feulgen-positive granules connected by fibrils.

Electron Microscopic Observations

The first good electron micrographs of animal kinetochores were published by Harris (1962; see also Harris 1965, Harris and Mazia 1962)

and by Nebel and Coulon (1962). Satisfactory fixation was still a problem in those days, but the kinetochores in dividing sea urchin eggs could be clearly recognized as irregularly shaped, electron-dense granules at the surface of the chromosomes where they are apparently attached to MT (Harris 1962). Most remarkable was a difference in staining intensity between the kinetochores and the remainder of the chromosomes in preparations where the fixative had dispersed or partially extracted the chromosomal fibers.

Nebel and Coulon (1962) interpreted the kinetochores of metaphase I pigeon spermatocytes as having the shape of an acorn with MT attached to the convex side of the cup. The details presented in their model (their Figure 12), however, are not all discernible in the only low-power electron micrograph included (their Figure 11). At best one can distinguish a dense band, 2,000-4,000 A long, following the outline of the chromosome and separated from the latter by a clear zone of approximately the same width. The chromosome proper appears denser at this site; poleward of the dark band a less dense matrix can be seen. The authors interpreted the MT to penetrate the kinetochore and terminate in the chromosome.

Since these early studies a number of papers have appeared describing the fine structure of kinetochores. The most detailed study of the kinetochores of invertebrate cells was that by Luykx (1965a, b) on Urechis eggs. Despite apparent fixation problems the dense-light-dense banding was evident, particularly on meiotic chromosomes. The author noted that the density of the kinetochore appeared to increase from prometaphase to anaphase. The dense material was seen to closely follow the curvature of the chromosome surface. The deep layer was

often less dense than the superficial layer and more variable in appearance. Approximately 10-25 MT, some of which seemed to end in the deep layer, could be counted per kinetochore. On mitotic chromosomes the triple-layered structure was less frequent. DNAse treatment indicated little or no DNA in the kinetochore region, or increased resistance of kinetochore DNA to the enzyme (Luykx 1965a).

Wettstein and Sotelo (1965) found that the kinetochores in Gryllus spermatocytes consist of essentially the same 100 A fibrils as the remainder of the chromosome, but the fibrils seemed more densely packed in the kinetochore. The shape of these kinetochores resembles that of a thick nail or screw deeply anchored in the body of the chromosome.

Grasshopper spermatocytes have ovoid kinetochores embedded in a cup (Brinkley and Nicklas 1968, Nicklas 1971, and personal communication; see also Brinkley and Stubblefield 1970, Figures 26 and 27). An electron-dense "axial core" is embedded in a mass of less dense 50-80 A fibrils. In general appearance these kinetochores seem to resemble plant kinetochores (Bajer and Molè-Bajer 1969, Wilson 1968) more than animal kinetochores.

A different kind of kinetochore in invertebrates is the diffuse kinetochore described by Buck (1967) in the bug Rhodnius. He interpreted the finely granular material on the surface of metaphase chromosomes as representing the kinetochore, but noticed the relative paucity of spindle MT attached to this structure. Ris (Ris and Kubai 1970) reported on a preliminary basis that no such material could be found on chromosomes in spermatocytes of the homopteran insect Philaenus. Rather, the MT seemed to penetrate deeply into the chromosome where they end blindly.

Mammalian kinetochores are by far the most intensely studied. Besides papers devoted specifically to mitosis or kinetochores, there are numerous isolated electron micrographs in the literature showing various profiles of mammalian kinetochores (e.g., Flaks 1971, Hu 1971). Unfortunately, some of the most frequently cited papers on the ultrastructure of mammalian cells in mitosis (e.g., Krishan and Buck 1965, Murray et al. 1965) do not show kinetochores at high magnifications. At best, one can make out that they consist of three layers or bands, like those described by Nebel and Coulon (1962). Robbins and Gonatas (1964, Figure 19) presented a detailed picture of an early anaphase kinetochore in a HeLa cell. The three layers are very clear; MT seem to insert into the outer layer. Barnicot and Huxley (1965) also published electron micrographs showing the kinetochores of cultured newt heart cells as three-layered structures. They interpreted the kinetochores to consist of material different from the chromosomes, based on different stainability. In this context it is interesting to note that the kinetochores of the alga Oedogonium (Pickett-Heaps and Fowke 1969) and the moss Mnium (Lambert 1970) are also triple-layered, as are those of Barbulanympha (Hollande and Valentin 1968), which has an intranuclear spindle.

Jokelainen (1965a) described kinetochores in fetal rat kidney as short bands separated from the chromosomes by a clear area, or as two parallel bands, in which case the second band was in direct contact with the chromosomal material. In subsequent papers (Jokelainen 1965b, 1967, 1968) he developed his concept of kinetochore maturation and his kinetochore model. Maturation occurs during prometaphase and is asynchronous for sister kinetochores. It involves the appearance of

the outer layer and a reduction in size of the kinetochoral patch as it becomes anchored to the spindle MT (Jokelainen 1965b). The outer layer is embedded in a moderately dense substance, part of which persists at metaphase as the middle layer of the kinetochore and the so-called corona (Jokelainen 1967). Jokelainen's model (1967) depicts the kinetochore as a trilaminar disk, 2,000-2,500 A in diameter, at the surface of the chromosome, sometimes slightly recessed, sometimes projecting. The outer layer is 300-450 A thick, the middle layer 150-300 A, and the inner layer 150-250 A. The corona over the outer layer measures approximately 300 A in thickness. Evidence for the disk-like appearance came from para-equatorial sections showing kinetochores in face view. The outer disk, which is finely granular or fibrillar, stains consistently, while the density of the chromosomes varies with the staining method employed. The inner layer is highly electron-dense, and roughly granular or fibrillar. Four to seven MT are attached to each kinetochore, apparently penetrating the outer and middle layers and sometimes ending in the chromosome.

Brinkley and Stubblefield (1966, 1970) presented a different model of mammalian kinetochores. In colcemid-arrested Chinese hamster cells the kinetochore appears as a 200-300 A wide band, made up of two 50-80 A threads. This band is embedded in a less dense matrix and follows the curvature of the chromosome surface at a distance of approximately 100 A. In the less dense matrix the authors detected 50-80 A fibrils apparently looping out from the main band. This description was based on kinetochores without attached MT, but according to the authors the kinetochores of untreated cells are very similar. The model of Brinkley and Stubblefield (1966, 1970) describes

the kinetochore as consisting of two lampbrush-like structures, each made up of two closely associated 50-80 A axial filaments from which numerous 50-80 A fibrils loop out laterally. The axial filaments extend along the surface of the chromosome, their ends being inserted into the latter. Microtubules attach to the axial filaments in sheets or bundles. According to their most recent report (Brinkley and Stubblefield 1970) there is little change in the structure of the kinetochores in Chinese hamster and rat kangaroo cells from prophase to metaphase. The kinetochores are mature in late prophase or in prometaphase, regardless of whether MT are attached or not.

An electron micrograph recently published by McIntosh and Landis (1971, Figure 4) supports Jokelainen's model (1967). In this paraequatorial section of the metaphase plate three kinetochores are shown as circular patches of less dense material. On the other hand, the kinetochores of colcemid-treated cells, on which Brinkley and Stubblefield (1966, 1970) mainly based their model, may be atypical. For example, very clear images of a double-banded outer layer embedded in a less dense matrix are produced by the alkaloids vinblastine and vincristine, both of which disorganize MT (George et al. 1965, Journey et al. 1968, Journey and Whaley 1970, Krishan 1968).

Microtubules and kinetochores as seen in thin sections are not preserved in whole-mount preparations of metaphase chromosomes (e.g., DuPraw 1968). Instead, chromosomal fibers can be seen to cross between sister chromatids in the centromere region (see also Abuelo and Moore 1969). Interesting, but unexplained, is the presence of four dense granules at the centromere of Chinese hamster cells subjected to certain treatments during isolation (Stubblefield and Wray 1971).

Function

In addition to the role of the kinetochore in chromosome movement as discussed in a previous section, Luykx (1970) reviewed five other possible functions: (1) Initiation of synapsis and localization of chiasmata; (2) terminalization of chiasmata; (3) chromosome condensation or coiling; (4) association of sister chromatids; and (5) formation or assembly of chromosomal spindle fibers. The latter is the most interesting in the context of this review.

When chromosomal fibers are irradiated between the centromere and the pole in anaphase cells, birefringence disappears from the irradiated region and distal to it. Restoration of birefringence takes place within a few minutes. When, however, the centromere itself is irradiated, birefringence disappears from the whole length of the chromosomal fibers, including the distal non-irradiated portion, and restoration does not occur for a long time (Inoué 1964). Electron micrographs have shown that a great proportion of spindle MT is arranged in bundles associated with the kinetochores (Brinkley and Landis 1970, Brinkley and Stubblefield 1970, Jokelainen 1967). These observations have led to the idea that the kinetochore may play an active role in the assembly and/or orientation of MT (e.g., the "organizing center" of Inoué 1964). Further support for this idea has been drawn from observations of apparent microtubular connections between meiotic sister kinetochores (Luykx 1965b) and mitotic non-sister kinetochores (Bajer 1970). As long as clear evidence from serial sections is lacking, however, such configurations have to be regarded with skepticism. On the other hand, the occurrence of individual chromosomal spindles, either as an anomaly (e.g., Dietz

1969, Koopmans 1958) or as part of normal spindle development (Hughes-Schrader 1948), seems to indicate that chromosomes alone are capable of organizing spindle MT. Similarly, Roth (1967) suggested that in spindle reformation after cold shock the spindle MT gradually extend from the chromosomes towards the poles. These observations have been interpreted to mean that spindle fiber material is being continuously assembled and oriented at the kinetochore throughout prometaphase and metaphase, but the exact role of the kinetochore is not as yet clear (see Luykx 1970).

Equally interesting in this context are ideas of the kinetochore as a specialized "gene" (Brinkley and Stubblefield 1970) or a gene product (Luykx 1970). Even if we accept the universal occurrence of DNA in the centromere region as a fact, we must bear in mind that the relationship between DNA and the kinetochore at the fine structural level is not at all resolved. Brinkley and Stubblefield (1970) have proposed that the lateral loops of their lampbrush-like kinetochores consist of DNA, which codes for long RNA molecules that bind with protein subunits to form MT. This elaborate hypothesis stands on rather shaky ground. Luykx (1970), on the other hand, proposed the DNA in the kinetochore region "may therefore be viewed as a 'kinetochore organizer', similar to the nucleolar organizing region of the chromosome in a number of ways. It is responsible for the synthesis or assembly of an essential organelle that remains associated with a specific chromosomal site, is often associated with blocks of heterochromatin, remains relatively uncoiled during mitosis, and probably contains a large number of identical genes" (Luykx 1970).

Chromosomal and Mitotic Aberrations

Chromosomal aberrations occur spontaneously in certain organisms (e.g., Brandham 1970, Vig 1970). Far more frequent, however, are induced aberrations. Shaw (1970) presents a long list of agents (clastogens) that can cause chromosome damage. The agents range from nucleic acid analogs, antibiotics, drugs, and pesticides, to ionizing and UV radiation, temperature shock, and weightlessness. Certain viruses are well-known biological clastogens (e.g., Nichols 1970, Nichols et al. 1964).

Only some of the elementary aspects of the induction of chromosomal and mitotic aberrations can be reviewed here. The emphasis will be on chemical clastogens. Radiation-induced aberrations will be referred to only to the extent that they elucidated basic facts that also apply to chemicals (for detailed reviews on radiation-induced aberrations see Bacq and Alexander 1955, Evans 1962, Hollaender 1954, Lea 1962, Wolff 1963).

Cellular Events

Kihlman (1966) distinguished three types of effect of chemicals on dividing cells and chromosomes: (1) Prevention of cells from entering mitosis [e.g., 5-fluorodeoxyuridine, FUdR (Taylor 1963)]; (2) interference with active stages of division [e.g., spindle poisons, such as colchicine (Eigsti and Dustin 1955)]; (3) production of chromosomal aberrations [e.g., streptonigrin (Cohen et al. 1963)]. It is characteristic for many chemicals that they affect mitosis and chromosomes (see also reviews by Biesele 1962, Deysson 1968, Gelfant 1963). For example, FUdR inhibits mitosis and also fragments

chromosomes (Hsu et al. 1964). Other chemicals are primarily chromosome-breaking agents, but at the same time they affect the mitotic rate. To discriminate between chromosomal and mitotic effects, Deysson (1968) classified the cytological effects of antimitotic substances as follows: mitodepressive (lowering the mitotic rate), mitostatic (no proliferation), mitoclasic (disturbances of the mitotic apparatus), and chromatoclasic (induction of aberrations). Generally, the lowest effective concentration of a given chemical is mitodepressive. The same, or a slightly higher concentration produces chromosomal aberrations. Higher concentrations, besides inducing chromosomal anomalies, cause preprophase inhibition (mitostatic effect), and still higher concentrations destroy cells in mitosis.

Chemicals Versus Ionizing Radiation

Aberrations produced by ionizing radiation applied to cells in G_1 are of the chromosome type (e.g., Heddle 1969). The transition from chromosome to chromatid aberrations occurs at the end of G_1 (Evans and Savage 1963), but some authors maintain that both chromosome and chromatid aberrations can result from irradiation during S, depending on whether unreplicated or replicated parts of the chromosomes are hit (e.g., Casarett 1968). Chromatid aberrations only result from irradiation of cells in G_2, i.e., after completion of DNA synthesis. Subchromatid aberrations can be induced during prophase and, possibly, at the end of G_2 (see Heddle 1969). The term non-delayed effect used by Kihlman (1966) with reference to chemical clastogens and radiation implies aberrations produced after completion of DNA synthesis (chromatid and subchromatid aberrations), while delayed effects include chromatid and chromosome aberrations (induced during G_1 and S).

The often used term "radiomimetic" chemicals for substances that induce chromosome damage is rather misleading. As already mentioned, ionizing radiation produces both non-delayed and delayed effects, while most chemicals (e.g., alkylating agents) produce delayed effects only (Kihlman 1966). Exceptions are streptonigrin (SN) and 8-ethoxycaffeine (EOC), which produce effects very similar to X-rays. Increased oxygen tension, which drastically increases the frequency of aberrations induced by X-rays (Bacq and Alexander 1955, Evans 1962, Lea 1962) has little or no effect with many chemical clastogens (Kihlman 1966). Perhaps the most significant difference between X-rays and chemicals is that the former produce aberrations more or less randomly in a particular chromosome, while aberrations induced by the latter tend to be localized in the heterochromatin (Nichols et al. 1964, Revell 1963).

Hypotheses on the Formation of Chromosomal Aberrations

The general or breakage-first hypothesis as described by Kihlman (1966) proposes that the primary event produced by a clastogen is a chromatid or chromosome break in a continuous interphase chromosome. The ends at the point of breakage may rejoin to restore the original configuration (restitution), they may remain open, or they may rejoin with other open ends. Illegitimate fusion of ends from different breaks results in sister-union or various types of exchanges.

According to the exchange hypothesis proposed by Revell (1955; see also Revell 1963) the primary event is not a break, but some other kind of lesion. The lesion may revert to normal or to another state incapable of forming an exchange. If two primary events occur close enough in space and time, an exchange initiation stage may follow.

During subsequent stages of chromosome development, the aberration is transformed into a real chromatid exchange. Revell (1955) presented data that are in good agreement with his hypothesis and Kihlman (1966) came to the same conclusion based on more recent work. However, in experiments especially designed to test the two hypotheses, Heddle and Bodycote (1970) found that neither, as usually interpreted, is entirely correct. Rather, they concluded that deletions are of two types, according to mode of origin, but they were unable to identify the two types morphologically.

Morphology and Mitotic Behavior of Aberrant Chromosomes

The following discussion is restricted to chromosomes with localized kinetochores.

"Gaps"

"Gaps," or "achromatic lesions" are Feulgen-negative regions of variable size in chromatids (Evans 1963, Scheid and Traut 1970). In Vicia they often resemble the normal nucleolar constriction. Gaps are aberrations of the non-delayed type, since they can be induced by X-rays in prophase nuclei (Evans 1963). The question of chromatid continuity across the gap is important here, because gaps would have to be scored as true breaks if the chromatid were really interrupted. Many investigators (see Evans 1963 for references) have observed some sort of material crossing gaps. Furthermore, the chromosome segment distal to the gap moves normally and seems attached to the main body of the chromosome at anaphase. If gaps were true breaks, they should give rise to chromatid or chromosome aberrations at the second division after exposure, but this is not the case (Evans 1963). Another

interesting point is that in Vicia and Trillium Feulgen-negative regions similar in appearance to gaps can be induced by exposure to low temperature. Electron microscopic examination of whole-mounted and thin-sectioned chromosomes indicates that some gaps are true breaks, while others are traversed by chromosomal fibrils (Brinkley and Shaw 1970). Similar results were obtained by Scheid and Traut (1971) with the scanning electron microscope. They found that gaps represent distinct "notches" which in some cases are traversed by two parallel strands.

Acentric fragments

A break without reunion produces an acentric fragment (Evans 1962, Kaufmann 1954, Kihlman 1966). If the break involves only one chromatid the fragment is single; it consists of two "sister chromatids" if the entire chromosome is broken. Such fragments are usually lost during division, or they are included at random in daughter cells where they form micronuclei (Humphrey and Brinkley 1969, Kihlman 1966, La Cour 1953). Carlson (1938) attributed apparent migration of acentric fragments towards the poles at anaphase to more than chance movement, but he made his observations on smear preparations. Bajer (1958) and Bajer and Molè-Bajer (1963) recorded the behavior of fragments in irradiated Haemanthus endosperm by time-lapse cinemicrography. The majority of fragments were eliminated from the spindle, either at prometaphase or during ana- and telophase. A few fragments, however, moved in the spindle region in a more than random fashion, sometimes from the equator to one pole and back. The authors attributed these movements to the activity of neocentric fibers. In rat kangaroo cells

exposed to X-rays, Humphrey and Brinkley (1969) confirmed by electron microscopic analysis of thin sections that fragments lack kinetochores.

Bridges

An exchange between centric portions of two broken chromatids or chromosomes results in the formation of an anaphase bridge if the two centromeres move to opposite poles (Evans 1962, Hair 1953, Kaufmann 1954, Kihlman 1966, Koller 1953). Subchromatid bridges (side-arm bridges) arise from intrachromosomal exchanges. The unit of breakage and exchange in these aberrations was generally assumed to be a half-chromatid (Heddle 1969, Kihlman 1966). Brinkley and Humphrey (1969) examined X-ray-induced side-arm bridges in rat kangaroo cells with the electron microscope and found that the diameter of these chromatid connections was considerably less than that of a half-chromatid. The authors conceded, however, that chromosome movement during anaphase might have stretched the connections, which appeared to consist of chromosomal fibers of the usual dimensions (see also Brinkley and Shaw 1970).

Anaphase bridges exist as direct connections between two centromeres, or as interlocked dicentrics (Koller 1953). The thickness and length of these bridges vary; they usually break during ana- or telophase, but may persist into interphase (Hair 1953, Koller 1953). Cinemicrographic studies by Bajer (1963, 1964) on the behavior of dicentrics in Haemanthus endosperm revealed interesting facts: normally, dicentrics break abruptly, but in slightly unhealthy cells they do not break, but form long, thin, sticky bridges. Interlocked dicentrics show two kinds of behavior: they cut one through the other,

and the broken ends rejoin; or they uncoil and do not break at all. Whether or not a bridge breaks or is stretched depends on its length and the position of the kinetochores relative to the equator at metaphase. Breakage at anaphase is due to the pulling force of the chromosomal fibers; at telophase it is caused by the phragmoplast. Sister chromatid bridges tend to break at apparently weak points which are sometimes seen as constrictions. Movement after breakage is scarcely faster than the initial anaphase speed, indicating there is no accumulated tension in the pulling mechanism. Humphrey and Brinkley (1969; see also Brinkley and Shaw 1970) observed apparent gaps within anaphase bridges in rat kangaroo cells. These gaps were constrictions, presumably caused by anaphase tension, within which three classes of chromosomal fibrils could be seen.

Chromosome "stickiness"

When cells are irradiated in late prophase, "sticky" bridges can be observed at the following anaphase (Carlson 1954). Chemical clastogens, e.g., nitrogen mustard, also produce this effect (Koller 1953). Stickiness has been interpreted to be the consequence of surface changes on the chromosomes, changes that make chromosomes adhere to each other if they happen to come in contact (Carlson 1954, Casarett 1968). Apparently, this aberration is reversible: if mitosis is delayed after treatment, stickiness does not occur. The nature of the sticky material remains obscure. Hsu et al. (1965) noted that in Chinese hamster cells nucleolar material sometimes remains attached to the ends of sister chromatids, forming apparent chromatin bridges at anaphase.

Streptonigrin: A Chemical Clastogen

Streptonigrin (SN) is a metabolite of Streptomyces flocculus. It has the formula $C_{24}H_{22}O_8N_4$, and the following structure (Rao et al. 1963):

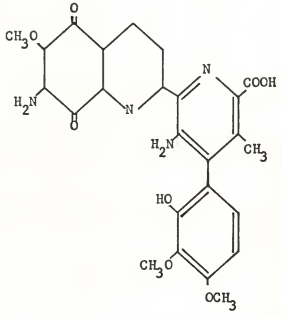

The drug behaves as a weak acid with quinoid properties. It induces phage release in lysogenic bacteria (Levine and Borthwick 1963) and initiates rapid breakdown of E. coli DNA in vivo (Radding 1963). Inhibition by SN of DNA synthesis and of DNA-dependent RNA synthesis was reported by Koschel et al. (1966) for a cell-free system, and by Young and Hodas (1965) for tissue culture cells. Streptonigrin caused single strand breaks in calf thymus DNA (Mizuno and Gilboe 1970). The latter authors also found that SN preferentially binds to DNA during the S phase.

Cohen et al. (1963) investigated the effect of SN on cultured human leukocytes. The mitodepressive effect of SN appeared related to concentration and length of exposure. The mitotic rate was significantly depressed in cells exposed for 36 hr to 0.01 and 0.1 μg/ml SN, but not in cultures treated with 0.001 μg/ml SN. The chromosome-

breaking effects of SN were of the delayed and non-delayed type. Aberrations occurred in cells treated as late as 2 hr before fixation. Among the aberrations observed were chromatid and isochromatid breaks, acentric fragments, dicentric chromosomes, cleavage or severe attenuation of the centromere region, telomeric fusion of sister chromatids, "stickiness," uncoiling of chromosomes, and severe fragmentation or degeneration of the entire chromatin material. Chromosomal damage appeared to be non-randomly distributed, chromosomes 19, 20, 21, 22, and the Y being relatively stable. Cohen (1963) further studied the non-randomness of aberrations produced by SN in chromosomes 1, 2, and 3 of cultured human leukocytes. While X-rays induced random breaks, SN preferentially affected the pericentric regions of chromosomes 1 and 2, as well as the area of the secondary constriction of chromosome 1. Breaks in chromosome 3, although fewer in number, were distributed at random. The telomere regions of all three chromosomes, and the short arm of chromosome 2 appeared relatively resistant to SN.

Kihlman (1966) concluded from the work by Cohen et al. (1963) that SN is able to break chromosomes during G_2. A similar finding had been reported for root tip cells of Vicia faba (Kihlman 1964). Exposure of cells to 2-5 µg/ml SN for 1 hr produced subchromatid (cells in early prophase), chromatid (cells in G_2 and S), and, possibly, chromosome exchanges (cells in G_1). However, Puck (1964) reported that SN does not affect mammalian cells after completion of DNA synthesis. In this respect SN may be similar to 8-ethoxycaffeine (EOC) and other drugs which have non-delayed effects in plant cells, and delayed effects, or hardly any effects at all, in mammalian tissue culture cells (see Kihlman 1966).

Jagiello (1967) described chromosomal aberrations induced by SN in mouse eggs. In vitro, metaphase I chromosomes of ova treated with 1.0 μg/ml SN were agglutinated beyond recognition; 0.1 μg/ml SN induced achromatic gaps and breaks in approximately 40% of the ova. Severe chromosome damage also occurred in ova of mice, to which SN had been administered subcutaneously.

Streptonigrin is still used in in vitro and clinical studies on tumor chemotherapy (Carter et al. 1968, Oleson et al. 1961). Like many other antitumor drugs it is more active against lymphoma than against solid tumors.

Colcemid: A Spindle Poison

Colchicine is an alkaloid isolated from Colchicum autumnale, whose anti-mitotic effect has been under investigation for over 30 years (see reviews by Biesele 1958, Deysson 1968, Dustin 1963, Eigsti and Dustin 1955, Gelfant 1963, Kihlman 1966). The structural formulas of colchicine (from Kihlman 1966) and its synthetic analog colcemid (demecolcine, N-deacetyl-N-methylcolchicine; from Schär et al. 1954) are given below.

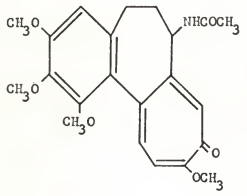

Colchicine

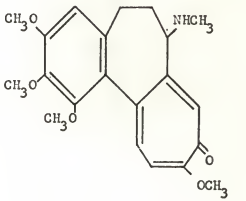

Colcemid

The effect of colcemid on plant and animal cells is essentially the same as that of colchicine (see Gelfant 1963), but the former is less toxic and more efficient in animal tissue (Schär et al. 1954).

Levan (1938) coined the term "c-mitosis" for the peculiar morphological changes in dividing Allium cells under the influence of colchicine. Chromosomes in c-mitosis are scattered in the cytoplasm, sister chromatids being held together in the centromere region. At "c-anaphase," sister chromatids fall apart and at "c-telophase," because of the absence of a mitotic spindle, all the chromosomes are included in one polyploid restitution nucleus (see also the cinemicrographic analysis of c-mitosis in Haemanthus endosperm by Molè-Bajer 1958). In animal cells the division of the centromere region is delayed until "c-telophase," i.e., "c-anaphase" is omitted (Levan 1954).

Besides Levan's (1938) classical scattered metaphase, other chromosomal arrangements, such as "star-mitosis" and "clumped" or "ball" metaphase, can be observed in both animal and plant cells (e.g., Gaulden and Carlson 1951, Deysson 1968). The effect depends on the concentration and the time of exposure.

For many years it was commonly accepted that colchicine and its analogs arrest dividing cells at metaphase. Sentein (1961) objected to calling colchicine purely a metaphase poison, because he also found arrested prophases, anaphases, and telophases in his material. Brinkley et al. (1967) demonstrated that in Chinese hamster cells arrested in mitosis by treatment with 0.06 µg/ml colcemid the two pairs of centrioles are surrounded by the chromosomes in a configuration different from a typical metaphase. After reversal of the inhibition,

centriole pairs move to opposite poles and a normal metaphase plate is established prior to anaphase segregation. Furthermore, at the concentration used some MT were still present, notably on the kinetochores facing the centrioles (see also Brinkley and Stubblefield 1966). Jokelainen (1968) furnished more evidence that the precise mitotic stage at which cells are arrested may depend on the concentration applied. He found no typical metaphases in fetal rat kidney tissue after treatment of pregnant rats with 0.12 mg/kg colchicine, but metaphases were present in fetuses of rats treated with 0.08 mg/kg.

The conclusion, drawn from birefringence studies (Inoué 1952) and the behavior of chromosomes in colchicine-treated cells (Levan 1938, Molè-Bajer 1958), that this chemical disorganizes spindle MT, has received support from biochemical studies by Borisy and Taylor (1967a, b). They found that colchicine binds to a 6S protein from isolated mitotic apparatus. This protein showed good correlation with the occurrence of MT and was considered to be a subunit of MT.

Statement of Purpose

The objective of this investigation was threefold: (1) To fill gaps in our knowledge of the structural changes accompanying the build-up of the chromatic and achromatic apparatus during normal mitosis in animal cells. Particular attention was devoted to controversial or less well-studied aspects of mitosis, such as kinetochores and the nuclear envelope. (2) To study possible structural alterations in the mitotic apparatus produced by the agents applied or by the presence of aberrant chromosomes (e.g., dicentrics). (3) To elucidate the fine structure of aberrant chromosomes, with particular reference to kinetochores and chromosome architecture.

MATERIALS AND METHODS

Cell Culture

The PtK_2 cell line was initiated in 1961 by Kirsten H. Walen (Walen and Brown 1962) from a kidney of an adult male rat kangaroo, Potorous tridactylis (Marsupialia). The male karyotype consists of ten autosomes, one X chromosome bearing the nucleolus organizer, and two Y chromosomes (Figure 1. Shaw and Krooth 1964, Walen and Brown 1962).

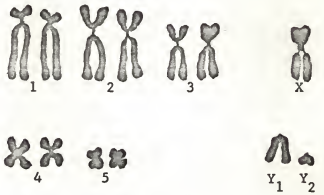

Fig. 1. Karyotype of the male rat kangaroo (Potorous tridactylis). Note the heterochromatic region near the centromere on the X chromosome (nucleolus organizer). Drawn after a micrograph by Shaw and Krooth (1964).

The PtK_2 line, however, is aneuploid, the number of chromosomes in the reference stock varying from 11 to 14 (Anonymous 1967). An extra, long subtelocentric chromosome is present in the majority of cells.

According to Walen (1965) the generation time in Eagle's medium with 4% fetal calf serum (FCS) is 28-32 hr. The low number and the individuality of chromosomes make this line particularly suitable for cytogenetic and labeling studies.

I obtained an ampule of frozen cells from the American Type Culture Collection and started a culture in April, 1970. After preliminary experiments this culture was given up in September, 1970, because of a suspected contamination by a microorganism (mycoplasma or fungus). A new culture with fresh cells was initiated in October, 1970. Only cells from this culture were used in the experiments described.

Cells of the stock culture were grown in square glass bottles in Eagle's minimum essential medium (MEM; GIBCO), supplemented with 10% FCS (GIBCO). Cells were harvested with trypsin-versene at weekly intervals and subcultured at appropriate dilutions. Fresh complete medium (MEM with 10% FCS) was supplied once between transfers. Cells to be used for experiments and controls were seeded in Falcon 30-ml flasks and left to attach overnight. Cultures were maintained at 37°C, but handling was carried out at room temperature.

Chemical and Physical Treatments

Streptonigrin

Streptonigrin (Pfizer and Co., Inc.) was obtained from Cancer Chemotherapy, NCI, NIH, Bethesda, Md. A stock solution of 250 µg/ml was prepared shortly before use by dissolving the powder in the diluent supplied. The stock solution was diluted volumetrically in distilled water, pH 8.0, to a concentration of 0.25 µg/ml. After sterilization with a millipore filter, the final concentrations of 0.05 µg/ml and

0.01 µg/ml were prepared under sterile conditions by dilution with MEM. No serum was added to avoid possible binding of SN by serum proteins.

Cell monolayers in Falcon 30-ml flasks were rinsed once with MEM before the drug was added. Control cells were treated in the same manner, except that they were exposed to MEM alone instead of the drug. The cells were incubated for 4 hr at 37°C. The flasks were then rinsed twice with complete medium and the cells were left to recover in the incubator in a third change of fresh complete medium. Approximately 24 hr later the medium was changed once more. After a total recovery period of 48 hr the cells were fixed in situ according to the standard schedule (see below).

Colcemid

A stock solution of 0.5 µg/ml was prepared by dissolving crystalline colcemid (CIBA) in distilled water, pH 6.4. This solution was sterilized with a millipore filter and further dilutions were prepared with sterile complete medium. Treatment A was 0.05 µg/ml colcemid for 2 hr at 37°C, followed by two rinses with complete medium and recovery for 1 hr at 37°C in a third change of medium. Treatment B was 0.25 µg/ml colcemid for 15 min at 37°C without a recovery period. Control cells were left undisturbed and were fixed at the same time as treated cells.

Cold

Flasks were seeded as usual and the cells left to attach overnight at 37°C. The medium in the experimental flask was then poured off and replaced by complete medium of 0-4°C. The flask was immediately placed in a pan with ice water so that its lower portion was immersed. After

1 hr exposure the medium was replaced by cold glutaraldehyde of the usual strength and buffered as usual (see fixation schedule). Initial fixation was 15 min in the cold, after which the flask was brought to room temperature and the standard fixation schedule was followed from here. One control consisted of cells kept at 37°C and fixed cold as above. The second control consisted of cells not exposed to cold and fixed at room temperature.

Fixation and Embedding

The standard fixation schedule, modified from Brinkley et al. (1967), was as follows:

(1) Decant the culture medium and add 3.1% glutaraldehyde (GA) buffered with Millonig's phosphate buffer without sucrose (Millonig 1961), pH 7.3. After a few minutes add a fresh change of GA. The cells are fixed for a total of 1 hr at room temperature.

(2) Rinse with two changes of buffer, 10 min each, at room temperature.

(3) Postfix for 1 hr at room temperature in similarly buffered 2% osmium tetroxide (OsO_4).

(4) Dehydrate in 25% and 50% ethanol, 10 min each. Prestain in cold 2% uranyl acetate in 70% ethanol for 2 hr to overnight. Rinse with two changes of cold 75% ethanol, 10 min each. Ten min 90% ethanol; the cold solution is added and the flasks then brought to room temperature. Subsequent steps are all carried out at room temperature; three changes, 10 min each, of 90% hydroxypropyl methacrylate (HPMA); 15 min each of 95% and 97% HPMA.

Enbed in Luft's Epon (Luft 1961) as follows. A ratio of 1 part of mixture A to 2 parts of mixture B gave the best results.

2 parts HPMA : 1 part Epon for 15 min

Equal parts of HPMA and Epon for 15 min

1 part HPMA : 2 parts Epon for 30 min

2 changes of pure Epon, 30 min each

Add fresh pure Epon and burn holes in the top of the culture flasks with a hot glass rod. Drain off excess Epon until a layer about the thickness of a glass slide is left. Leave overnight at room temperature then transfer to 60°C for 24 hr or longer.

Preparation of Cells for Light and Electron Microscopy

The basic procedure was adopted from Brinkley et al. (1967). After curing, the bottom of the flask with the adhering Epon wafer is cut out. Wafer and flask bottom are separated by alternately cooling the sandwich in liquid N_2 and thawing in tap water. Once separation has started at the edge, the Epon wafer can be snapped loose.

For light microscopy (scoring of aberrations, determination of mitotic indices) wafers are placed cell layer up on the stage of a phase contrast microscope. Detailed examination of cells is possible by using oil immersion objectives.

The area around cells selected for thin sectioning is marked with a sharp needle under low power. Several high magnification pictures at different levels of focus are then taken. A disk with the marked area is cut out with a cork borer of suitable diameter. The piece of Epon is roughly trimmed and glued to the tapered end of a plastic peg, cell layer up. Fine trimming to the boundaries of the trapezoidal or

rectangular area containing the cell or cells is done after curing of the resin glue.

As a rule, blocks were sectioned in a plane parallel to the cell monolayer (horizontal plane; see Figure 2). For special sections (para-sagittal = vertical; para-equatorial = orthogonal to the spindle axis; see Figure 2) blocks were mounted differently. A scratch was made on the surface of the Epon wafer, under low power, either parallel to the spindle axis or at a right angle to it and as close to the selected cell as possible. A disk with the marked cell was cut out, roughly trimmed, and mounted in the clamp chuck of an ultramicrotome. By cutting thick sections with a glass knife the block could be faced to the level of the scratch or even closer to the cell, when periodical checking under a microscope was possible. If necessary, the angle of the face relative to the spindle axis could still be corrected. Finally, the block was mounted on a peg with the face up.

Serial sections were cut with a diamond knife on a Porter-Blum MT-2 microtome and picked up on formvar-coated, carbon-stabilized rectangular hole grids (LKB Instruments, Inc.). Sections were poststained with uranyl acetate (Watson 1958) and lead citrate (Reynolds 1963) and examined in a Hitachi HU 11-E electron microscope with a 50-nm objective aperture and operated at 75 kV.

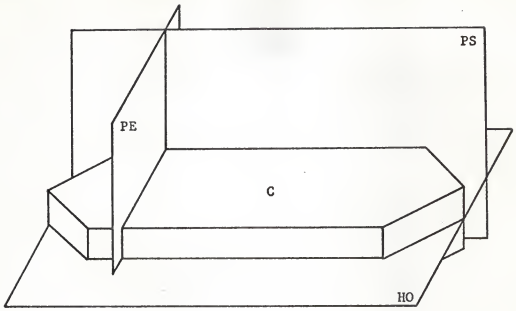

Fig. 2. The three planes in which blocks were sectioned. C: Cell in mitosis; the spindle axis is assumed to be along a line between the two pointed ends. HO: Horizontal plane. PE: Para-equatorial plane. PS: Para-sagittal plane.

RESULTS AND OBSERVATIONS

Normal Mitosis

This section is based on light and electron microscopic observations on untreated cells, either used as controls for the various treatments, or fixed directly from the stock culture.

Interphase

Although interphase is not a mitotic stage, it makes sense to describe the structure and spatial orientation in the interphase cell of those components and organelles that take part in the formation and function of the mitotic apparatus.

Figure 3 shows a grazing section of an interphase nucleus. Pore-annulus complexes of the nuclear envelope are cut at different levels. They appear as circles at the level of the envelope, and as circles surrounded by a "halo" at the level of the underlying chromatin. Central dense granules can be seen in some of the profiles. Where the section passes below the complexes, their position is indicated by achromatic holes in the chromatin. Whorls of polyribosomes are visible on oblique sections of the nuclear envelope. In the cytoplasm, two centrioles are present, approximately at a right angle to each other. Obliquely sectioned membrane elements, probably of a Golgi complex, can be seen in their vicinity. Microtubules, though more numerous around the centrioles, pass in various directions, without apparent specific orientation to the latter. Details of centriolar structure at different levels are shown in the four serial sections in Figure 4.

Osmiophilic, granular or fibrillar material surrounds the centriole at one end (Figure 4a). The short rays radiating from the triplets (Figure 4b) give the whole structure the appearance of a pinwheel. Such images are rare. Dense, spherical particles with a lighter core and aura (Figure 4c), often quite numerous, are exclusively associated with centrioles and are present during all the stages of the cell cycle. An intracentriolar vesicle, shown in an approximately median section in Figure 4d, is often found in the lumen of centrioles. Satellites and microtubules can be seen in all four sections (Figures 4a-d).

The appearance of the interphase nucleus in transverse sections varies. Three representative nuclei are shown in Figure 5. The chromatin is either dispersed (Figure 5a), or it includes heterochromatic chromocenters to a variable extent (Figures 5b and 5c). Nuclei like the one in Figure 5c are very likely in late cytokinesis or very early prophase. Of 34 interphase nuclei examined, 12 had dispersed chromatin, the remainder contained chromocenters of variable size and extent. At higher magnification, chromatin fibers, approximately 130 A and 250 A in diameter, can be seen cut at various angles (Figure 6). A very dense core, 70-80 A in diameter, appears in a few cross sections of 250 A fibers. Nucleoli are large and prominent in interphase cells (Figure 5). Granular and fibrillar components are mixed (Figure 7). Nucleolus-associated chromatin is found within the nucleolus and at its periphery (Figures 5 and 7). Intranuclear vesicles occur in some nuclei (Figure 5a). The wall of these vesicles is finely fibrillar and they often, perhaps always, contain granules or particles 250-400 A in diameter. However, densely packed granules of similar size and appearance also occur free in the karyoplasm.

Prophase

The centrioles duplicate at the onset of prophase. Therefore, two parent-daughter centriole pairs are found in early prophase cells (Figure 8a). Four serial sections of the same centrioles (Figures 8b-e) reveal that each daughter centriole is closely associated with its parent at approximately a right angle. Daughter centrioles appear shorter than mature centrioles (compare Figure 8b with Figure 3), but have the same diameter (approximately 2,200 A). At this stage relatively few MT converge on, or radiate from, each parent centriole. An early stage of centriole migration is illustrated in Figures 9a and 9b. One of the two centrioles shown (C_1) is possibly a daughter centriole. It is cut almost perfectly at a right angle to its axis. The structure and arrangement of the tubular triplets is particularly clear (Figures 9c-e). The cartwheel at the proximal end appears in three adjacent sections (Figures 9b-d), but hub and spokes are most distinct in Figure 9c. The triplets seem to be embedded in amorphous osmiophilic material. Bars, approximately 80 by 480 A, possibly cross sections of plates, appear between the triplets (Figure 9e). Numerous satellites are present in the general area of the two centriole pairs (Figures 9a and 9b). In many, perhaps all, mid-prophase cells the centrioles lie in an invagination or pocket of the nuclear envelope (e.g., Figure 11a). At this stage numerous MT are present, forming an "aster" around the centrioles. The radial arrangement of these MT also imposes radial orientation on other organelles, notably mitochondria (Figure 11b). Migration of centrioles relative to nuclear changes (chromosome condensation, fragmentation of the NE) varies considerably, so that by

the end of prophase the two pairs may have moved a short distance only, or they may lie at opposite poles (see Figures 18a and 19).

Progressive condensation of chromatin is indicated by the appearance, during very early prophase, of large heterochromatic patches (compare Figure 8a with Figure 5). Discrete chromosomes are present in mid-prophase cells (Figures 10 and 11a). Their "mottled" appearance (see also Figure 13) is suggestive of incomplete condensation. During condensation many, possibly all the chromosomes are attached to the nuclear envelope along their entire length or with their telomeres (Figures 11a and 13). In transverse sections of nuclei in early prophase the chromosomes appear to be attached by "stalks" (Figure 13), but grazing sections reveal that this appearance is due to achromatic "holes," enlarged compared to interphase (compare Figure 12 with Figure 3). In late prophase, however, strand-like connections between chromosomes and the nuclear envelope are real (Figure 14).

No kinetochores are discernible in early prophase (Figure 8a). In sections of nuclei in mid- and late prophase kinetochores appear as roughly circular patches of finely fibrillar material in slight constrictions of chromosomes (Figures 11a, 15, and 17). Serial sections revealed that these kinetochores are globular and 5,000-8,000 A in diameter. I cannot state with certainty that the diameter decreases with advancing prophase. The doubleness of the chromosomes is evident in sections showing both sister kinetochores (Figures 15 and 17). The lesser electron density of the kinetochores compared to the chromosomes is very distinct (Figures 10, 11a, 15-17). Slightly more opaque kinetochore granules at the surface of the sister chromatids (Figure 17) are very rarely seen.

The nucleolus, still intact in very early prophase (Figure 8a), fragments into several masses of granular material (Figures 10 and 11a), some of which are apparently associated with chromosomes (Figure 11a).

The nuclear envelope remains intact until the end of prophase, but the pore-annulus complexes become more fuzzy (Figure 12). Polyribosomes are found on the nuclear envelope throughout prophase (e.g., Figure 11a).

Prometaphase

The breakdown of the nuclear envelope, indicating the transition from prophase to prometaphase, is gradual, but structural changes involving MT and kinetochores are more striking. Fragmentation of the nuclear envelope always begins nearest the centrioles (Figures 18a and 19). Fragments are undulated or form vesicles. The telomeres of chromosomes at the periphery of the "nucleus" are often trapped in compartments formed by undulated, still intact portions of the nuclear envelope (Figure 18b). With progressive development of the spindle apparatus, envelope fragments become smaller and scarcer, but some persist at the periphery of the spindle until late prometaphase (Figures 20, 26, and 29). Disappearing central granules indicate early stages of the breakdown of pore-annulus complexes (Figures 21a and 21b). The entire complexes on fragments of the nuclear envelope become fuzzy and disappear by mid-prometaphase (Figure 21). Polyribosomes can be found on clearly identifiable fragments until late prometaphase (Figures 21, 26, and 29).

Chromosome condensation continues throughout prometaphase (Figures 18-20, 26-30). The chromosomes detach from the nuclear envelope as the

latter fragments, and they gradually lose their "mottled" appearance. Most kinetochores in very early prometaphase still resemble prophase kinetochores (Figure 22a), but some are differentiating into more complex structures. For example, the sister kinetochores of the chromosome in Figure 22b, although apparently not attached to MT, exhibit a slightly denser band within the fibrillar matrix. Such internal structures may be more common than it appears, but due to their relative indistinctness they would not appear in ever so slightly oblique sections. A rather unusual case is illustrated in Figures 22c and 22d. This chromosome of the cell shown in Figure 18 was situated in the area distant from the centrioles, i.e., near the intact portion of the nuclear envelope. Several obliquely sectioned MT lie outside the envelope opposite the "outer" kinetochore, which also contains a short band. Serial sections revealed no MT inside the nuclear envelope. The other sister kinetochore, facing in the direction of the distant centrioles, resembles a typical prophase kinetochore.

As prometaphase progresses, kinetochores become more variable in appearance. Structural differentiation depends in each individual case upon the position and orientation of the chromosome relative to the spindle poles. Sister kinetochores of chromosomes near a pole are dissimilar (Figures 23 and 24). As a rule, the kinetochore facing the near pole is attached to MT and consists of moderately opaque, finely fibrillar material (K, K_2, in Figure 20; K_2 in Figures 23 and 24). A banding pattern is discernible in some of these kinetochores (Figures 23a and 23b), which are quite often also stretched (K, K_2, in Figure 23a; K_2 in Figures 24b and 24c). This makes it impossible to determine where the MT end. In contrast, the kinetochore facing the distant pole

resembles typical prophase kinetochores (e.g., K_1 in Figure 24), or it consists of a dense band embedded in the fibrillar matrix (K_1 in Figures 23a and 23c). The band can be seen in several adjacent sections, which suggests it represents a transverse section of a flat or convex plate approximately 300 A thick and 3,500 A in diameter. In each case few or no MT are associated with such a kinetochore.

Sister kinetochores of chromosomes lying near the future equator of the spindle are similar if both are unobstructed, i.e., if there is no nearby obstacle (such as another chromosome) between them and the respective pole (Figure 25). Usually, these kinetochores are more or less stretched, with or without bands, and attached to MT. If one of the sister kinetochores is obstructed by a neighbor chromosome lying very close, it resembles prophase kinetochores (not shown, but similar to K_1 in Figure 24a), while the other kinetochore resembles the unobstructed kinetochores described above.

Microtubules are found in the "nucleus" as soon as the nuclear envelope breaks down (Figures 18, 22, and 23). At first they are more numerous in the vicinity of the centrioles (Figure 18), but as the latter take up their position at opposite poles, MT are abundant in the center of the spindle (Figure 20). Surprisingly, most of the MT are associated with kinetochores and few, if any, continuous tubules seem to be present. However, a more careful, quantitative analysis would be necessary to establish this with certainty.

Remnants of the nucleolus disappear completely and the nucleolar organizer appears on the X chromosome (Figures 19 and 25).

Figures 26-30 illustrate further progression of prometaphase. Fragments of the nuclear envelope, still found between and around some

chromosomes during mid-prometaphase (Figure 26), become smaller and move to the periphery of the spindle in late prometaphase (Figures 29 and 30a). Nuclear pore complexes have disappeared approximately at the stage shown in Figure 26, but some polyribosomes are still present on the fragments of the nuclear envelope. Peripheral segments of double membrane in late prometaphase cells have ribosomes on both faces, thus resembling rough ER (Figure 29).

As the spindle develops, mitochondria, ER, and other large cellular organelles and components are excluded from its area (compare Figure 20 with Figure 29), but ribosomes, mostly monosomes, are abundant. Bundles of MT in the center of the spindle run more or less straight along the pole-to-pole axis, while peripheral bundles are slightly arched (Figures 26 and 29). An exceptional case is shown in Figure 32, where rather disoriented MT curve sharply towards the centriole. Angular configurations of kinetochore MT, as shown in Figure 20, no longer occur. Still, most of the bundles of MT are associated with kinetochores (Figures 26-29, and 30a). It is very difficult to determine whether the MT of other bundles (e.g., Figure 28) are interpolar, or whether they are associated with kinetochores not visible in the same section. Quite frequently, a bundle of MT passes near the kinetochores of a maloriented chromosome (e.g., Figure 39). Transchromosomal MT are outstanding in rather thick sections (Figure 30b). Skew MT, as well as "wavy" MT, occur quite frequently, but they always make up a small proportion of the total number of spindle MT (Figures 27, 28, 30a, and 33).

Orientation of the centrioles relative to the axis of the fully formed spindle is variable (Figure 29). This has also been confirmed in cells in meta- and anaphase.

The chromosomes condense further until they appear as solid, very electron dense rods or blocks (compare Figure 26 with Figure 29). Sister chromatids are still tightly joined, but their individuality is apparent in transverse or peripheral longitudinal sections of chromosomes (Figures 27, 29, 30a, 31, and 33), or in situations where the sister kinetochores are stretched (Figure 34). In the latter case, one or several achromatic holes appear in the kinetochore region.

The diversity of kinetochore structure is still remarkable during mid- and late prometaphase (Figures 26-29, 30a, 31, 33-41). At a glance there seems to be no general pattern of differentiation, but a careful comparison of the structure of sister kinetochores with the position of the chromosomes in the spindle gives a better insight. First, we can distinguish between chromosomes lying on or near the equator of the spindle (Ch_1 and Ch_2 in Figure 27; Ch_3 in Figure 28; the chromosomes in Figures 30a and 33-36), and chromosomes lying closer to one pole (malpositioned chromosomes; Figure 26; Ch_3 in Figure 27; Ch_1 in Figure 28; Figures 29 and 37-40). Generally speaking, more chromosomes occupy an equatorial position in late than in early prometaphase (Figures 20, 26, and 29). The sister kinetochores of equatorial chromosomes are similar if both are unobstructed, i.e., if no major obstacle lies along a line from the kinetochore to the pole (Figures 27, 30a, 33, 34, and 36); they are dissimilar if one is unobstructed, the other obstructed by a neighbor chromosome (Figures 33 and 35). Unobstructed kinetochores are irregularly shaped and fuzzy (Figures 28 and 36), fuzzy cones with a trace of bands (similar to K_1 in Figure 38), or distinctly triple-banded (Figures 27 and 33-35). It appears that the clarity of the three bands increases with advancing prometaphase. Unobstructed

kinetochores are quite often stretched (Figures 27, 28, 31, 33, and 36), and they are always attached to bundles of MT.

Obstructed kinetochores of equatorial chromosomes appear as patches of finely fibrillar matrix within which a denser band or patch can be seen (Figures 33, 35, and 41). Serial sections make it clear that the bands do not represent fibers, but sections of oddly shaped three-dimensional structures (e.g., Figures 35 and 41). The width of the bands varies from 250-400 A. In appearance and dimensions they are comparable to the outer layer of triple-banded kinetochores, except that they often exhibit a partly double-banded, partly beaded substructure (Figure 41). Furthermore, obstructed kinetochores are always attached to very few, if any, MT.

Sister kinetochores of maloriented chromosomes most commonly are also dissimilar. As a rule, the kinetochore facing the near pole resembles the unobstructed kinetochores of equatorial chromosomes (Figures 27, 37, and 38), while the kinetochore facing the far pole resembles obstructed kinetochores (Figures 27, 37, and 38). Figure 40 illustrates a rare exception to this rule. On both these maloriented chromosomes the kinetochore oriented towards the near pole is compact, and attached to MT, while the other kinetochore is fuzzy and stretched, but also attached to MT.

Figure 39 illustrates another rare case. The sister kinetochores of this maloriented chromosome are very similar in every respect; both are relatively undifferentiated masses of matrix with only a trace of a band. Most remarkable is that the matrix seems to cover almost the entire small side of the chromosome (Figure 39c).

The difference in electron density between the kinetochore matrix and its band on one hand, and the chromosome proper on the other hand, is obvious in many of the figures cited, but particularly in grazing sections of kinetochores (e.g., Figures 33b, 35c, and 36). Interesting, but very rarely seen, are chromatin "strands" between stretched sister kinetochores (Figures 31 and 36). It is difficult to determine, even at high magnification, if the fibers in these strands are finer than normal chromosomal fibers, or if they are more densely packed, and arranged more or less in parallel.

Metaphase

Cells in full metaphase are quite rare, probably because this stage is of very short duration. Most cells judged to be in metaphase, based on light microscopy, turn out, upon examination of thin sections, to be either in very late prometaphase or very early anaphase.

Chromosomes at metaphase are aligned on the equator of the spindle, at least with their kinetochore region (Figure 42). Typically, the non-aligned telomeric portions of the long chromosomes extend beyond the periphery of the spindle into the cytoplasm (insets of Figures 42-44). All the kinetochores in normal metaphase cells are triple-banded (Figures 42 and 43). Bundles of kinetochore MT converge towards the poles (Figure 42). Within a bundle the MT are more or less parallel, but a few non-kinetochore MT slant across. Wavy MT occur mainly between chromosomes. Overall, the paucity of non-kinetochore MT is remarkable.

Figure 43 represents a para-sagittal section. The plane of sectioning was not precisely at a right angle to the chromosomes,

therefore only one of the two sister kinetochores can be seen. Kinetochore profiles are virtually identical with those seen in horizontal sections (compare Figure 43 with Figure 42). Sister chromatids are separated by grooves relatively devoid of ribosomes and ground substance. However, the separation, which actually indicates late metaphase to very early anaphase (see also inset of Figure 43), is incomplete, for large "bridges" still connect the sister chromatids.

In para-equatorial sections the metaphase plate appears as shown in Figure 44. Three kinetochores with associated MT can be seen. Other MT occur singly or in small clusters, or they are arranged in bundles which may belong to kinetochores not included in this section. Microtubules penetrating chromosomes are surrounded by a clear halo.

Anaphase

Sister chromatids, now more properly called daughter chromosomes, separate from each other at the onset of anaphase. In the light microscope they still appear as parallel rods (Figure 45, inset). Because the chromosomes are somewhat frayed, their separation at very early anaphase (Figure 45) is less distinct in thin sections, except for the kinetochore region. The latter is spaced farther apart than the telomere region (Figures 45 and 46), and this trailing of the telomeres is more pronounced during later anaphase (Figure 47; inset of Figure 50; Figure 51a). The daughter chromosomes lose their individuality during late anaphase and each set forms a large mass of densely packed chromatin near the respective pole (Figure 52). The nucleolus organizer (NO) is enclosed in this mass.

A striking phenomenon is illustrated in Figures 46-48. Daughter chromosomes in very early and early anaphase are connected by electron dense strands. First believed to be an aberration, it was found in six of seven early anaphase cells. The chromosomes of the seventh cell had short strands of similar appearance extending from the rather widely separated kinetochore regions into the interzone. The same was observed in one mid-anaphase cell. In the latter two cases the strands were extremely tapered towards the interzone, giving the impression of connections gradually drawn out and finally ruptured. In the majority of early anaphase cells the strands connect the kinetochore regions of daughter chromosomes. I have counted as many as six strands in serial sections. However, in the cell shown in Figure 47, and also another very similar anaphase, a few strands connected the mid-region of daughter chromosomes.

The diameter of these strands varies from approximately 400 A to 900 A. Short strands are usually thicker, and long strands very frequently are thinnest approximately midway between daughter chromosomes, while they are thicker at their base (i.e., point of attachment; Figures 46 and 47). The staining properties of the strands are identical with those of chromosomes, and the structure is that of fine and/or densely packed fibers.

Kinetochores vary in appearance from more or less straight to convex, "stalked," or angular (Figures 46-49). The three layers are very distinct except in sections that cut a kinetochore obliquely or peripherally (Figures 46 and 47). In para-equatorial sections the kinetochores appear as circles of moderate electron density, within which cross sections of MT can be seen (Figure 50). In late anaphase

the triple-layered character of the kinetochores is less clear, but still recognizable (Figures 51b and 52). Most kinetochores in very late anaphase cells appear in depressions on the poleward face of the chromatin mass (Figure 53). The less dense band in Figure 53 is approximately 500 A wide and set off from the chromatin by a 250 A wide clear band. The chromatin immediately underlying the kinetochore is denser and less obviously fibrillar than the remainder of the chromosomal mass. Remarkable is the decreasing number and degree of organization of kinetochore MT in late anaphase (compare Figures 46-49 with Figures 51-53).

Spindle elongation is the rule in PtK_2 cells (Figure 51a). The interzone is still free of cytoplasmic organelles even after the chromosomes have almost reached the poles. Pieces of double membrane, some with ribosomes, are found at the periphery of the spindle area, particularly around the two sets of chromosomes (Figure 51a). Interzonal MT are scarce. Mitochondria, vesicles, and ER invade the interzone in very late anaphase (Figures 52 and 55b). The cytoplasm begins to constrict in the equatorial region (Figure 52, inset), where stem bodies appear. The latter consist of amorphous, osmiophilic material, within which MT are closely packed (Figures 54 and 55a). It is difficult to determine from these sections whether the MT terminate in the stem bodies or beyond. Both possibilities are likely. One MT in Figure 55a clearly passes through the stem body. Its total length visible in this section was 3 μ.

It is possible that pieces of double membrane as seen in Figure 51a become involved in the reconstitution of the nuclear envelope. More typically, however, small cisternae and vesicles appear on the

surface of the chromatin masses in late anaphase (Figure 52). Oblique sections of such membranes reveal the presence of nuclear pore complexes. Some of the cisternae obviously are, or have originated from, RER as indicated by the presence of ribosomes (Figure 52). The location of the membrane pieces varies, depending on the level of the section. Usually, the majority of the membrane cisternae and vesicles is apposed to the lateral faces of the chromatin masses.

Figure 56 shows a pair of centrioles in early anaphase. As during prometa- and metaphase, the moderately osmiophilic, amorphous material surrounds that centriole on which the MT more or less converge. Direct connections between MT and any part of the centrioles are never observed.

Telophase and Cytokinesis

Reconstruction of the nuclear envelope continues during telophase, apparently by coalescence of the small vesicles and cisternae seen in anaphase cells. Extensively reformed NE first appears on the lateral faces of the chromatin mass, as well as on the polar face, except directly opposite the centrioles (Figures 57 and 58). Nuclear pore complexes, complete with central granules, are present on chromatin-associated membranes irrespective of size and location (e.g., Figure 58). The spacing between the two membranes of the NE remains irregular until late telophase (Figures 57-60). Quite frequently, pieces of NE are trapped within the reforming nucleus, probably giving rise to the deeply invaginated pockets seen in many interphase cells.

Figures 60 and 61 illustrate progressive decondensation of the chromatin. This process begins even before the NE is completely

restored, but large heterochromatic patches persist until interphase (late stages of cytokinesis).

The less dense component of kinetochores, still present during early telophase (Figure 57), has disappeared by the time the NE is completely reconstructed (Figures 59 and 60). The inner, dense layer becomes an extremely osmiophilic patch on the inner membrane of the NE (Figures 59 and 60). Most commonly, the entire NE is indented at these sites, and quite frequently the inner membrane with the dense patch is deeply invaginated (Figure 60). Microtubules can be seen extending poleward from these kinetochores, but the nature of this association cannot be determined precisely.

During cytokinesis a cleavage furrow in the former equatorial region separates the two daughter cells, except for a stem, whose length and diameter vary depending on the distance between daughter cells (Figures 61 and 62). The stem bodies seen in late anaphase and early telophase have fused to form the midbody, an irregular band of osmiophilic material in the stem. Numerous MT from both daughter cells converge in the midbody, but the dense material obscures details in these paraxial sections. Normally, the midbody remains between the daughter cells even after these have completely separated and moved far apart from each other. Eventually, it seems to be lost. On rare occasions the midbody is included in the peripheral cytoplasm of one of the daughter cells, but this is most likely an abnormal condition.

C-Mitosis

Treatment A (0.05 µg/ml colcemid for 2 hr 1 hr recovery) produces an accumulation of cells with "scattered" metaphases (Figures

63 and 64). C-mitotic cells are much less compressed along the axis vertical to the growth surface than normal mitotic cells. The extreme is illustrated by the near-spherical cell in Figure 63. Differences among c-mitotic cells are evident in the variable shape at the level of the light microscope (compare the insets of Figures 63 and 64). Ultrastructural variations relate to the distribution of membrane elements and mitochondria. For example, in the cell shown in Figure 63 membrane vesicles and cisternae, as well as mitochondria, are distributed throughout the area occupied by the chromosomes, although the former are more numerous at the periphery. In contrast, the area of the chromosomes in Figure 64 contains very few small vesicles. Numerous vesicles and larger cisternae, some of them rough ER, are arranged almost concentrically at the periphery of this area. Mitochondria are also excluded. In this respect the cell in Figure 64 resembles a prometaphase more than a metaphase, but the degree of condensation of the chromosomes does not bear this out.

The centrioles, embedded in amorphous or finely fibrillar material of moderate electron density, were always found at the periphery of the area occupied by the chromosomes in the few cells examined (Figures 63 and 64). Four centrioles are present in each cell. They do not differ structurally from centrioles in untreated cells.

Kinetochores appear as dense bands embedded in a less dense fibrillar matrix and following the curvature of the chromosomal surface, or as patches of less dense material (Figures 63, 64, 92-98). This depends on the angle and the level of the section. No MT at all were found in such cells. Treatment B (0.25 µg/ml colcemid for 15 min, no recovery) produces strikingly different effects. As with treatment

A, the usual criteria for determining mitotic stages do not apply. Nevertheless, light microscopic examination of cells subjected to treatment B revealed stages resembling pro- and prometaphase rather than metaphase. One cell was in late telophase or cytokinesis. The chromosomes, fairly distinct in the light micrographs (insets of Figures 65 and 66), were extremely difficult to see by direct observation.

Electron microscopy confirmed the above observations and revealed interesting details. The central area of the cells in Figures 65 and 66 consists of a coarsely granular or fibrillar ground substance in which the chromosomes are embedded. The separation of this area from the cytoplasm is almost perfect; with the exception of small membrane vesicles all the larger organelles are excluded. In the cell in Figure 65 large pieces of double membrane, probably fragments of the NE, are present at the border between central area and cytoplasm. Grazing sections revealed no pore-annulus complexes on these fragments, although colcemid does not destroy their integrity on the NE of interphase nuclei (Figure 68). Chromosomes are highly dispersed, making the recognition of sister chromatids difficult (Figure 65). The dark centromeric granules of chromosomes in the light micrograph are patches or balls of more tightly packed, perhaps also finer, chromosomal fibers. There seems to be one patch per sister chromatid, and, as revealed by serial sections, connections between chromatids exist in this region. Kinetochores in the usual sense are lacking, but a vesicular space relatively poor in fibers and filled with a less dense substance can be recognized adjacent to the dense patches.

The cell in Figure 66 differs from the above description by the absence of large membrane cisternae and the higher degree of chromosome condensation. It is remarkable, in this context, that the chromatin of all the interphase cells subjected to treatment B is completely dispersed (compare Figure 67 with Figure 5). The fibers in the primary constriction of the chromosomes in Figure 66 are also finer, or more tightly packed, or both. In this case, however, a distinct less dense kinetochore band is present in the vesicular space.

Despite the relatively high concentration of colcemid used in treatment B, a few MT were found in interphase cells (Figure 68), but not in c-mitotic cells. In some of the latter, numerous bundles of microfibrils, approximately 70 A in diameter, were present in the central area (Figure 69).

Mitosis in Cold-Treated Cells

Exposure to 0-4°C does not accumulate metaphase cells. Cells at all stages of mitosis are present in the unsynchronized cultures used. The general ultrastructural features of prophase correspond to control cells, except for the presence of intranuclear clusters of granules approximately the size of ribosomes (Figure 70). Kinetochores of cells in mid-prophase consist of less dense, fibrous material in constrictions of chromosomes (Figure 72). A mitotic spindle in the usual sense does not exist in prometa-, meta-, and anaphase cells, although centrioles are situated at opposite poles (Figures 71 and 75). Most of the few MT present are associated with kinetochores. An amorphous , moderately osmiophilic substance coats the microtubules, whose walls appear as stark lines (Figures 73 and

75). Fully differentiated kinetochores exhibit the familiar triple-banded profiles (Figure 75), though less distinctly than in normally fixed control cells. The fuzziness of kinetochores and MT is not caused by the initial cold fixation, because these structures are well preserved in similarly fixed cells not previously exposed to cold (Figure 74). The paucity of MT is also obvious in the midbody region of cells in cytokinesis (Figure 76). Centrioles are not structurally altered by exposure to cold (Figure 77).

Chromosomes are normally condensed, except for achromatic holes, which are prominent at all stages of mitosis (e.g., Figure 71). Remarkable is the great number and increased clarity of chromosomal granules in cold-treated compared to control cells (Figures 70-72, and 75).

Kinetochore Fine Structure

I have already described in detail the fine structure of kinetochores from prophase to late prometaphase. To establish a basis for the discussion of kinetochore models, this section is devoted to an in-depth study of kinetochores in normal meta- and early anaphase, colcemid- and cold-treated cells.

Figure 78 shows five of seven serial sections in the horizontal plane of a kinetochore in a cell in very early anaphase. Most of the sections were too thick (approximately 800 A) to reveal details concerning the attachment of MT. However, two things are very clear: the triple-banding, and the greater length of the kinetochore in the median sections (Figures 78b and 78c) compared to the peripheral sections (Figures 78a, 78d, and 78e). Thinner sections (500-600 A),

also approximately median, of other kinetochores are presented in Figures 81-84. These kinetochores were sectioned transversely, except those shown in Figure 83, where obliquely cut kinetochore MT indicate the sections were tangential. Kinetochore profiles very similar to those in horizontal sections can be seen in para-sagittal sections (Figure 85).

Kinetochores in metaphase cells are rarely flat. Most commonly, they are undulated or S-shaped (Figure 42), more seldom concave (Figure 85a). In very early anaphase the kinetochores of small chromosomes in the center of the spindle are more or less flat (Figures 46, 48, and 82), and at a slightly later stage the kinetochores of such chromosomes are convex (Figure 84). The kinetochores of the long chromosomes at the periphery of the spindle are convex or more irregular in early anaphase (Figures 47 and 49). In mid-anaphase, S-shaped and more exotic profiles of kinetochores are prevalent.

Triple-banded kinetochores in paraxial median sections are 4,000-6,700 A long. A faintly staining corona, approximately 400 A wide and consisting of fine fibrils embedded in an amorphous matrix, covers the kinetochores on the poleward side (Figures 78 and 84). The width of the three bands varies, both within and between kinetochores. Average values were 390 A for the outer, 270 A for the middle, and 400 A for the inner band. The outer band consistently stains less intensely than either the inner band or the chromosome proper (Figures 84 and 85a). This is very clear in the image seen on the screen of the electron microscope, but in micrographs printed on contrasty paper the difference is obscured (e.g., Figures 78, 82, and 83). Figure 80 shows a peripheral section of a stretched kinetochore in a late prometa- or

metaphase cell. This section was picked up on an uncoated 200-mesh grid. The difference in contrast between the chromosome and the kinetochore is undeniable.

The basic structure of the outer band is finely granular in highly condensed kinetochores (Figures 78, 81-84), but in grazing sections of less condensed kinetochores, 30-50 A fibrils are visible (Figure 80). Superimposed on the fine granularity of condensed kinetochores is a structure of coarse granules or fibers, giving the band a knotted appearance (Figures 78, 81-85). The structure and electron density of the middle band are very similar to the corona (Figures 78b and 84). The inner band is continuous with the chromosome (Figures 78b and 84), but in very early anaphase it may be connected to the main body of the chromosome by a "stalk" of chromatin, giving it the appearance of a mushroom (compare Figure 84 with Figure 46). The fibers of the inner band seem to be identical with the fibers of the chromosome. The greater opacity may be due to denser packing, but an interesting alternative is the presence of a very fine amorphous substance, which is lacking in the remainder of the chromosome.

Microtubules attach to the kinetochore at a variable angle. Three conditions must be fulfilled in paraxial sections to determine how far the MT penetrate into the kinetochore: (1) The section must be thin (500 A); (2) the MT in question must not be cut obliquely near the kinetochore; and (3) the section must be approximately median. These conditions are fulfilled in Figure 82. The MT marked with an arrow penetrates the outer layer and ends at the interface with the middle layer. The different impression created by an obliquely sectioned MT is demonstrated in the somewhat thicker section of Figure

81. The straight MT marked with an arrow terminates in the outer layer, while the obliquely sectioned MT marked with an arrowhead seems to penetrate into the inner layer. Skew MT passing in front of a kinetochore occur occasionally (Figure 79).

One metaphase cell was sectioned in a para-equatorial plane from one pole across the metaphase plate into the opposite half-spindle. Of the 24 kinetochores examined, all were apparently cut head-on (e.g., Figures 86 and 87), except one, which was sectioned at a slightly oblique angle. This kinetochore belonged to a chromosome at the periphery of the metaphase plate. To determine which of the MT of a chromosomal bundle were kinetochore MT, serial micrographs of eight different chromosomes and associated MT, at final magnifications between 40,000 and 62,500, were analyzed. In the last section of the series, MT in the vicinity of the chromosome were marked with one color. Proceeding poleward, newly emerging MT at the kinetochore were marked with a different color. The average number of kinetochore MT was 26, the range 16-40. This agrees well with estimates from paraxial serial sections. I was unable to ascertain if the number of kinetochore MT is correlated with chromosome size. The average number of MT bypassing the kinetochore was 5 (range 0-9). It is rather arbitrary to choose these bypassing MT from the population of non-kinetochore tubules, the only criterion being their proximity to the chromosome in question.

The kinetochores in para-equatorial sections are roughly circular patches of variable electron density, depending on the level of the section (Figures 86-88, and 91). The diameter varies from approximately 3,400 A for obviously convex kinetochores to 6,000 A for flatter kinetochores.

The kinetochore of Figure 86 was most likely similar to those in Figures 78, 81, and 82. The first section of the kinetochore itself shows a moderately opaque patch of finely fibrillar material (Figure 86d). I interpret this as the outer layer. Fewer MT are visible than in the preceding sections, indicating they terminate at this level. Remarkable are less opaque circles whose diameter is similar to the inner diameter of MT. They mark the terminals of kinetochore MT, the wall of which cannot be seen because its opacity is the same as that of the outer layer. A few MT can be followed one section farther (Figure 86e), because the kinetochore is not perfectly flat, but as the sections pass through the inner layer (Figure 86f) and through the chromosome (Figures 86g and 86h) all the kinetochore MT have disappeared. The middle layer is always obscured by the more opaque outer or inner layers, because the sections are thicker than the middle layer. Even a very thin section would have to pass just between inner and outer layers of a perfectly flat kinetochore in order to show middle layer only, a very unlikely event.

Figure 87 shows two adjacent sections of two more convex kinetochores. The moderately opaque patches in Figure 87b again represent part of the outer layer in which terminals of MT are visible. The kinetochore shown in Figure 88 was most likely similar to those in Figure 83. The section grazed the apex of the inner layer (large arrow) which seems embedded in the less opaque outer layer. The latter is clearly set off from the chromosome.

Occasionally, a single MT is found to penetrate the kinetochore and to extend deeply into the chromosome (Figure 89). Whether such MT pass completely through the chromosome is not clear.

I found no intertubular connections and arms on MT in sections passing close to the kinetochores. Figure 90 shows what presumably is a bundle of kinetochore MT at a greater distance from the chromosome. Two apparent cross-bridges and two arms can be seen.

Anaphase kinetochores in para-equatorial sections are very similar to metaphase kinetochores, except that most of them are more convex, i.e., MT at the periphery of the kinetochores terminate one or two sections after the apical MT have disappeared (Figure 91).

Kinetochore profiles in colcemid-treated cells are quite different from the triple-banded structures in untreated cells (Figures 92-98). Figure 92 represents an approximately median longitudinal section of two chromosomes. A longitudinal section along line C-D and perpendicular to that of Figure 92 would produce a face-on view of the kinetochore as in Figure 93. A transverse section along line A-B, also perpendicular to that of Figure 92, would produce an image as in Figure 94. The kinetochore bands in sections such as in Figures 92 and 94 are approximately 400 A wide, are embedded in a less opaque, fibrillar matrix, and closely follow the surface of the chromosome. The bands are slightly less electron dense than the chromosomes (Figure 92), but again this characteristic is obscured in contrasty prints (Figures 94, 97, and 98). I consider these bands equivalent to the outer layer of kinetochores in untreated cells. There is no inner layer on any of the chromosomes in colcemid-treated cells, and the kinetochores are never attached to MT. The outer layer is apparently made of two 150 A sheets held together at various points. This accounts for the transverse and longitudinal sections showing two

bands knotted together (Figures 92, 94, 97, and 98), as well as for the fibrous structure in grazing sections (Figures 93, 95, and 96).

Further evidence for the contention that the bands are actually transverse sections of irregularly undulated (K_1 in Figure 92; Figures 94 and 97), convex (K in Figure 92), or almost flat sheets (K_2 in Figure 98), came from careful analysis of serial sections of chromosomes whose orientation relative to the plane of sections was known from phase contrast micrographs. The diameter of these sheet-like kinetochores is 5,000-9,500 A. Values of 7,000-8,000 A are most common.

Figure 95 illustrates rather unusual, exotic kinetochore profiles. Kinetochore no. 1 seems to consist of two bands converging at their ends. Additional bands were visible at the same locus in three adjacent serial sections. Similar observations were made on the undulated kinetochore no. 2.

In contrast to the single-banded kinetochores of colcemid-treated cells, the metaphase kinetochores of cold-treated cells are triple-banded as in Figure 75. The bands are fuzzier, but their relative opacity is very similar to that of kinetochores in untreated cells. Kinetochores of cold-treated cells are also attached to MT, but these are few in number.

Chromosomal and Mitotic Aberrations

Untreated Cells

Frequency of aberrations

To score the frequency of chromosomal and mitotic aberrations, Epon wafers with the embedded cell monolayers were scanned with the

phase contrast microscope at a magnification of 300. Obviously aberrant, as well as doubtful cells were examined at magnifications of 625 and 1,560. Acentric fragments, maloriented chromosomes, and other aberrations (e.g., multipolar spindles) were scored in metaphase cells; fragments, lagging chromosomes, and dicentric bridges were scored in anaphase cells. The results are presented in Table 1.

The cumulative frequency of normal and abnormal cells is less than 100%, because cells that could not be clearly identified as normal or abnormal were included in the sample, but not assigned to either category. The difference between the total frequency and 100% is the frequency of these "doubtful" cases.

Gross and fine structure of aberrations

Acentric fragments and dicentric bridges.--Figures 99-101 illustrate one of the most common types of aberration in anaphase cells, viz., a single dicentric bridge and fragments. These bridges, formed by a subterminal exchange between sister chromatids, are more or less attenuated, probably depending on the degree of spindle elongation. In both cells shown the kinetochores of the dicentric chromosome were perfectly normal (e.g., Figure 100). There was nothing unusual about the fibrous structure of the bridged chromosomes. The fragments in these cells were located in the cytoplasm at the periphery of the spindle (insets in Figures 99 and 101). Analysis of serial sections of several such cells revealed the truely acentric nature of the fragments.

Dicentric bridges, single or multiple, also occur in telophase cells. In this case the intact bridges cross the region of the

Table 1.--Frequency of chromosomal and mitotic aberrations in untreated meta- and anaphase cells (streptonigrin control).

Mitotic Stage	No. of Normal Cells	No. of Abnormal Cells	Total No. of Cells Examined	Percent Normal Cells	Percent Abnormal Cells
Metaphase	90	23	135	66.7	17.0
Anaphase	56	5	66	84.9	7.6
Total	146	28	201	72.7	13.9

equatorial constriction. Two cells in cytokinesis were found with "nuclear" bridges connecting the daughter nuclei through the compact midbody. One of these cells was examined in the electron microscope. Nuclear pore complexes were present on the NE wrapping the bridges.

Lagging chromosomes.--The second most common type of aberration in anaphase cells is laggards. Only a few such chromosomes could be examined in serial sections. Representative profiles of kinetochores of two laggards are shown in Figure 102. These chromosomes were lying near or at the periphery of the spindle (inset in Figure 102a). Characteristically, a bundle of arched MT was present at the kinetochores, which were oriented towards the center of the spindle. Some of these MT apparently bypassed the chromosome, while others seemed to terminate in the fuzzy kinetochores (Figure 102). The bundle of MT associated with laggard no. 1 (Figure 102a and inset) also seemed to be associated with laggard no. 2 (inset in Figure 102a) in the opposite half-spindle. Numerous non-kinetochore MT near the laggards were oriented haphazardly. Kinetochores and MT of most of the chromosomes near the poles were normal. The chromosome in Figure 103 was an exception. The strange profile of its kinetochore in some of the serial sections may be due to a peculiar angle of sectioning. Some of the kinetochore MT, particularly in peripheral sections of the kinetochore (Figure 103b), were definitely odd.

In a similar cell one kinetochore of a laggard was very stretched and similar in structure to the one in Figure 102a.

Centriole aberrations.--The three major possible aberrations involving centrioles - abnormal number, abnormal structure, and abnormal position - are illustrated in Figures 104-107. The presence of four centrioles in interphase (Figure 104) presumably leads to multipolar mitosis. The prophase cell in Figure 105a was very similar to the one in Figure 11a, as far as chromosome condensation and kinetochore differentiation are concerned. However, the two pairs of centrioles were positioned on opposite sides of the nucleus (Figure 105a). Despite this obviously axial arrangement, very few MT were associated with each centriole pair (Figures 105b and 105c).

Figure 106 shows two serial sections of the pole no. 2 centrioles of the cell in Figure 29. Portions of three centrioles are visible. The one in the center was deformed to a cup-like structure. Because of missing sections, the precise architecture of, and relationship between, these centrioles could not be reconstructed. Microtubules converged on the osmiophilic masses left and right of center in Figure 106a.

Centriole aberrations also occurred in the anaphase cell of Figure 102. One of a pair of centrioles near pole no. 2 is shown in Figure 107a. The MT, however, converged on a different center (P_2), where amorphous, osmiophilic material was present. I am convinced that there was at least a third centriole at this spot, but I could not verify it, because some of the serial sections were missing. On the other hand, one serial section of the centriole shown in Figure 107a revealed a very osmiophilic particle in the lumen of the centriole (Figure 107b). In size and shape this particle was very similar to those found in the vicinity of centrioles at all stages of the cell cycle (e.g., Figure 4). At pole no. 1 of this anaphase cell there were probably also more than two centrioles (Figure 107c).

Streptonigrin-Treated Cells

Mitotic index and frequency of aberrations

The mitotic index was determined from cell counts made with the phase contrast microscope at a magnification of 200 or higher. Mitotic cells comprised all the stages from pro- to telophase. The control cells were the same used to compute the frequency of aberrations (see Table 1). The results are presented in Table 2.

The procedure for scoring aberrations was as described for untreated cells. The results are presented in Table 3.

The figures for meta- and anaphase cells are of relative value only, because the distinction between these stages is not sharp in highly aberrant cells. As for untreated cells, the cumulative frequency for 0.01 µg/ml SN in less than 100%, due to "doubtful" cases.

Gross and fine structure of aberrations

The cytological effect produced by the two concentrations of SN differs not only quantitatively, but also qualitatively. Generally speaking, the higher concentration induces more complex aberrations and bizarre mitotic figures are common (Figure 108). Ana- and telophase cells usually contain several dicentric bridges of variable diameter, probably depending on the degree of attenuation (Figures 108 c-f). Numerous acentric fragments are located at the periphery of these cells.

Chromatin strands connecting the kinetochore regions of daughter chromosomes occurred in cells in very early anaphase (Figure 109). The kinetochores of these chromosomes appeared normal. An apparent exception is illustrated in Figure 109. This kinetochore resembled certain prometaphase kinetochores (see Figures 35 and 41). Its associated MT passed over the adjacent chromosome.

Table 2.--Mitotic indices (MI) for streptonigrin-treated and untreated control cells.

Treatment	Total No. of Cells Counted	Cells in Mitosis	
		no.	% (MI)
Control	541	14	2.59
0.01 ug/ml SN	540	12	2.22
0.05 ug/ml SN	541	1	0.18

Table 3.--Frequency of chromosomal and mitotic aberrations in streptonigrin-treated cells.

Treatment	No. of Metaphase Cells		No. of Anaphase Cells		Total No. of Cells Counted	Percent	
	Normal	Abnormal	Normal	Abnormal		Normal Cells	Abnormal Cells
0.01 ug/ml SN	63	65	16	33	200	39.5	49.0
0.05 ug/ml SN	0	21	0	14	35	0	100.0

Many cells treated with 0.05 µg/ml SN contained chromosomes less condensed than normal (Figure 111). Chromosomal fibrils possibly cemented together by an amorphous substance formed more electron dense patches either at the surface of, or within, these chromosomes (Figures 111b and 111c).

Dicentric bridges very often contained strands of densely packed or finer-than-normal fibers that extended, at least in a few carefully studied cases, from one kinetochore to the other (Figures 110 and 111a). The kinetochores in cells with dicentric chromosomes were structurally normal, but their distance from the respective pole was more variable than in normal ana- and telophase cells (Figures 110a and 113). The kinetochores of dicentrics, in particular, seemed to lag.

Serial sections revealed the truely acentric nature of fragments irrespective of their position within a cell.

Nuclear envelope reconstruction begins near the poles, along the sides of the chromosomes. Small cisternae, already with nuclear pore complexes, are closely apposed to the chromosomes (Figure 112). It appears there is a gradient for this process from the polar regions to the interzone. For example, membrane cisternae may be found along the poleward portions of dicentrics and laggards, but not along the interzonal portions.

Late telophase cells with nuclear bridges through the midbody are more frequent in SN-treated than in control cells. An example is shown in Figure 116. The nuclei of the daughter cells were polymorphic. Pockets extended deep into the nuclei on the poleward side. Very electron dense patches within the nuclei, or on the inner membrane of the nuclear envelope lining the pockets, are remnants of the inner

layer of kinetochores (Figures 114-116). Numerous MT were observed penetrating from the pockets into the nuclei, indicating the envelope was not completely reconstructed. Pieces of double membrane, some bearing ribosomes (Figure 117a), were also found in the nuclei. Occasionally, ribosome-like particles appeared on both membranes of the nuclear envelope (117b).

Cells in late cytokinesis, connected by nuclear bridges across the midbody, can be identified with the light microscope. Surprisingly, however, a greater number of daughter cells connected by extremely thin bridges are found in thin sections. Many of these aberrations are of truely ultrastructural dimensions. The greater portion of the bridge shown in Figure 118 was only approximately 500 A in diameter. In this case no midbody was found between the two daughter cell. The bridge simply passed across the cleavage furrow into the other cell and expanded to a large nuclear bleb, which was in turn connected to the main nucleus by a similarly thin stalk. Both daughter cells also had micronuclei. A similar case is illustrated in Figure 119. The thin bridge passed through the compact midbody (Figure 119a). The drop-shaped nuclear bleb was connected to the main nucleus by a very thin stalk. Micronuclei were also present in both daughter cells (Figure 119b).

Centriole aberrations also occur in SN-treated cells, but apparently not more frequently than in untreated cells. In one of two daughter cells in cytokinesis the two centrioles were found unusually far from the nucleus and also remote from each other.

Fig. 3. Interphase. Grazing section of the nucleus. Note centrioles (C), Golgi complex (G), polyribosomes (R) on nuclear envelope, pore-annulus complexes at the level of the envelope (small arrows) and the level of the nucleus (large arrows), achromatic holes (H) in the peripheral chromatin (Chr) underlying pores. x 15,750.

Fig. 4a-d. Interphase. Four serial sections of a centriole. (a) Osmiophilic mass near distal end. (b) Probably the distal end. Note short rays radiating from triplets (arrows). (c) Probably near-median section. Note osmiophilic mass forming cylinder around the centriole, spherical particle (Pa). (d) Median section revealing intracentriolar vesicle (CV). Note satellites (S) in all four sections. x 100,000.

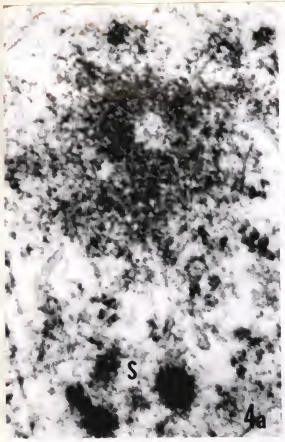
S
4a

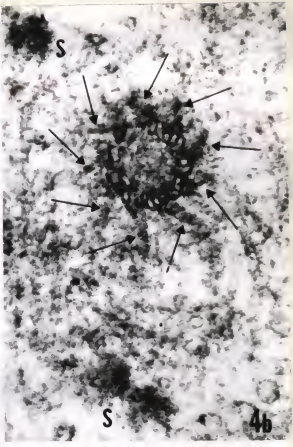
S
S
4b

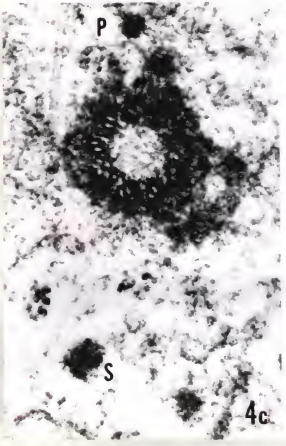
P
S
4c

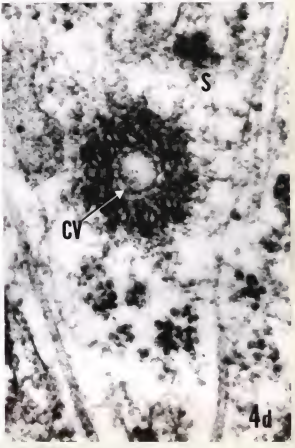
S
CV
4d

Fig. 5a-c. Interphase. Transverse sections of representative nuclei. (a) Dispersed chromatin (Chr). Note granular (Gr), and fibrillar (F) components of nucleolus (Nu); intranuclear vesicle containing particles (IV), nuclear envelope (NE). x15,750. (b) Moderate proportion of heterochromatin (HChr). x 15,750. (c) Relatively great proportion of heterochromatin. x 11,500.

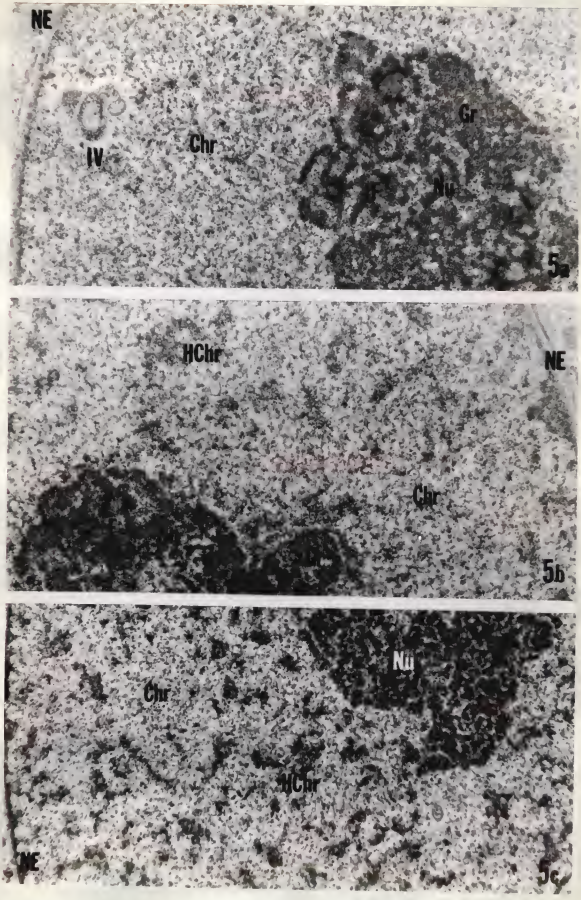
NE
IV
Chr
Gr
Nu
5a
HChr
NE
Chr
5b
Nu
Chr
HChr
NE
5c

Fig. 6. Interphase. Chromatin fibers in the nucleus of Fig. 5a. Note 250 A fibers (large arrows), 125 A fibers (arrowheads), 70-80 A core within some 250 A fibers (small arrows). x 75,000.

Fig. 7. Interphase. Portion of the nucleolus shown in Fig. 5b. Note granular (Gr), fibrillar (F) components; nucleolus-associated chromatin (Chr). x 30,000.

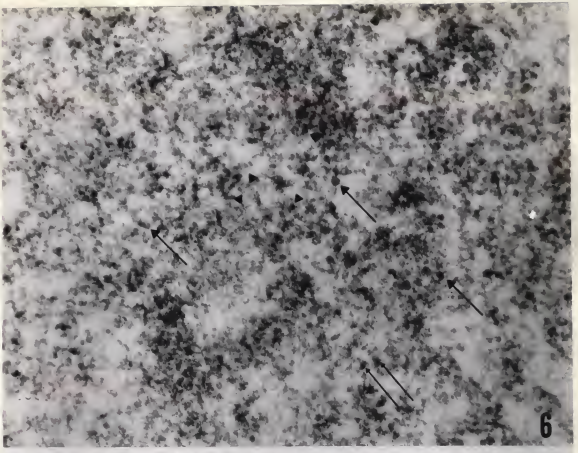
6

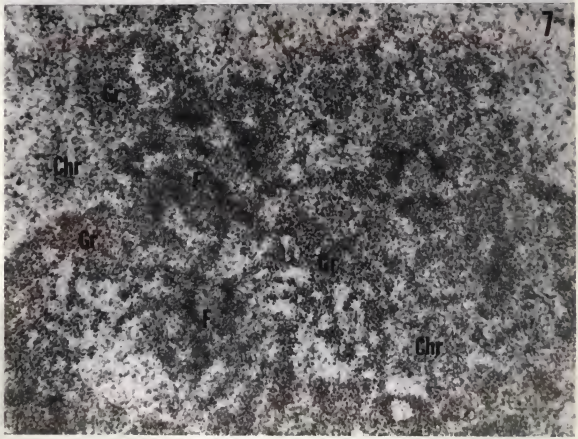
7
Gr
Chr
F
Gr
Gr
F
Chr

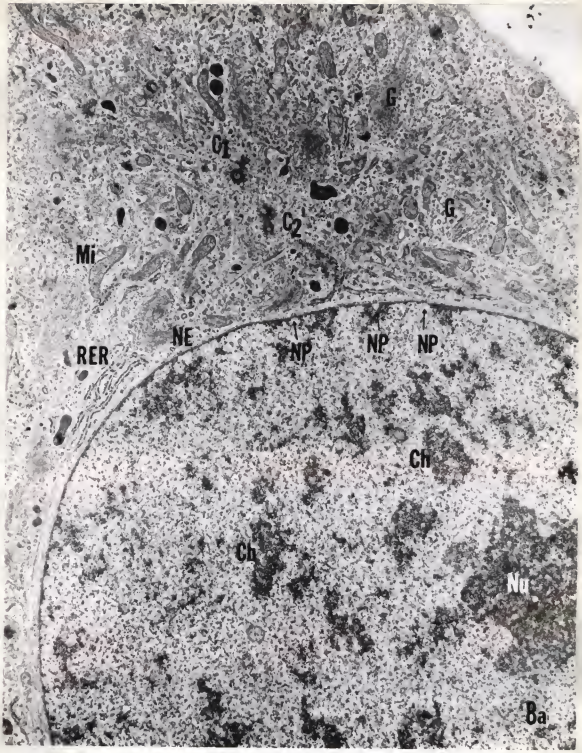

Fig. 8a. Very early prophase. Note two pairs of centrioles (C_1, C_2), condensing chromosomes (Ch), nucleolus (Nu). Nuclear envelope (NE) with pores (NP); Golgi complexes (G), rough ER (RER), and mitochondria (Mi) in the cytoplasm. x 11,500.

Fig. 8b-e. Very early prophase. Four serial sections of the two pairs of centrioles shown in Fig. 8a. Daughter centrioles (DC_1, DC_2) closely associated with parent centrioles (PC_1, PC_2). x 40,000.

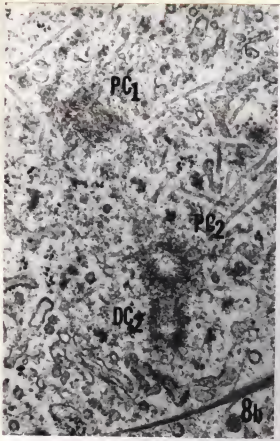
PC1
PC2
DC2
8b

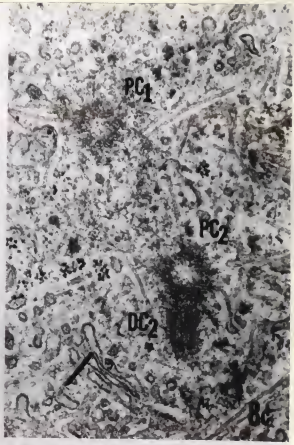
PC1
PC2
DC2
8c

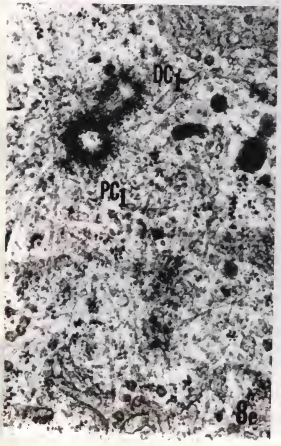
DC1
PC1
8e

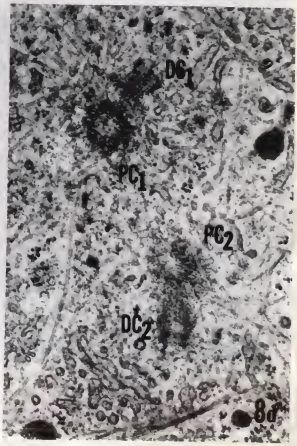
DC1
PC1
PC2
DC2
8d

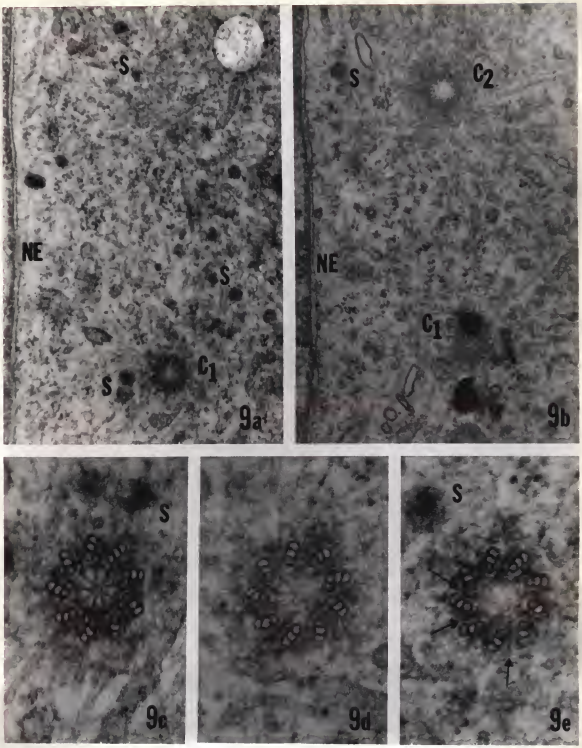

Fig. 9a-e. Very early prophase. Migration and structure of centrioles. (a), (b) Two serial sections showing one of each pair of centrioles (C_1, C_2). Note satellites (S). Black spots near C_1 in (b) are staining marks. x 40,000. (c-e) Three serial sections of centriole no. 1 (C_1). Note cartwheel structure with hub and spokes in (c) and (d), skew arrangement of tubular triplets; short, osmiophilic bars between triplets in (e). x 122,500.

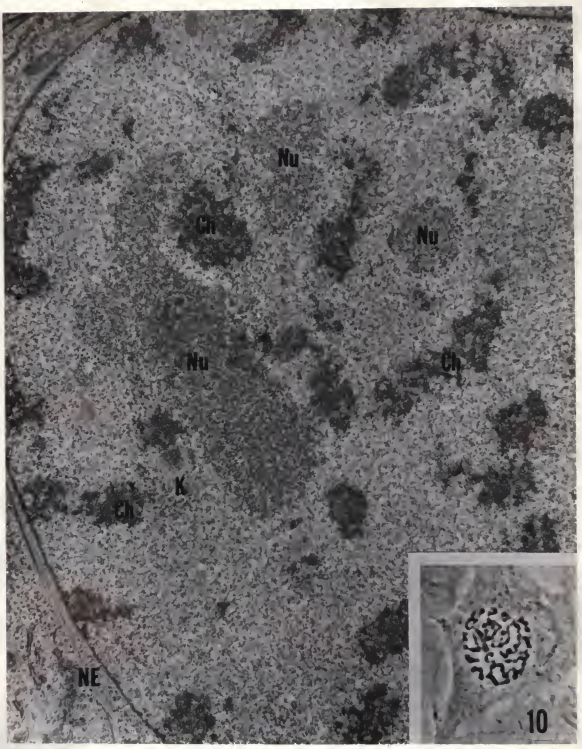

Fig. 10. Mid-prophase. Note dispersed nucleolus (Nu), chromosomes (Ch), kinetochore (K), intact nuclear envelope (NE). x 11,500. Inset: Phase contrast micrograph of the cell in plastic. (x 1,280).

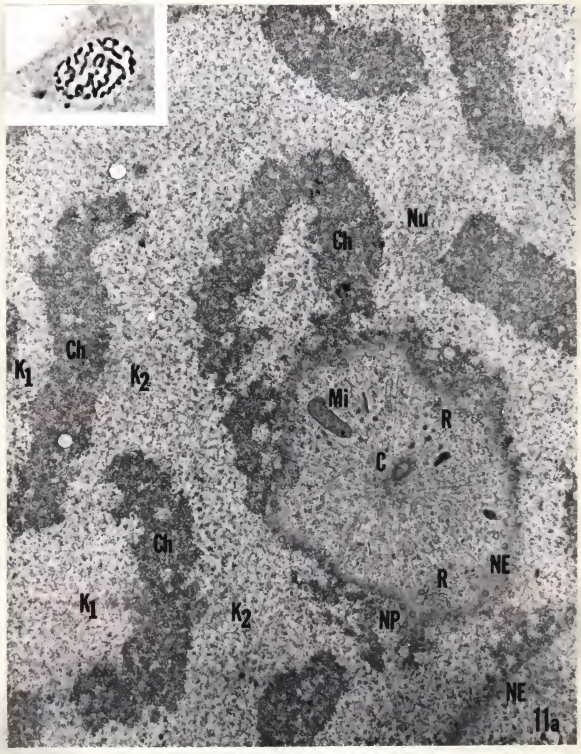

Fig. 11a. Mid-prophase. Centriole (C) in pocket of the nuclear envelope (NE). Note chromosomes (Ch) with sister kinetochores (K_1, K_2), remnant of the nucleolus (Nu). x 15,750. Inset: Phase contrast micrograph of the cell in plastic (x 1,280).

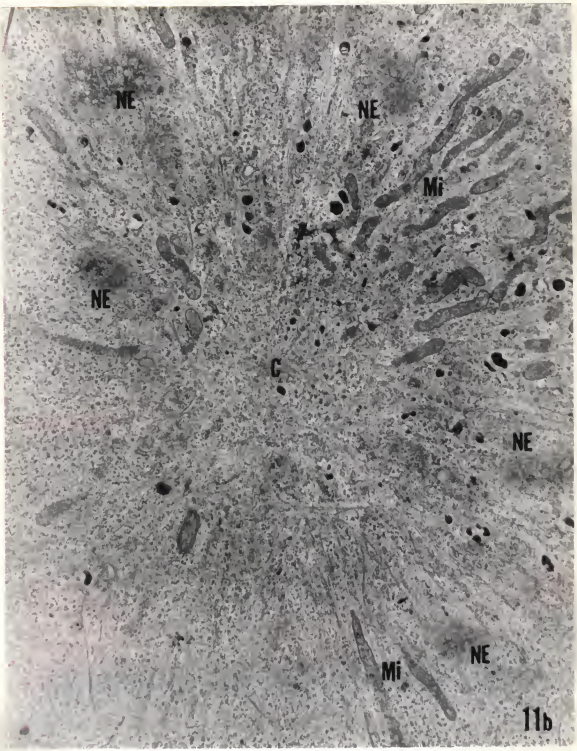

Fig. 11b. Mid-prophase. Serial section of the cell in Fig. 11a, at the periphery of the nucleus. Note microtubules converging at the location of the centrioles (C); the centrioles themselves not shown. Mitochondria (Mi) also radially oriented. Grazing sections of the nuclear envelope (NE). x 11,500.

Fig. 12. Early prophase. Grazing section of the nucleus. Note intact nuclear envelope (NE) with pores (NP), chromosomes (Ch) with large achromatic holes (H). x 30,000.

Fig. 13. Early prophase. Transverse (serial) section of the nucleus shown in Fig. 12. Note chromosomes (Ch) apparently attached to nuclear envelope (NE) by "stalks" (arrows). x 22,500.

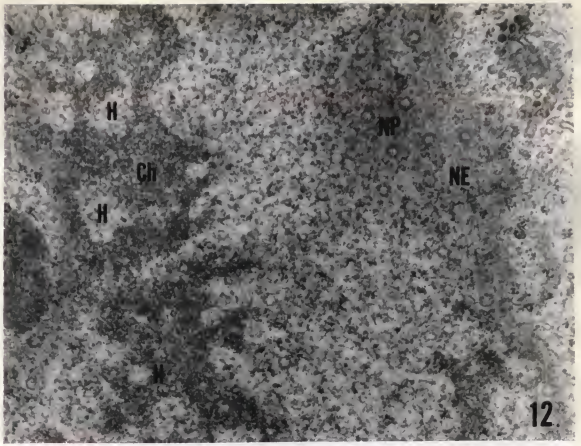
H
Ch
H
NP
NE
H
12

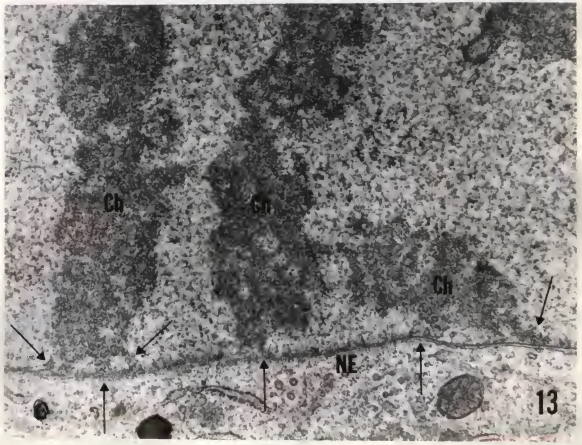
Ch
Ch
Ch
NE
13

Fig. 14. Late prophase. Chromosome (Ch) attached to the intact nuclear envelope (NE) by a "stalk" (arrow). x 57,500.

Fig. 15. Late prophase. Sister kinetochores (K_1, K_2) of two chromosomes (Ch_1, Ch_2). From the same cell as Fig. 14. x 30,000.

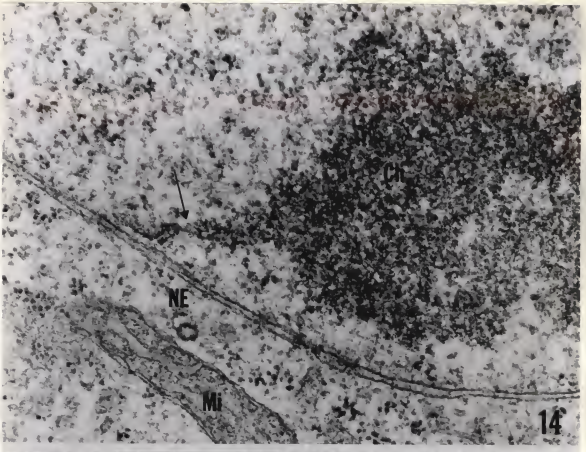
Ch
NE
Mi
14

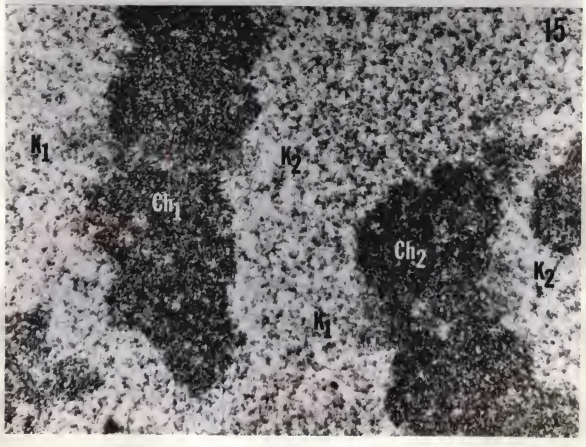
15
K1
K2
Ch1
Ch2
K2
K1

Fig. 16. Mid-prophase. Oblique section of a chromosome (Ch) and one of its kinetochores (K). From the cell shown in Fig. 10. Note difference in electron density between chromosome and kinetochore. x 62,500.

Fig. 17. Mid-prophase. Sister kinetochores (K_1, K_2) of a chromosome in the nucleus shown in Fig. 11a. Note doubleness of chromosome (Chd the two sister chromatids), kinetochore granules (KG). x 67,500.

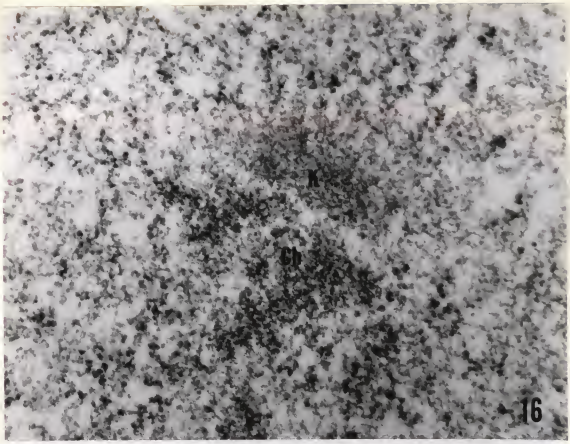
K
Ch
16

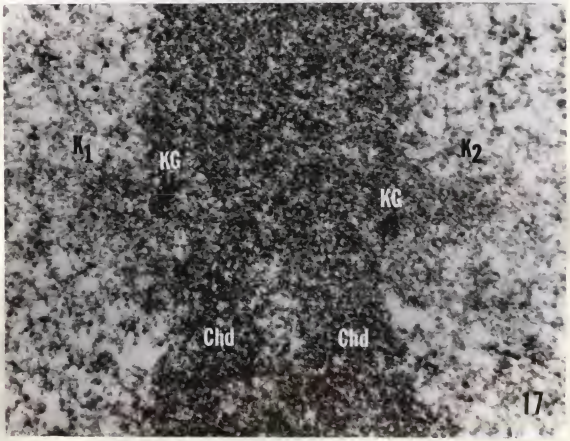
K1
KG
K2
KG
Chd
Chd
17

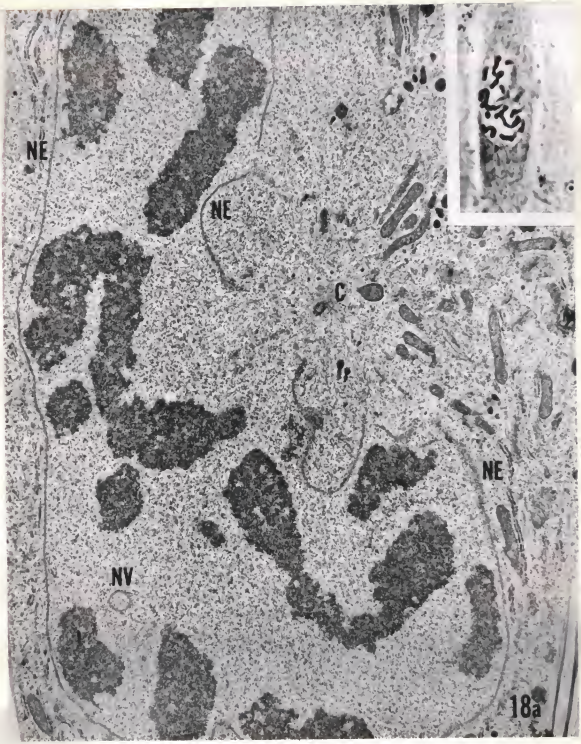

Fig. 18a. Very early prometaphase. Note fragmenting nuclear envelope (NE) near centrioles (C), intact NE on opposite side of "nucleus". One fragment formed a vesicle (NV). x 11,500. Inset: Phase contrast micrograph of the cell in plastic (x 1,280).

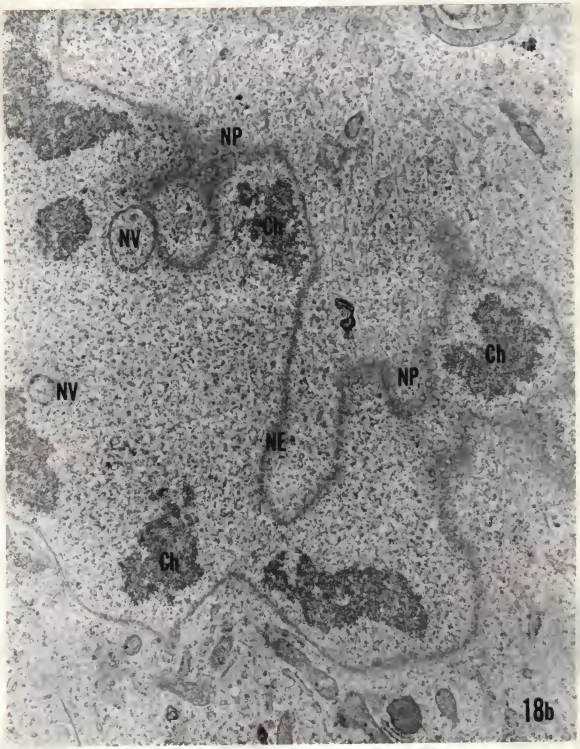

Fig. 18b. Very early prometaphase. Serial section of the cell in Fig. 18a. Nuclear envelope (NE) undulated around chromosomes (Ch), fragments formed vesicles (NV). Note nuclear pores (NP). x 15,750.

Fig. 19. Early prometaphase. Breakdown of the nuclear envelope (NE) near poles (P_1, P_2). Note nucleolus organizer (NO) on X chromosome. The white circle near the left margin is due to a hole in the supporting film; black spots are dirt and stain marks. x 7,750. Inset: Phase contrast micrograph of the cell in plastic (x 1,280).

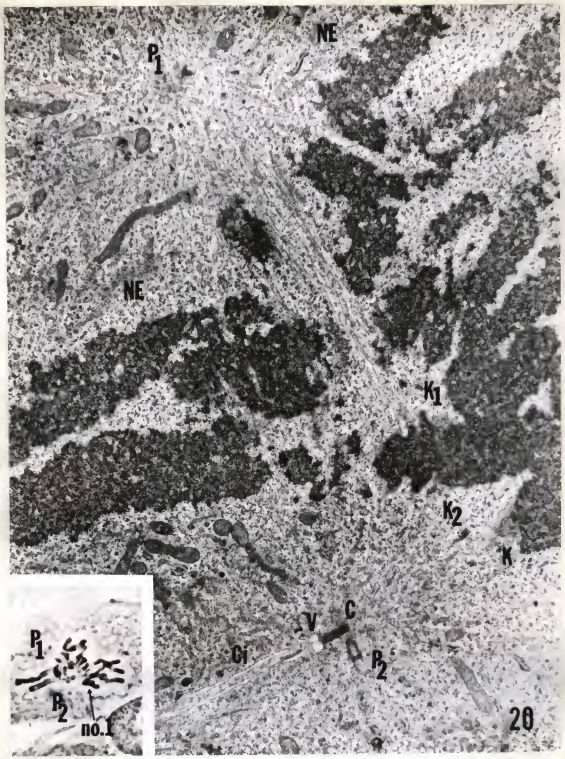

Fig. 20. Early prometaphase. Formation of the spindle. Most MT connect kinetochores (K) with the poles (P_1, P_2). Note vesicle (V) and elongated cisternae (Ci) at the proximal end of one of the centrioles (C) at pole no. 1 (P_1). x 11,500. Inset: Phase contrast micrograph of the cell in plastic; chromosome no. 1 is shown in Fig. 24 (x 1,280).

Fig. 21a-c. Early prometaphase. Grazing sections of the nuclear envelope at progressively later stages. (a) From the cell in Fig. 18; note eccentric pore granules (arrows). x 57,500. (b) x 40,000. (c) x 50,000. Compare pore-annulus complexes (NP), polyribosomes (R) in the three micrographs.

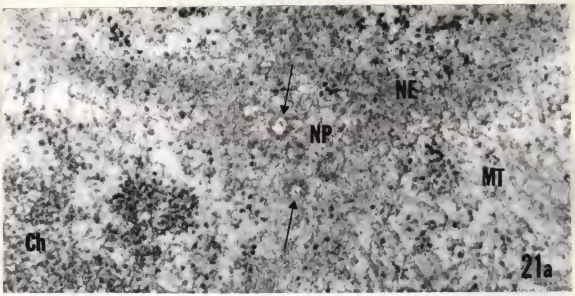
NE
NP
MT
Ch
21a

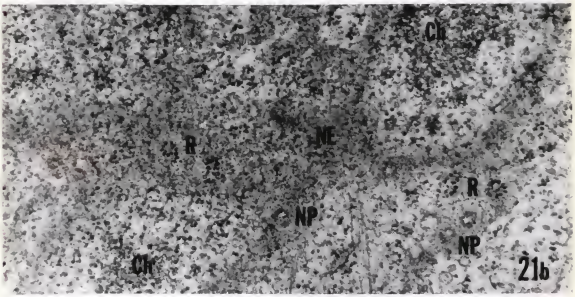
Ch
R
NE
R
NP
NP
Ch
21b

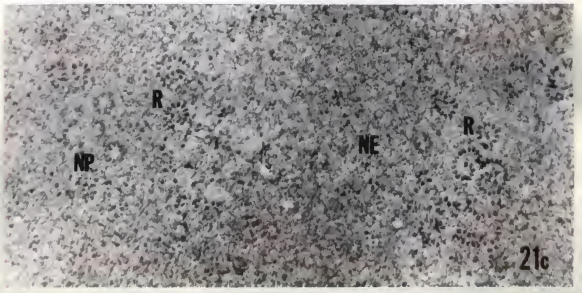
R
R
NP
NE
21c

Fig. 22a-d (continued on the following page). Early prometaphase. Kinetochores of the cell in Fig. 18. (a) Note appearance of kinetochores (large arrows) compared to prophase (e.g., Fig. 15). Oblique and cross sections of MT (small arrows), intrachromosomal MT (circles). x 30,000. (b) Sister kinetochores (K_1, K_2) with faint band (arrows). x 57,500.

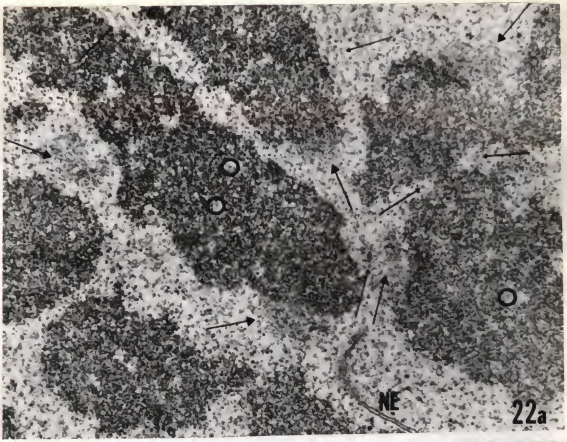
NE
22a

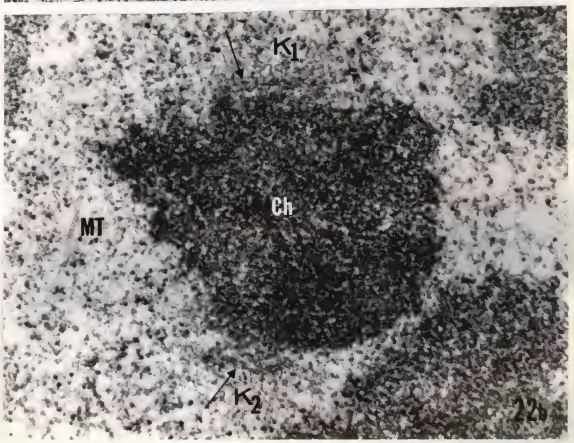
K1
Ch
MT
K2
22b

Fig. 22 (contd). (c) and (d) two serial sections of a chromosome near the intact nuclear envelope (NE). Note MT outside the NE, opposite one kinetochore (K_2); difference between the two kinetochores. x 57,500.

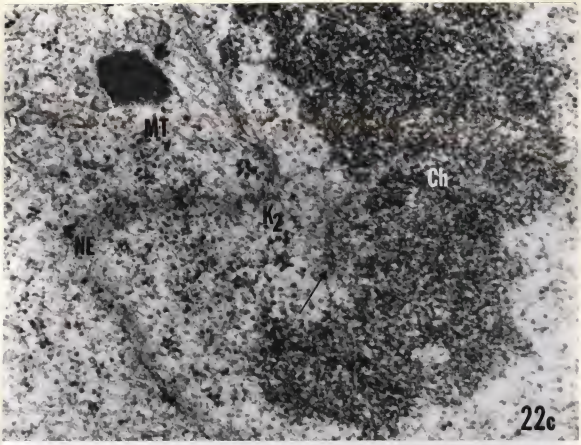
MT
Chr
K2
NE
22c

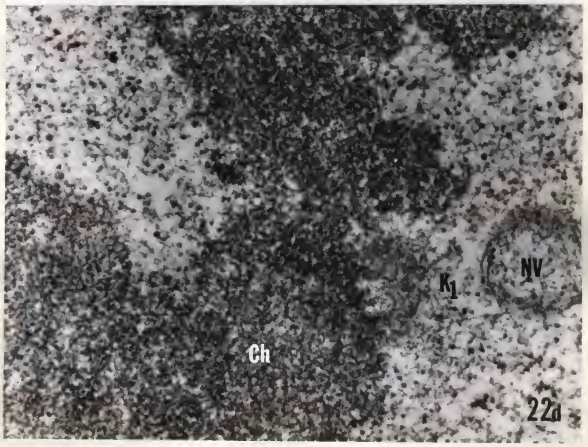
K1
NV
Ch
22d

Fig. 23a-c. Early prometaphase. Kinetochores of chromosomes near pole no. 2 of the cell in Fig. 19. (a) Note difference between kinetochores facing the near pole (K, K_2), and kinetochore facing the far pole (K_1). Arrows indicate bands. x 30,000. (b) and (c) two serial sections of another chromosome (Ch). Note differences, similarities between the kinetochore facing the near pole (K_2) and the kinetochore facing the far pole (K_1). Arrows indicate bands. x 30,000

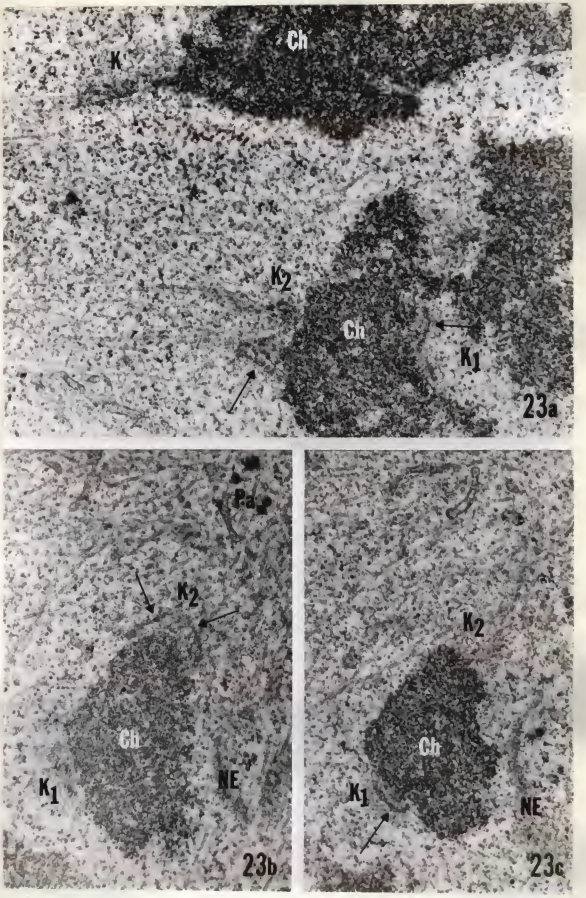
K
Ch
K2
Ch
K1
23a
Pa
K2
Ch
K1
NE
23b
K2
Ch
K1
NE
23c

Fig. 24a-c. Early prometaphase. Three serial sections of chromosome no. 1 shown in the inset of Fig. 20. Note stretching, attached MT, of the kinetochore facing the near pole (K_2); globular shape, lack of MT, of the kinetochore facing the far pole (K_1). x 30,000.

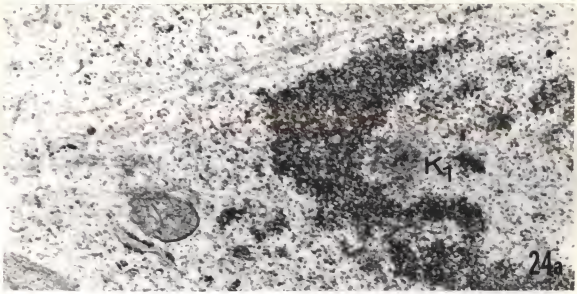
K1
24a

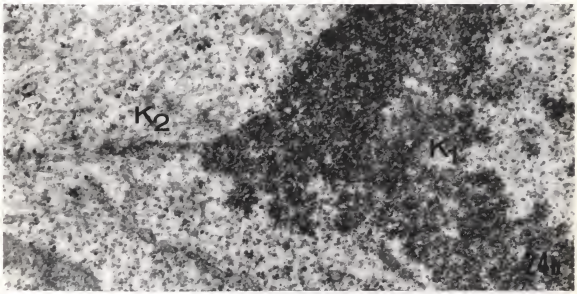
K2
K1
24b

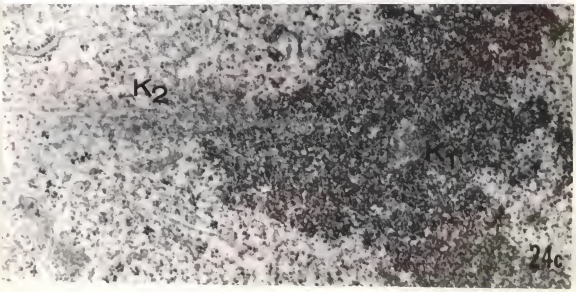
K2
K1
24c

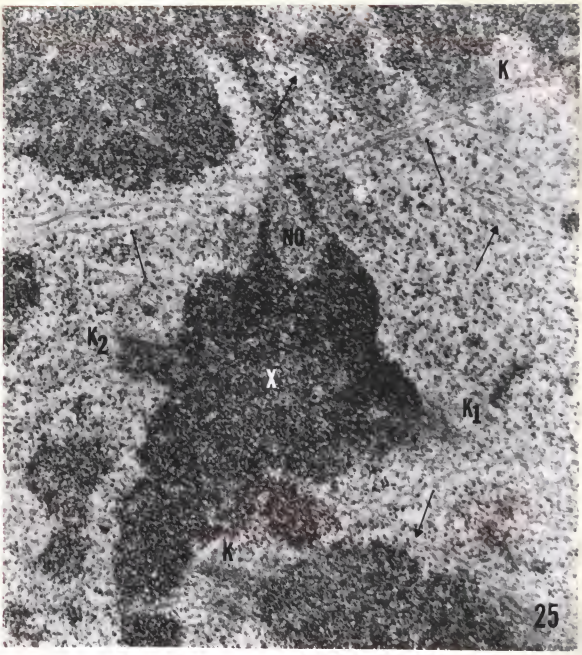

Fig. 25. Early prometaphase. Kinetochores in the equatorial region. From the cell in Fig. 20. Note unobstructed sister kinetochores (K_1, K_2) of the X chromosome, its nucleolus organizer (NO), other kinetochores (K). The direction of the spindle axis is indicated by MT marked with large arrows. Other MT are skew (small arrows). x 30,000.

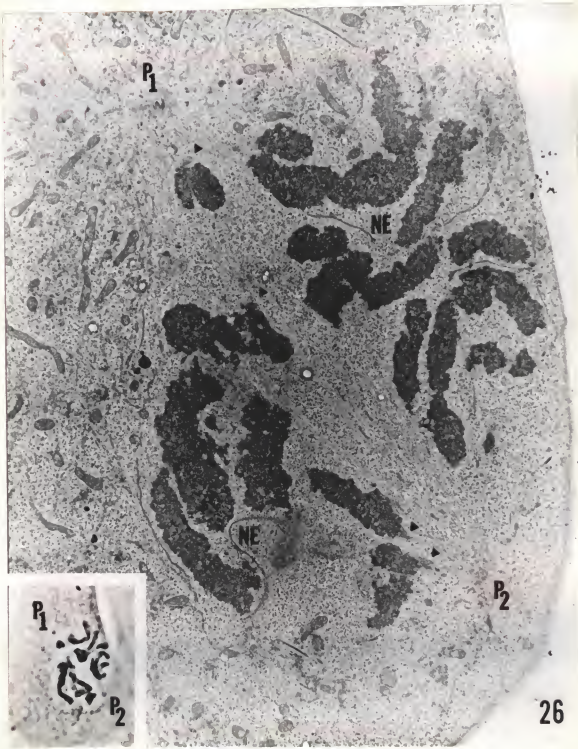

Fig. 2[illegible]. Mid-prometaphase. P_1, P_2, the two poles of the mitotic spindle. A centriole is visible at pole no. 1. Several kinetochores are indicated by arrowheads. x 7,750. Inset: Phase contrast micrograph of the cell in plastic (x 1,280).

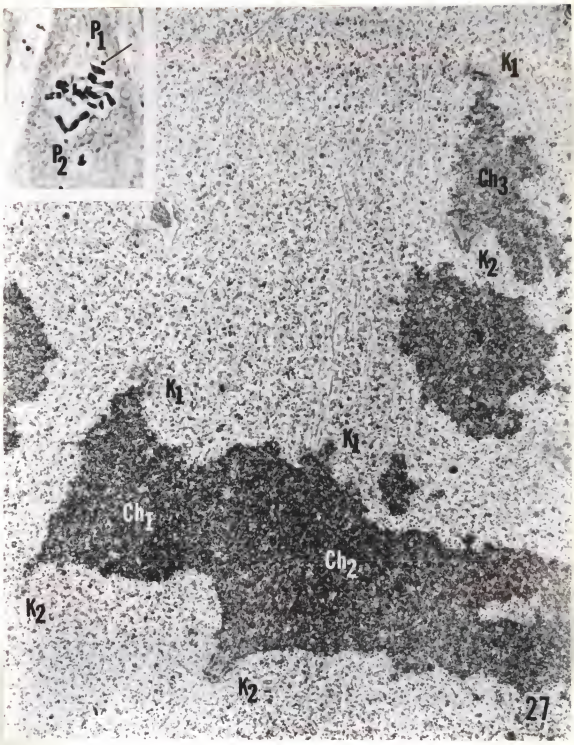

Fig. 27. Mid- to late prometaphase. Ch_1, Ch_2, two equatorial chromosomes. Ch_3 a chromosome displaced towards pole no. 1 (see arrow in inset). K_1, K_2, kinetochores oriented towards pole no 1 and pole no. 2, respectively. x 7,750. Inset: Phase contrast micrograph of the cell in plastic (x 1,280).

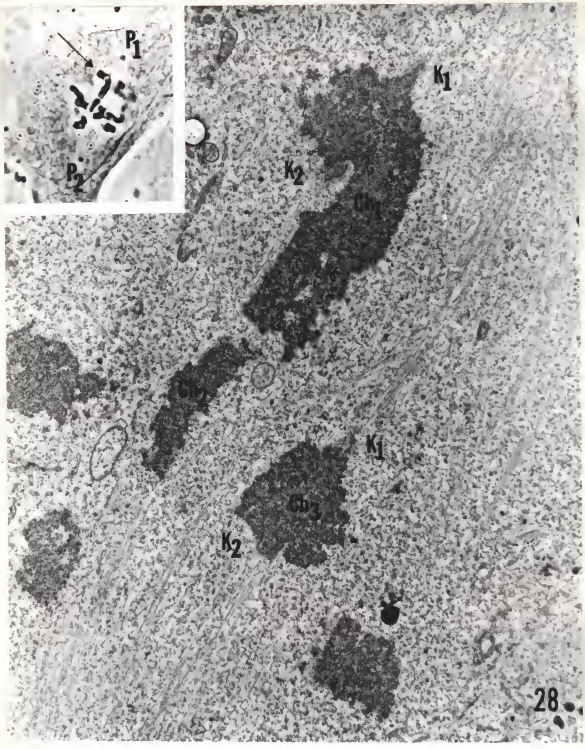

Fig. 28. Late prometaphase. Ch_2, Ch_3, two equatorial chromosomes. Ch_1 the chromosome displaced towards pole no. 1 (arrow in inset). K_1, K_2, the pole no. 1 and pole no. 2 kinetochores, respectively. x 11,500. Inset: Phase contrast micrograph of the cell in plastic (x 1,280).

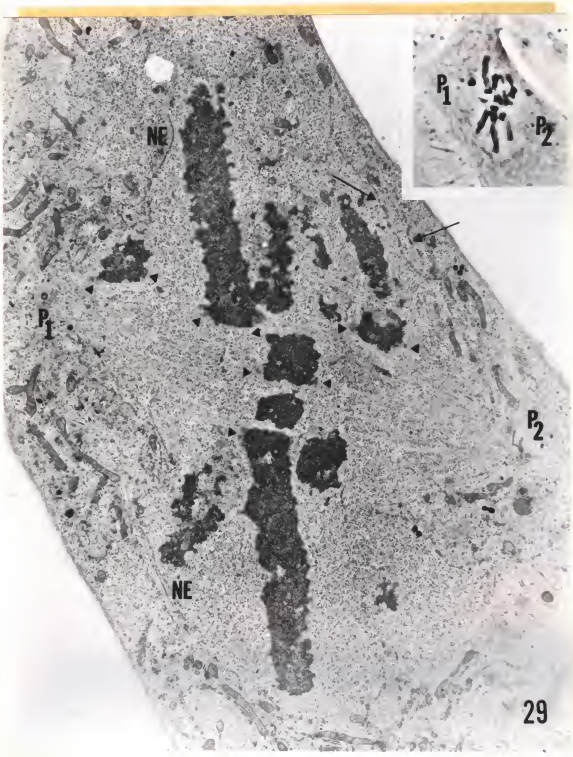

Fig. 29. Late prometaphase. Note the small chromosome near pole no. 1 (P_1). Kinetochores are marked by arrowheads. Fragments of the nuclear envelope (NE) at the periphery of the spindle. Pieces of double membrane with ribosomes (arrows). x 7,750. Inset: Phase contrast micrograph of the cell in plastic (x 1,280).

Fig. 30a, b. Late prometaphase. (a) Equatorial chromosomes with kinetochores (arrowheads). x 11,500. (b) Relatively thick section with transchromosomal MT (arrows). x 30,000.

Fig. 31. Late prometaphase. Equatorial chromosomes with kinetochores (arrowheads). Note chromatin strand connecting stretched kinetochore regions (arrow). x 15,750.

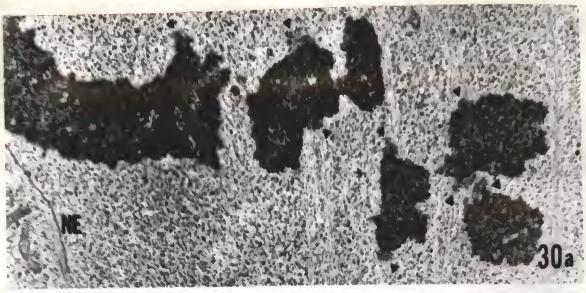
NE
30a

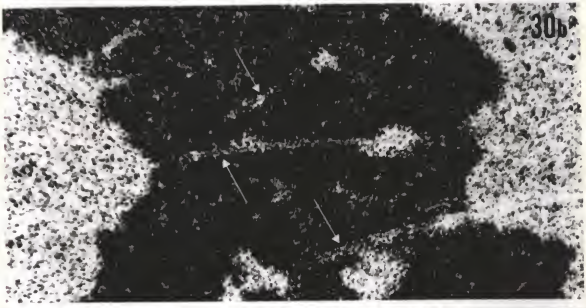
30b

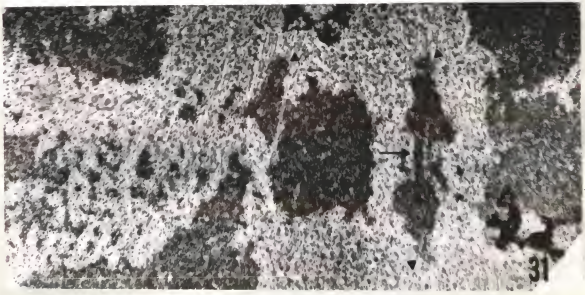
31

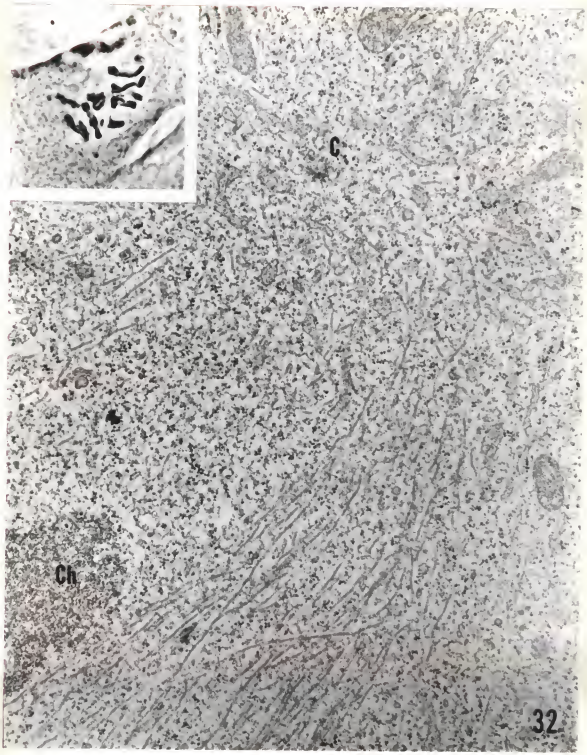

Fig. 32. Mid-prometaphase. Unusual arrangement of MT. x 22,500.

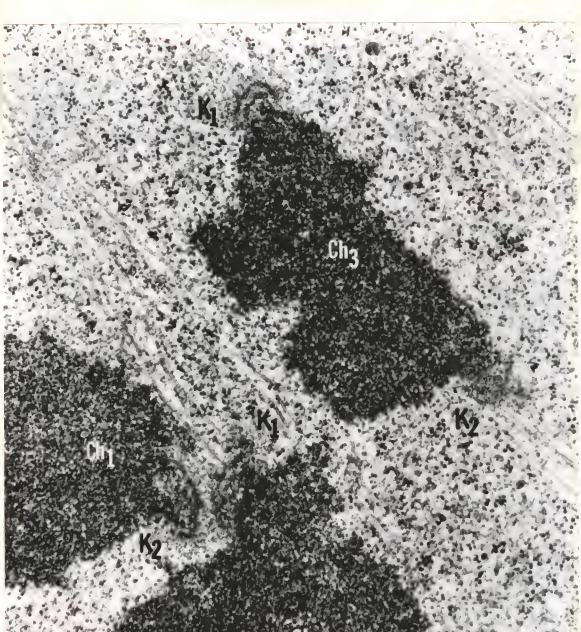

Fig. 33a. Late prometaphase. Three of the chromosomes shown in Fig. 30a at higher magnification. Unobstructed kinetochores (K_1 and K_2 of Ch_3, K_2 of Ch_2) and obstructed kinetochores (K_1 of Ch_2, K_2 of Ch_1). Note wavy and skew MT. x 40,000.

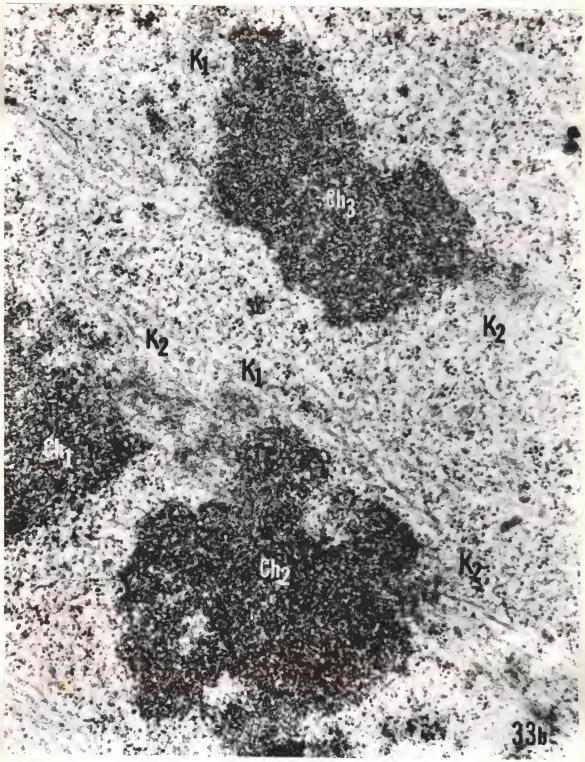

Fig. 33b. Late prometaphase. Serial section of the three chromosomes shown in Fig. 33a. x 40,000.

Fig. 34a-c. Late prometaphase. Three serial sections of an equatorial chromosome. From the same cell as Fig. 39. Note triple-banded kinetochores (K_1, K_2), transchromosomal MT (arrows). x 40,000.

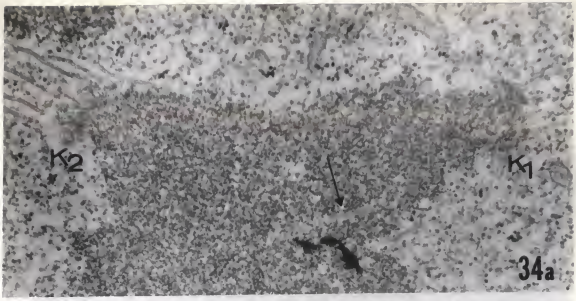
K2
K1
34a

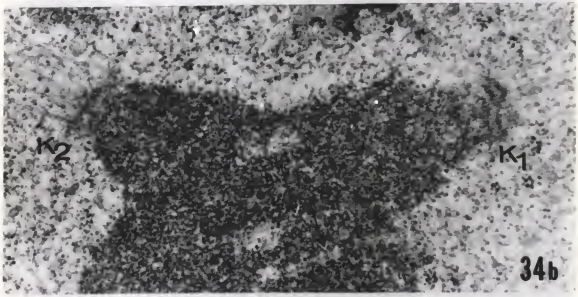
K2
K1
34b

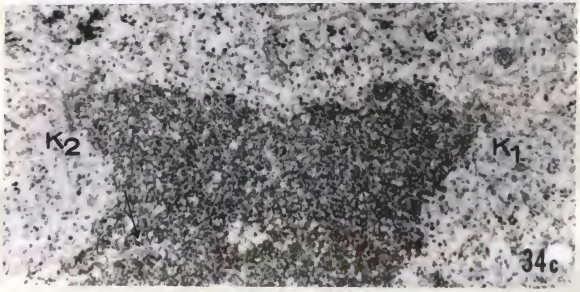
K2
K1
34c

Fig. 35a-c. Late prometaphase. Unobstructed (K_1) and obstructed (K_2) kinetochore of an equatorial chromosome. From the same cell as Fig. 41. Note difference in banding, shape, of the two kinetochores. x 50,000.

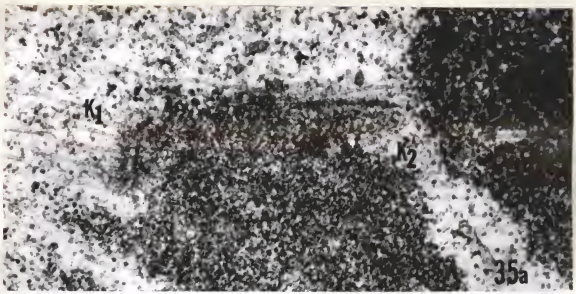

35a

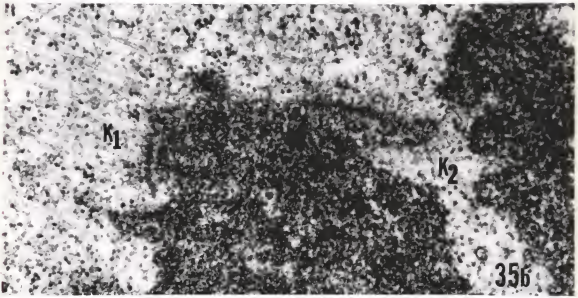

35б

35c

Fig. 36. Mid-prometaphase. An equatorial chromosome with stretched, fuzzy kinetochores (K_1, K_2). Note strand of chromosomal fibrils connecting the two kinetochore regions (arrows). x 30,000.

Fig. 37a, b. Late prometaphase. Two serial sections of the small chromosome displaced towards pole no. 1 in Fig. 29. Note fuzzy appearance of K_1, compact K_2 with single band (arrow in Fig. 37b). x 50,000.


K1
K2
36

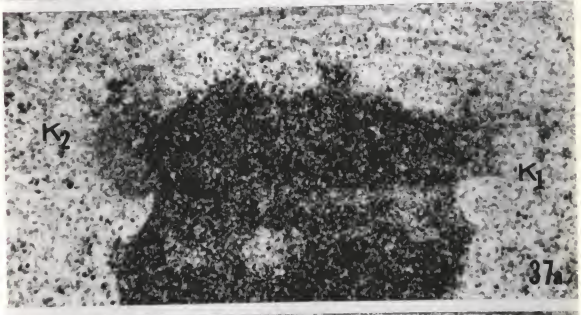
K2
K1
37a

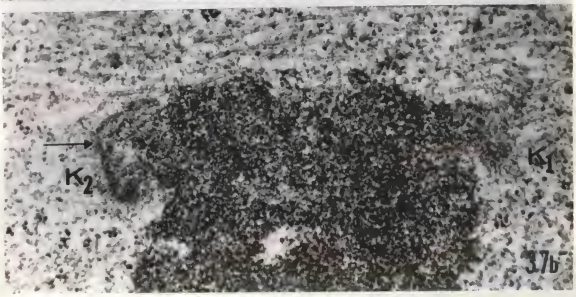
K2
K1
37b

Fig. 38a, b. Late prometaphase. Higher magnification of chromosome no. 1 shown in Fig. 28. Note single band of K_2 (arrowhead in Fig. 38a), faint triple-banding of K_1 (arrowhead in Fig. 38b). Arrows point to dark chromosomal granules. x 30,000.

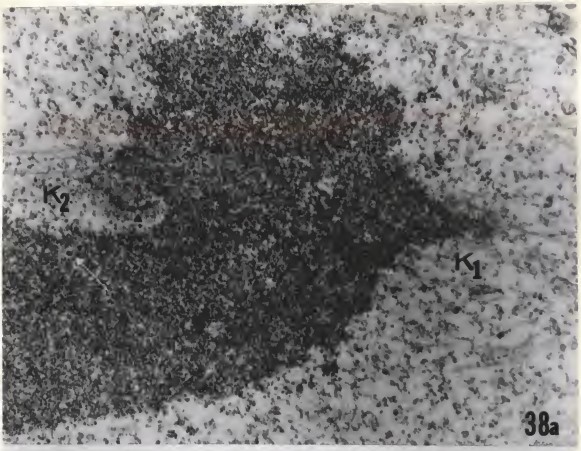
K2
K1
38a

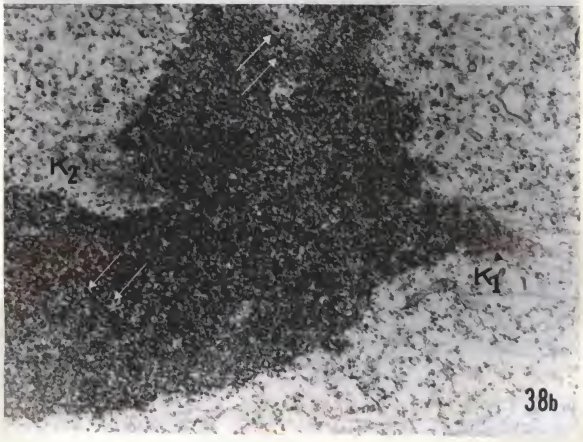
K2
K1
38b

Fig. 39a-e. Late prometaphase. Kinetochores of a chromosome displaced towards pole no. 2. K_1, K_2, the pole no. 1 and pole no. 2 kinetochores, respectively. Arrowheads indicate bands. Note bundle of straight, some skew and wavy MT, passing the kinetochores. x 40,000.

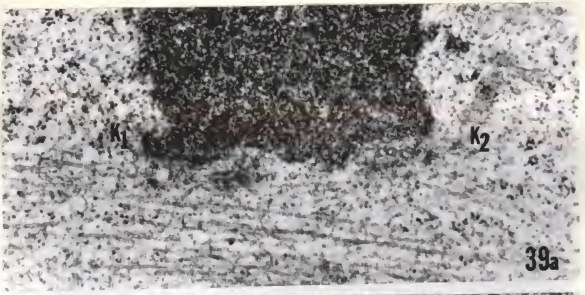
K1
K2
39a


K1
K2
39b

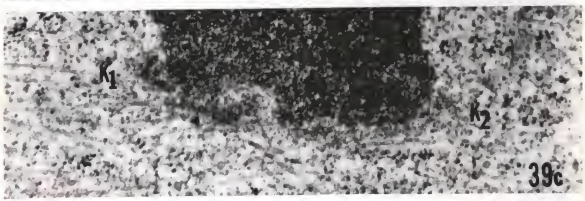
K1
K2
39c


K1
39d

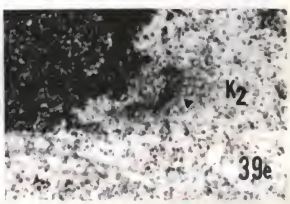
K2
39e

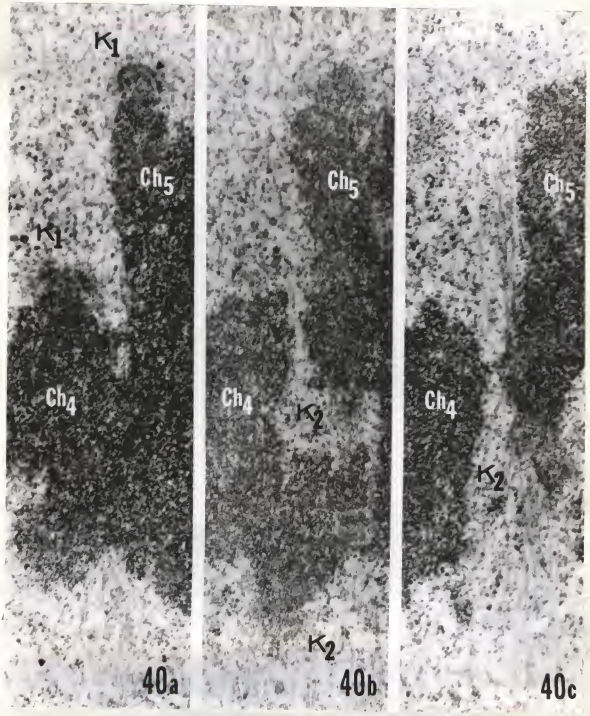

Fig. 40a-c. Late prometaphase. Two chromosomes (Ch_4, Ch_5) of the cell shown in Fig. 28 displaced towards pole no. 1. K_1, K_2, the pole no. 1 and pole no. 2 kinetochores, respectively. x 30,000.

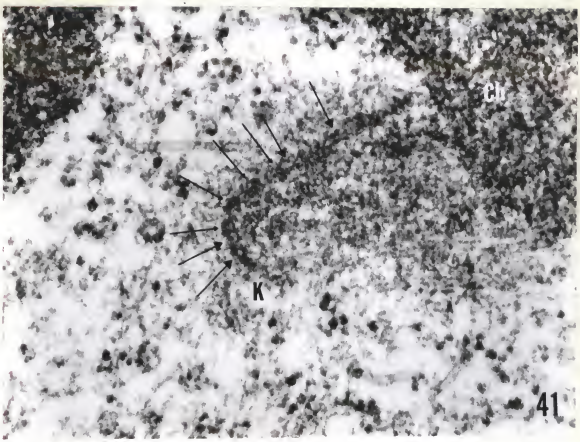

Fig. 41. Late prometaphase. Obstructed kinetochore (K) of an equatorial chromosome (Ch). Note double (large arrows) and beaded (small arrows) substructure of the moderately dense band. x 100,000.

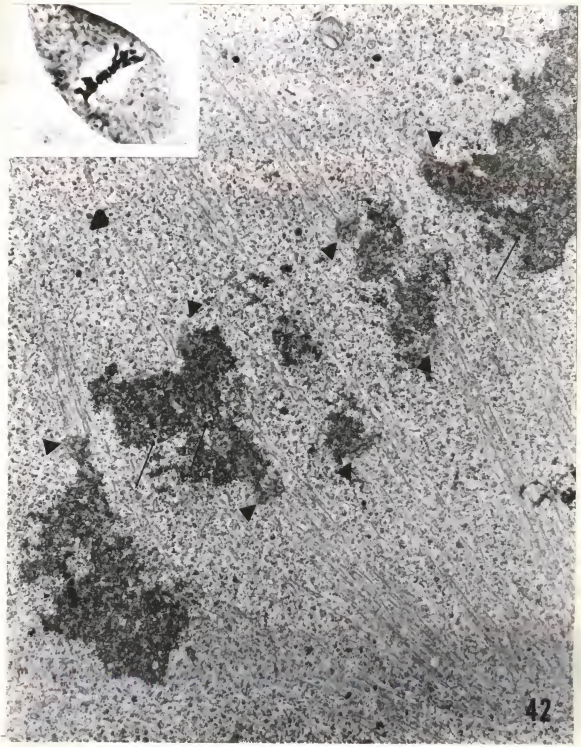

Fig. 42. Metaphase. Chromosomes aligned on the metaphase plate (horizontal section). Sister kinetochores (arrowheads) oriented towards opposite poles. Bundles of kinetochore MT converge towards the poles. Note dense chromosomal granules (arrows). x 15,750. Inset: Phase contrast micrograph of the cell in plastic (x 1,280).

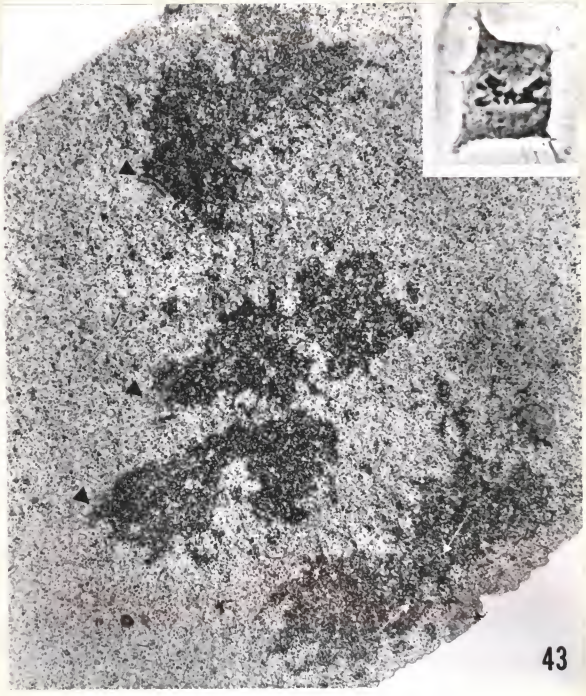

Fig. 43. Metaphase. Para-sagittal section showing four pairs of sister chromatids. Three kinetochores (arrowheads), one of them distinctly triple-banded and concave (upper left). Note dense chromosomal granules (arrows). x 22,500. Inset: Phase contrast micrograph of the cell in plastic (x 1,280).

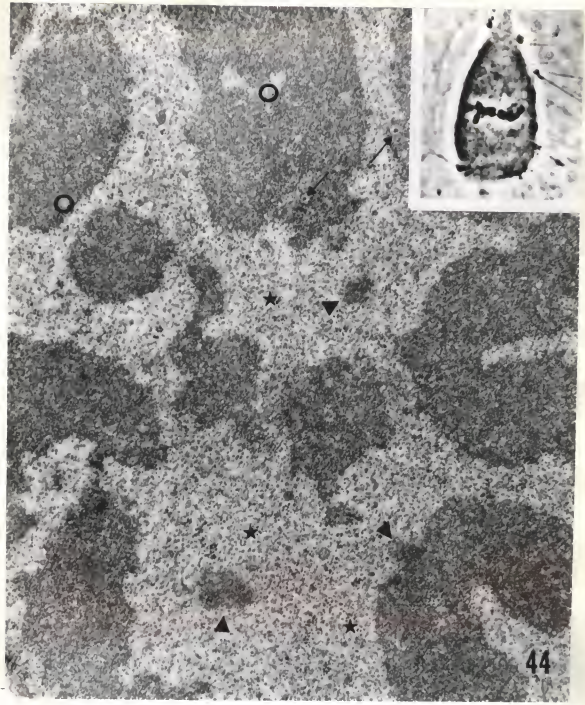

Fig. 44. Metaphase. Para-equatorial section showing three circular kinetochores (arrowheads). Note clusters of MT between chromosomes (*), intrachromosomal MT (circles), dense granules (arrows). x 22,500. Inset: Phase contrast micrograph of the cell in plastic (x 1,280).

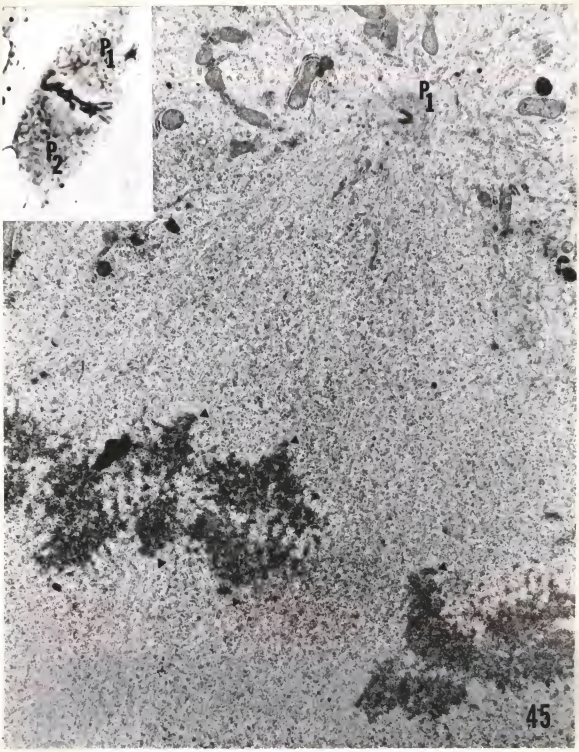

Fig. 45. Very early anaphase. Daughter chromosomes are "pulled" apart in the kinetochore region. Note "frayed" appearance of chromosomes; kinetochores (arrowheads), MT, and a centriole at pole no. 1 (P_1). x 11,500. Inset: Phase contrast micrograph of the cell in plastic (x 1,280).

Fig. 46. Very early anaphase. Several sister kinetochores (K_1, K_2) showing variation of profiles. K_1 in the upper left corner is sectioned obliquely or peripherally. Note the electron dense strand connecting kinetochores of the chromosomes left of center (arrow). x 22,500.

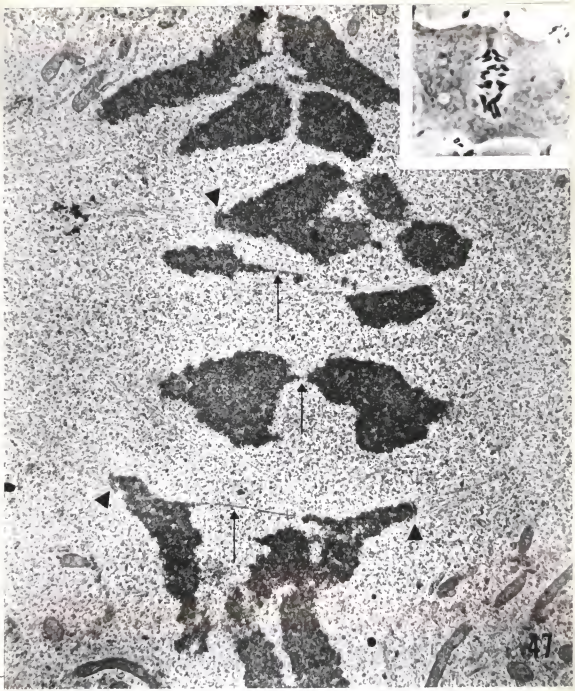

Fig. 47. Early anaphase. Telomeric regions of the separating daughter chromosomes trail the kinetochore regions. Several kinetochores (arrowheads) and connecting strands (arrows) are visible. Black spots are dirt. x 11,500. Inset: Phase contrast micrograph of the cell in plastic (x 1,280).

Fig. 48. Very early anaphase. Two pairs of daughter chromosomes (Ch_1, Ch_2) with their kinetochores (K_1, K_2) and associated MT. Note electron dense strands connecting kinetochore regions of daughter chromosomes (arrows). Serial section of the cell shown in Fig. 45. x 22,500.

Fig. 49. Early anaphase. Three representative kinetochores (K). The angular kinetochore near the right margin is cut obliquely or peripherally. Serial section of the cell shown in Fig. 47. x 30,000.

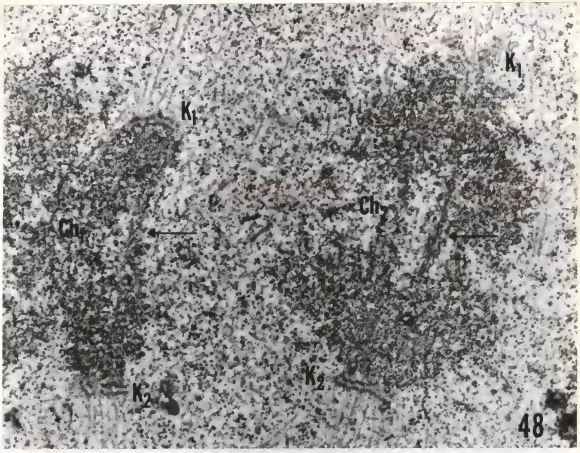
K1
K1
Ch1
Ch2
K2
K2
48


49
K
K
K

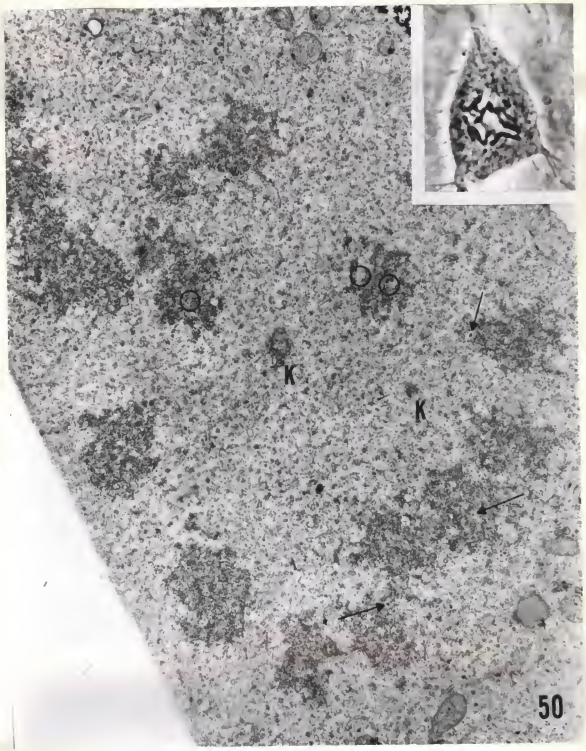

Fig. 50. Mid-anaphase. Para-equatorial section of the cell shown in the inset. Note two circular kinetochores (K), penetrating MT (circles), chromosomal granules (arrows). 15,750. Inset: Phase contrast micrograph of the cell in plastic (x 1,280).

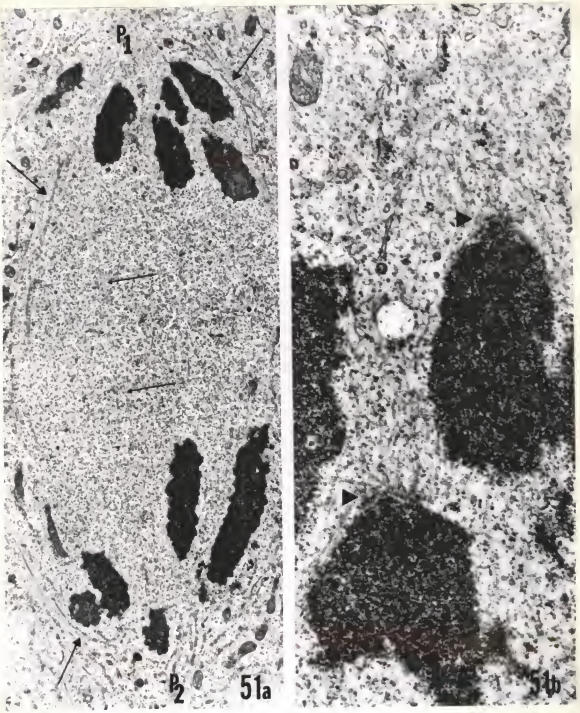

Fig. 51. Late anaphase. (a) Survey of elongated spindle showing two sets of chromosomes near opposite poles (P_1, P_2). Note pieces of double membrane at periphery of spindle area (large arrows), few interzonal MT (small arrows). x 7,750. (b) Detail of chromosome group at pole no. 1. Note rather indistinct kinetochores (arrowheads), MT crossing in front of chromosomes. x 30,000.

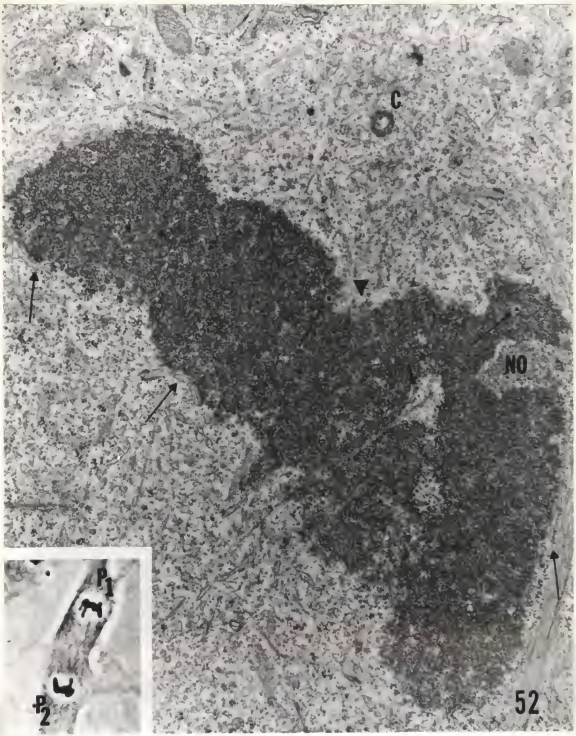

Fig. 52. Very late anaphase. Chromosomal mass near pole no. 1 (P_1). Note fuzzy kinetochore (arrowhead), membrane cisternae (large arrows), chromosomal granules (small arrows), nucleolus organizer (NO), and MT traversing the chromosomal mass. x 22,500. Inset: Phase contrast micrograph of the cell in plastic (x 1,000).

Fig. 53. Very late anaphase. Kinetochore (K) in depression on the poleward face of the chromosomal mass. Note less dense band (arrowhead), density of underlying chromatin, kinetochore MT. Arrows indicate chromosomal granules. Serial section of the cell shown in Fig. 52. x 75,000.

Fig. 54. Very late anaphase. Stem bodies (Sb) in the equatorial region. Serial section of the cell shown in Fig. 52. x 30,000.

Fig. 55a. Very late anaphase. Detail of stem body. Most MT seem to terminate in the stem body or to project a very short distance beyond it, but one MT (arrows) clearly passes through. x 57,500.

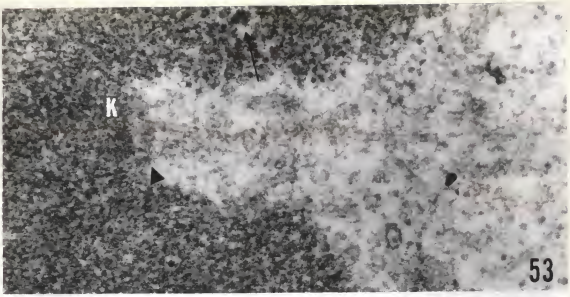
K
53

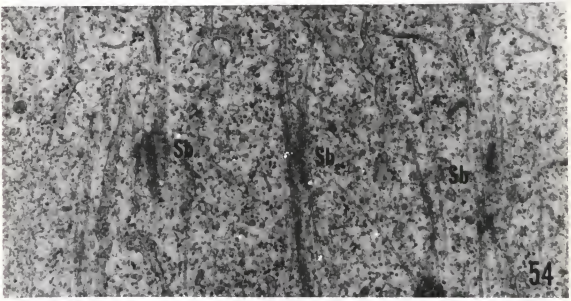
Sb
Sb
Sb
54

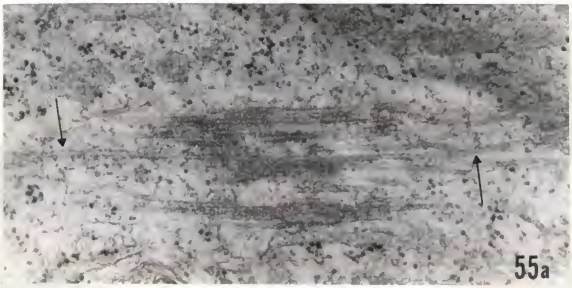
55a

Fig. 55b. Very late anaphase. Mitochondria (Mi), RER, vesicles (V), and MT in the constricted equatorial region. Serial section of the same cell as Fig. 55a. x 22,500.

Fig. 56. Centrioles in early anaphase. An unidentified particle (Pa) and, possibly, a satellite (S) are present. Note MT embedded in amorphous material surrounding the centriole on the right. x 75,000.

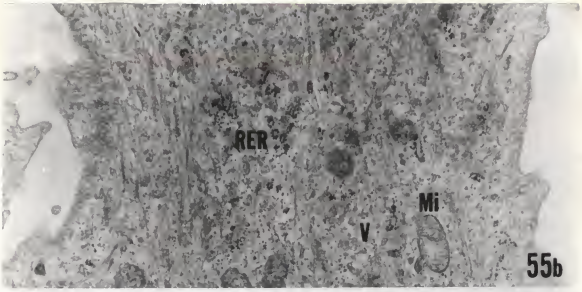
RER
Mi
V
55b

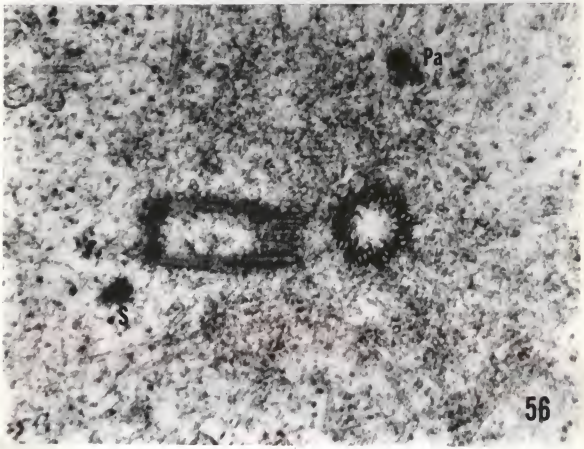
Pa
S
56

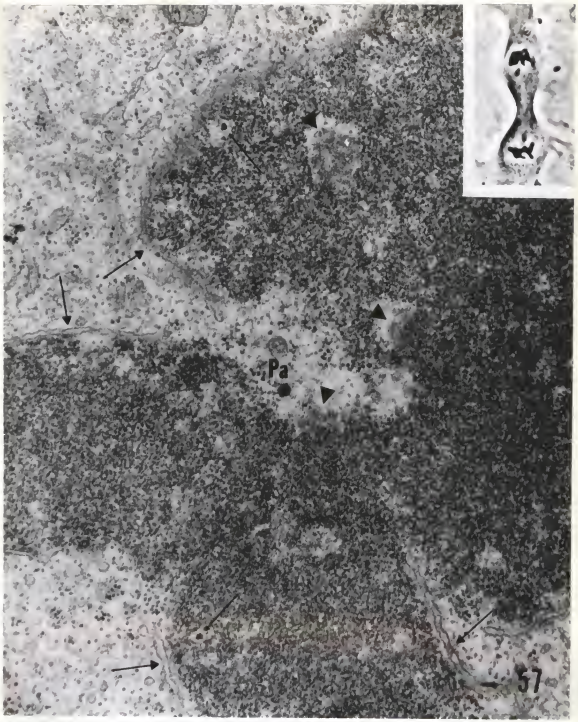

Fig. 57. Early telophase. Reconstitution of the nucleus. Three obliquely sectioned kinetochores within the chromatin mass (arrowheads). Note large pieces of chromatin-associated membranes (large arrows), chromosomal granules (small arrows), and spherical particle (Pa). x 30,000. Inset: Phase contrast micrograph of the cell in plastic (x 1,000).

Fig. 58. Early telophase. Obliquely sectioned nuclear lobe (NL) with pore-annulus complexes (NP). Transversely sectioned pieces of NE indicated by large arrows. Serial section of the cell shown in Fig. 57. x 57,500.

Fig. 59. Mid-telophase. Two kinetochores (K) in pockets on the polar face of the nucleus. Note MT (arrows) associated with the kinetochores. Serial section of the cell shown in Fig. 60. x 50,000.

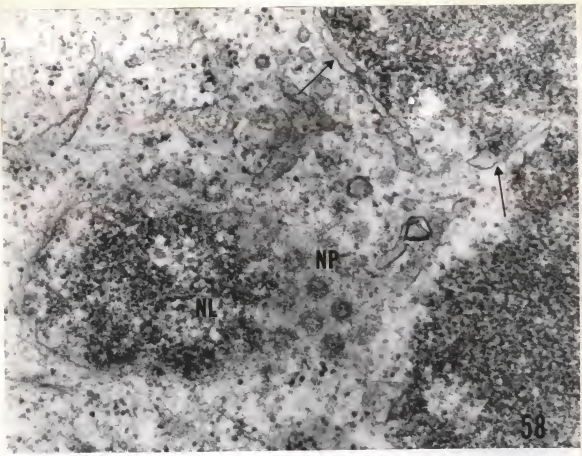
NP
NL
58

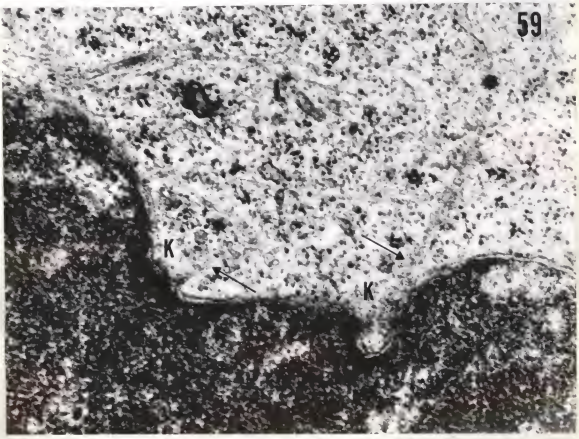
59
K
K

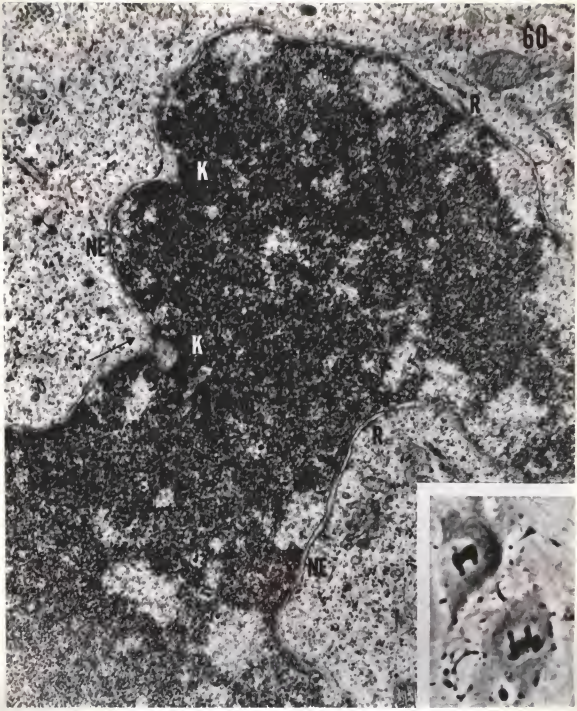

Fig. 60. Mid-telophase. Nuclear envelope (NE) completely surrounds the nucleus. A few ribosomes (R) present on the outer membrane of the NE. Two kinetochores (K) present on the polar face of the nucleus. Note MT (arrow) extending into the kinetochore pocket. x 30,000. Inset: Phase contrast micrograph of the cell in plastic. (x 1,280).

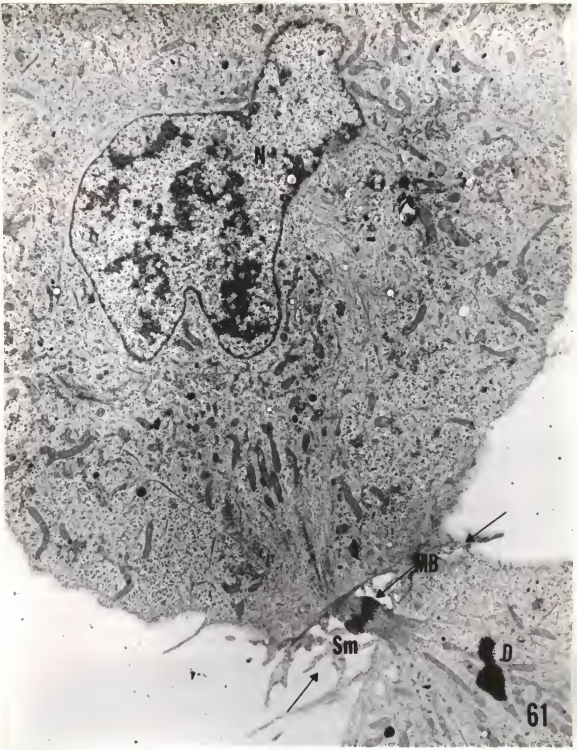

Fig. 61. Cytokinesis. Nucleus (N) of one daughter cell with large heterochromatic patches. Note cleavage furrow (arrows), stem (Sm), midbody (MB). Black spot (D) and small dots are stain marks. x 7,750.

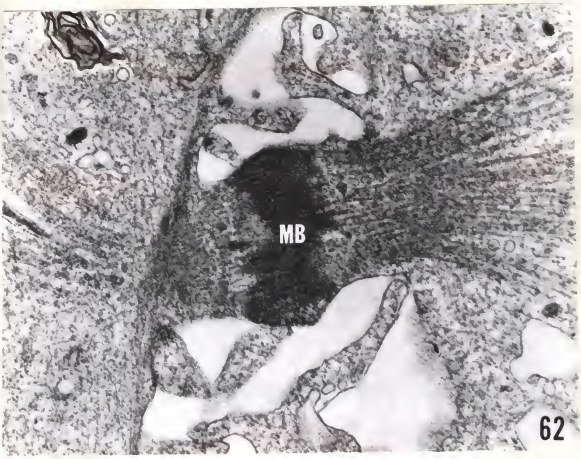

Fig. 62. Cytokinesis. Higher magnification of the stem and midbody (MB) shown in Fig. 61. x 30,000.

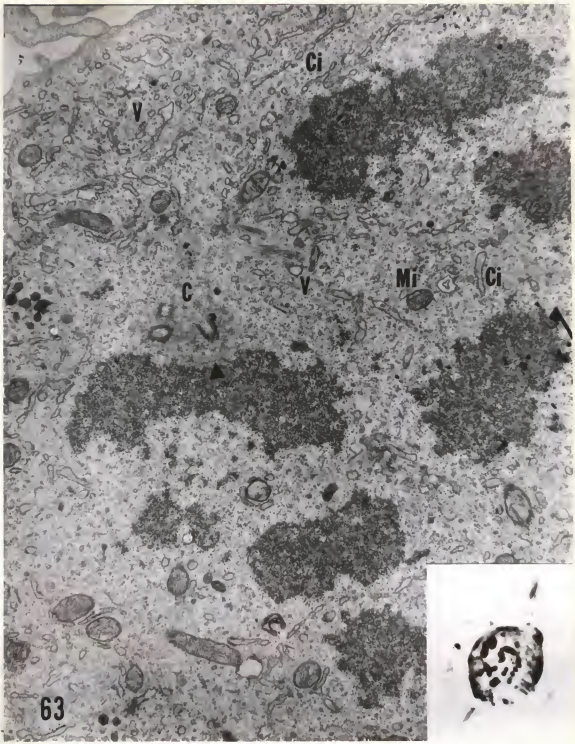

Fig. 63. C-metaphase. The chromosomes are scattered. Three of the four centrioles present in this cell can be seen (C). A kinetochore is opposite the centrioles (arrowhead). Mitochondria (Mi), vesicles (V), and cisternae (Ci) occur in the central area and at the periphery of the cell. Black marks are staining artifacts. x 15,750. Inset: Phase contrast micrograph of the cell in plastic (x 1,280). Treatment A.

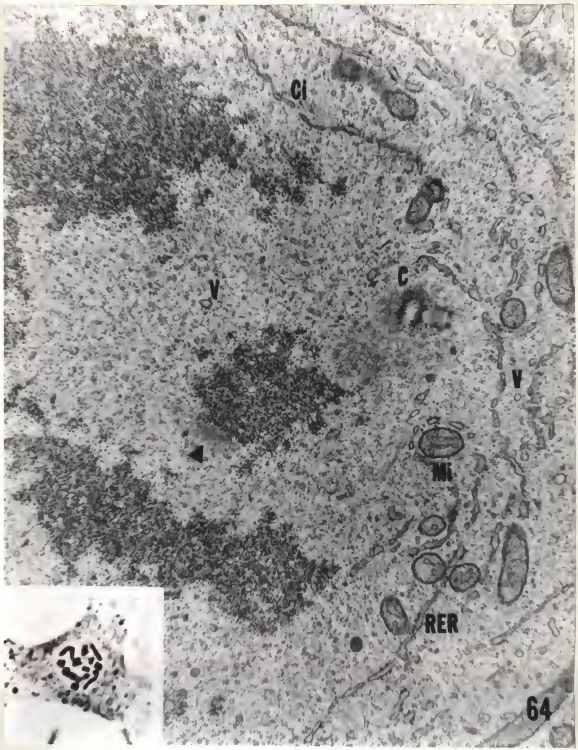

Fig. 64. C-metaphase. Two centrioles are visible (C). A kinetochore is indicated by the arrowhead. Vesicles (V) occur in the central and peripheral areas. Mitochondria (Mi), RER, and cisternae (Ci) are restricted to the peripheral area. x 22,500. Inset: Phase contrast micrograph of the cell in plastic (x 1,280). Treatment A.

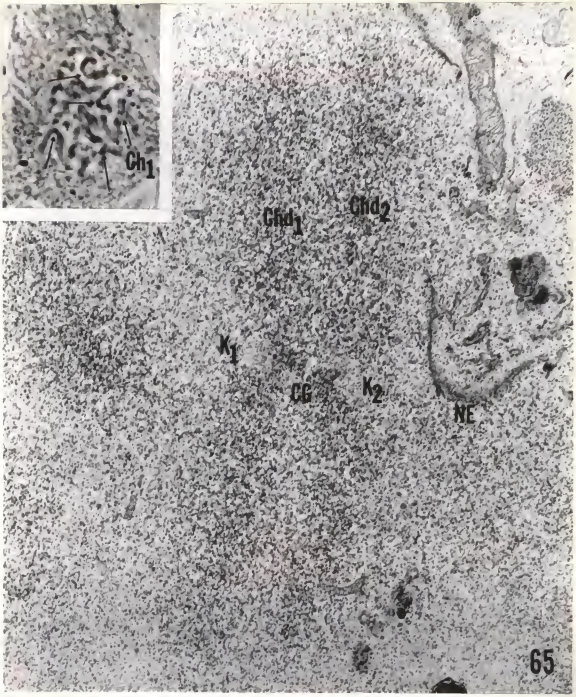

Fig. 65. C-mitosis. Chromosome at the periphery of the central area; Chd_1, Chd_2 its two sister chromatids. Kinetochores (K_1, K_2), centromeric granules (CG) in the primary constriction. The double membranes (NE) are probably fragments of the nuclear envelope. x 22,500. Inset: Phase contrast micrograph of the cell in plastic. Ch_1 the chromosome shown in the electron micrograph. Arrows indicate centromeric granules (x 1,280). Treatment B.

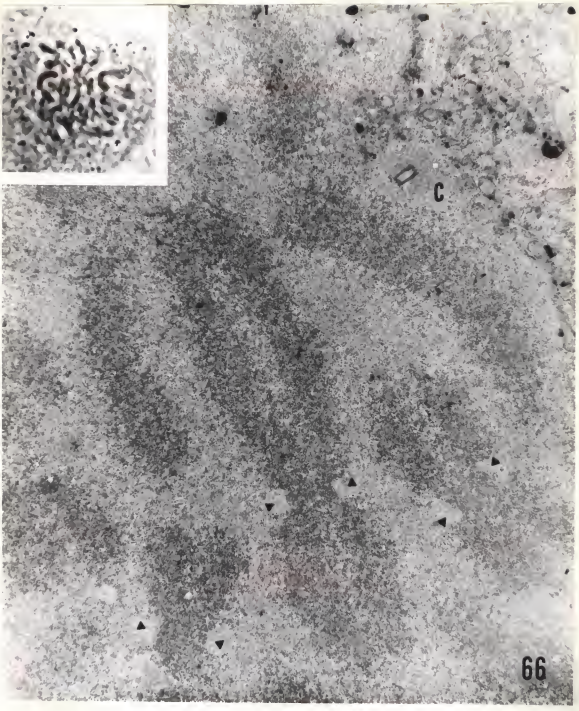

Fig. 66. C-mitosis. Several chromosomes with kinetochores (arrowheads) in the central area. A centriole (C) near the cytoplasmic area. x 11,500. Inset: Phase contrast micrograph of the cell in plastic. (x 1,280). Treatment B.

Fig. 67. Colcemid-treated interphase cell. Nucleus with dispersed chromatin (Chr), nucleolus (Nu), nuclear envelope (NE). x 15,750. Treatment B.

Fig. 68. Colcemid-treated interphase cell. Grazing section of the nuclear envelope (NE) with pore-annulus complexes (NP), helical polyribosomes (R). Note microtubules (MT), and microfibrils (MF). x 40,000. Treatment B.

Fig. 69. C-mitosis. Bundle of microfibrils (MF) in the central area. Same section as in Fig. 66. x 75,000. Treatment B.

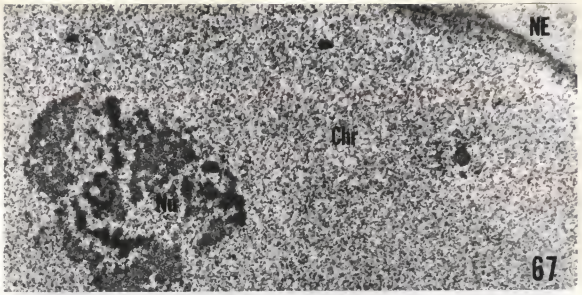
NE
Chr
Nu
67

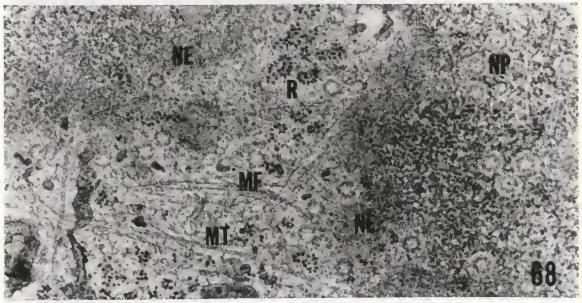
NE
R
NP
MF
MT
NE
68

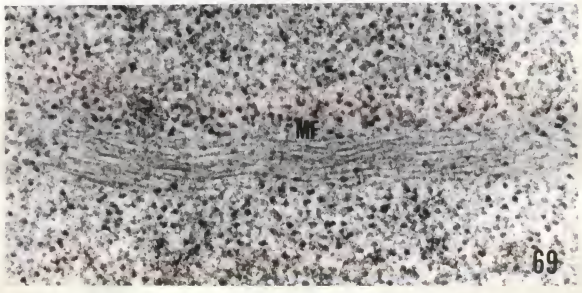
MF
69

Fig. 70. Cold-treated cell in mid-prophase. Note granular component of the dissolving nucleolus (Nu) and its associated chromosome (Ch), a kinetochore (arrowhead), clusters of intranuclear granules (arrows), and chromosomal granules (circles). x 11,500. Inset: Phase contrast micrograph of the cell in plastic. Note the intact NE (x 1,280).

Fig. 71. Cold-treated cell in mid-prometaphase. Three kinetochores (arrowheads) and a bundle of MT are visible. Note achromatic holes in chromosomes, numerous chromosomal granules. x 11,500. Inset: Phase contrast micrograph of the cell in plastic (x 1,280).

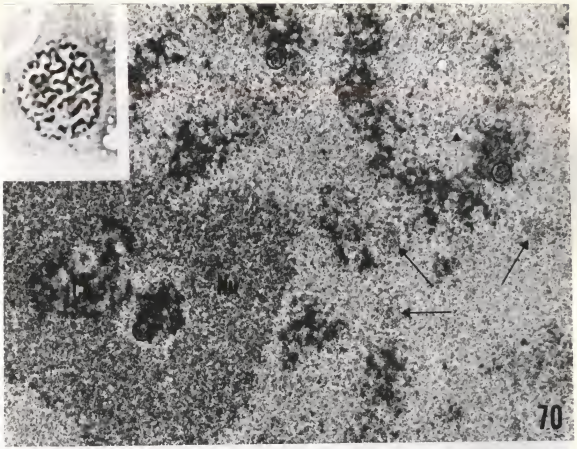
MV
70

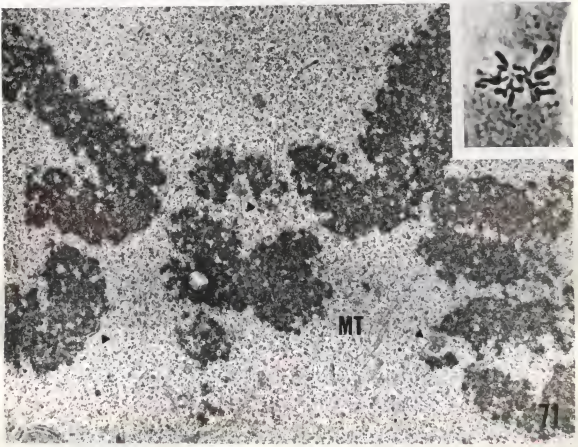
MT
71

Fig. 72. Prophase kinetochores of cold-treated cell. Sister kinetochores (K_1, K_2) lie in cup-shaped depressions. Fine fibrils seem to radiate from the less dense mass of K_2. Note chromosomal granules (circles). Serial section of the cell in Fig. 71. x 40,000.

Fig. 73. Cold-treated cell in metaphase. MT at higher magnification. Note amorphous coating, stark lines of MT walls. x 100,000.

Fig. 74. Cold-fixed control cell in metaphase. Three kinetochores (K) and numerous MT are visible. Compare with Fig. 76. x 30,000.

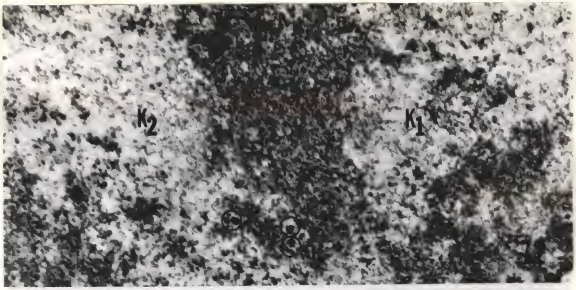
K2
K1

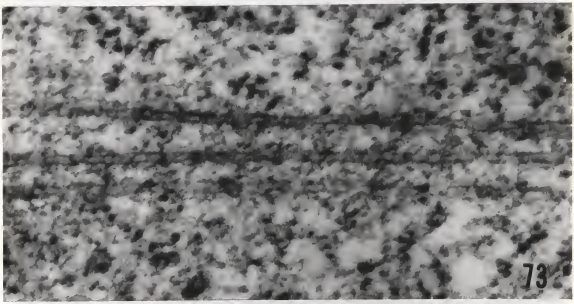
73


K
K
K

Fig. 75. Cold-treated cell in prometaphase. Note fuzzy, but triple-banded profiles of kinetochores (K), associated MT, centriole (C). x 30,000.

Fig. 76. Cold-treated cell in cytokinesis. The midbody (MB) connected to the daughter cell on the right by the stem (Sm). Serial sections at a different level revealed connection to the other daughter cell. Note MT, clumped ribosomes. x 22,500.

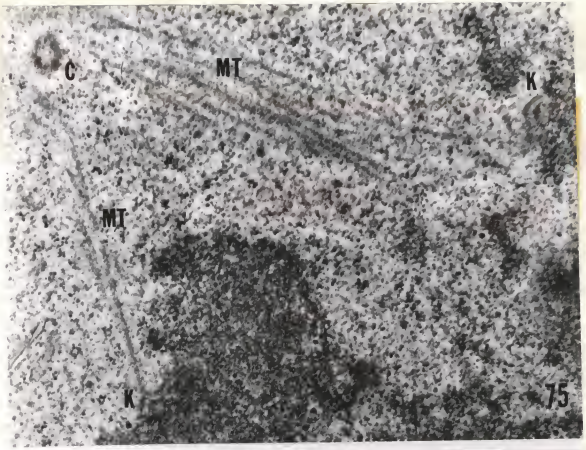
C
MT
K
MT
K
75

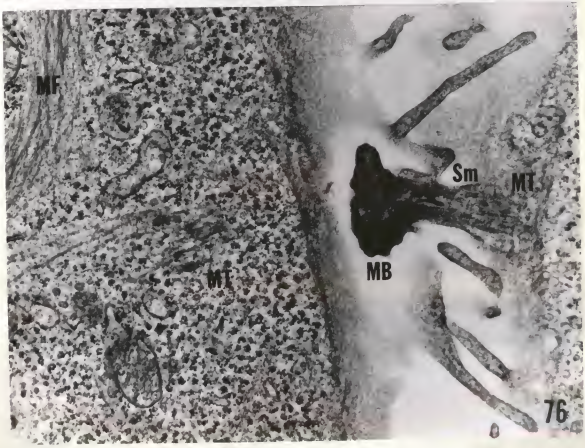
MF
Sm
MT
MT
MB
76

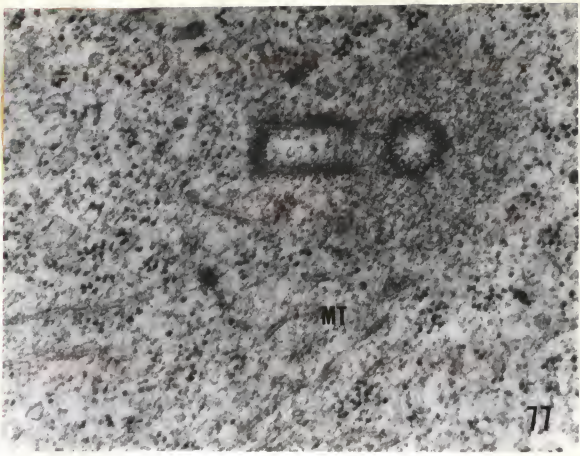

Fig. 77. Centrioles of cold-treated cell in metaphase. Note clarity of triplets in cross-section, amorphous or fibrillar material surrounding the same centriole. x 62,500.

Fig. 78a-e (continued on the following page). Five of seven serial sections of a kinetochore in very early anaphase. (a) Section no. 2. (b) Section no. 4; note corona (Co), outer band (KO), middle band (KM), and inner band (KI). (c) Section no. 5.

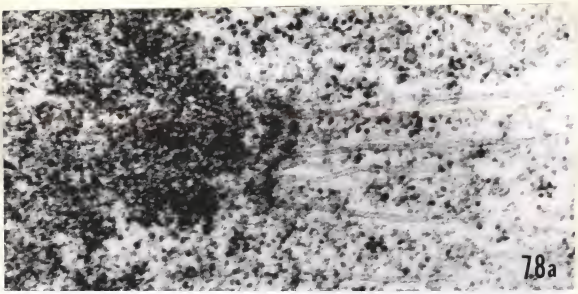

78a

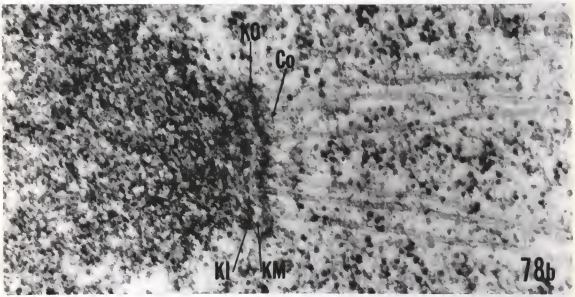

78b

78c

Fig. 78 (contd.). (d) Section no. 6. (e) Section no. 7. From the cell in Fig. 45. x 62,500.

Fig. 79. Peripheral section of a kinetochore in very early anaphase. Note the MT traversing in front of the kinetochore (arrow). From the same cell as Fig. 78. x 50,000.

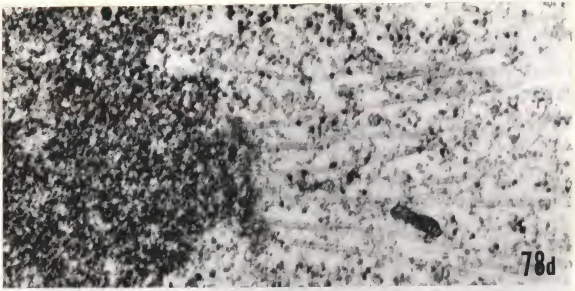
78d

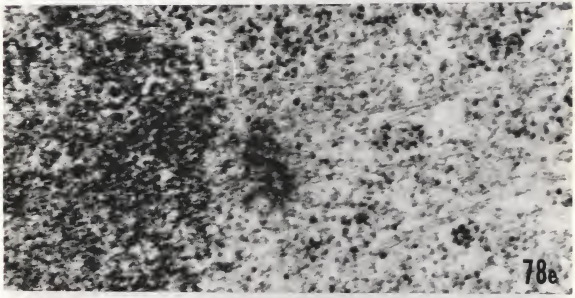
78e

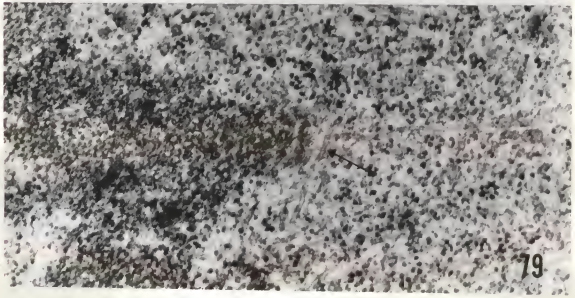
79

Fig. 80. Kinetochore in late prometa- to metaphase. Note 30-50 A fibrils (arrows) in outer layer (KO) of kinetochore, its lesser electron density compared to the chromosome (Ch). x 100,000.

Fig. 81. Metaphase kinetochore. A straight MT (arrow) ends in the outer layer (KO); an obliquely sectioned MT (arrowhead) seems to penetrate outer and middle layers. x 62,500.

Fig. 82. Kinetochore in very early anaphase. MT marked by arrow ends in the outer layer (KO). From the cell in Fig. 45. x 50,000.

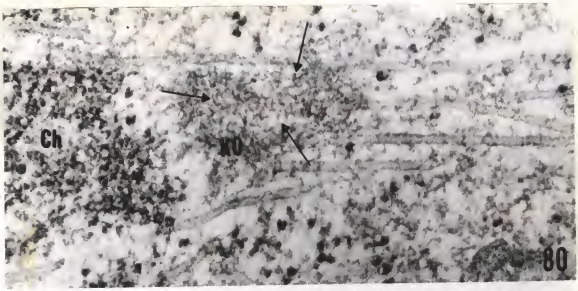
Ch
KO
80

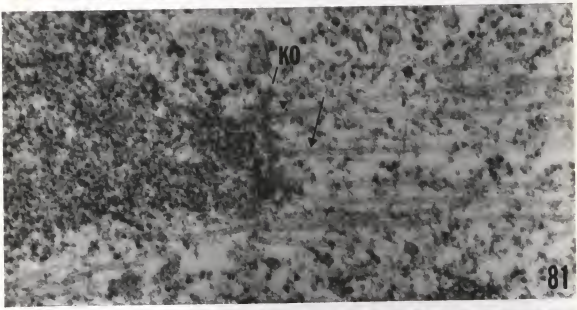
KO
81

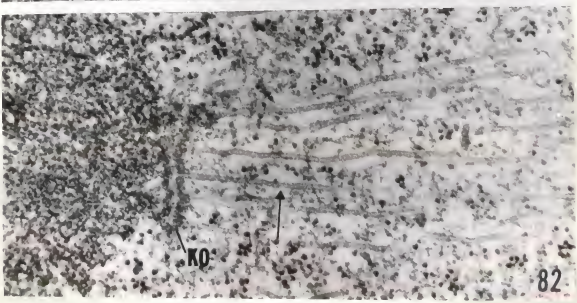
KO
82

Fig. 83a, b. Sister kinetochores in very early anaphase. Note obliquely cut kinetochore MT (some marked by arrows), shape of the kinetochores. From the cell in Fig. 45. x 50,000.

Fig. 84. Early anaphase kinetochore. Note corona (Co), outer (KO), middle (KM), and inner (KI) layers, lesser density of KO compared to KI. From the cell in Fig. 47. x 122,500.

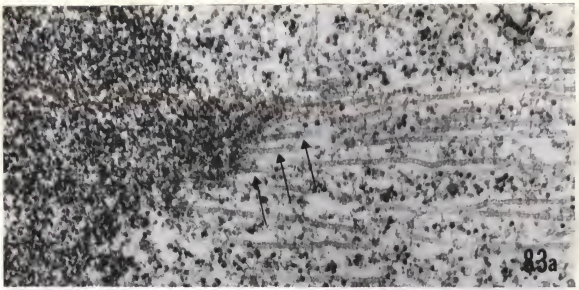
83a

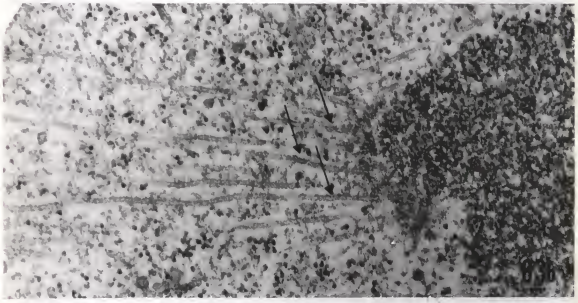
83b

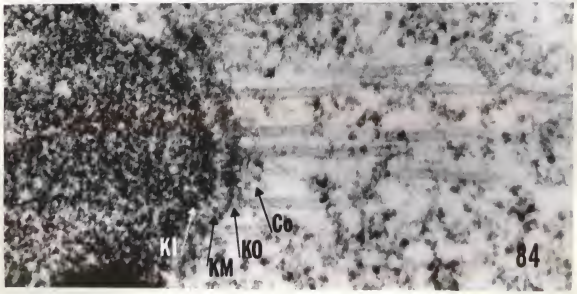
KI
KM
KO
Co
84

Fig. 85a-c. Three serial sections of a metaphase kinetochore (parasagittal). Note triple-layered profile, lesser density of outer layer (arrows) compared to inner layer. From the cell in Fig. 43. x 62,500.

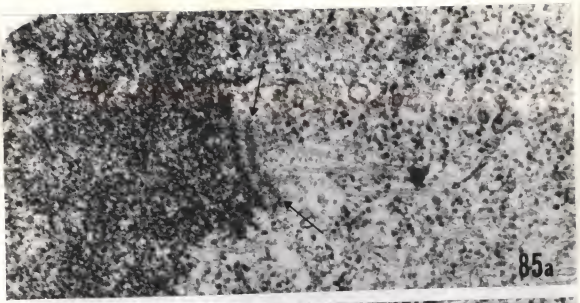
85a

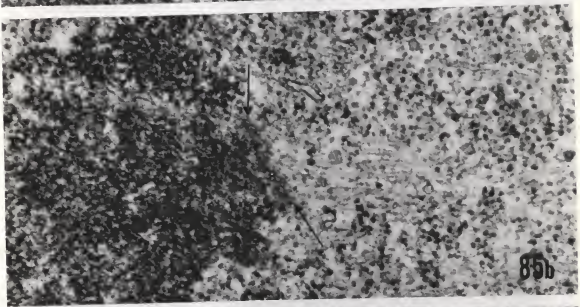
85b

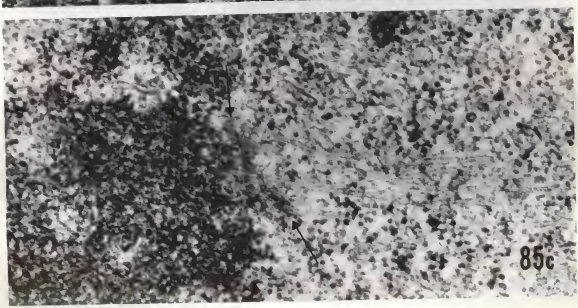
85c

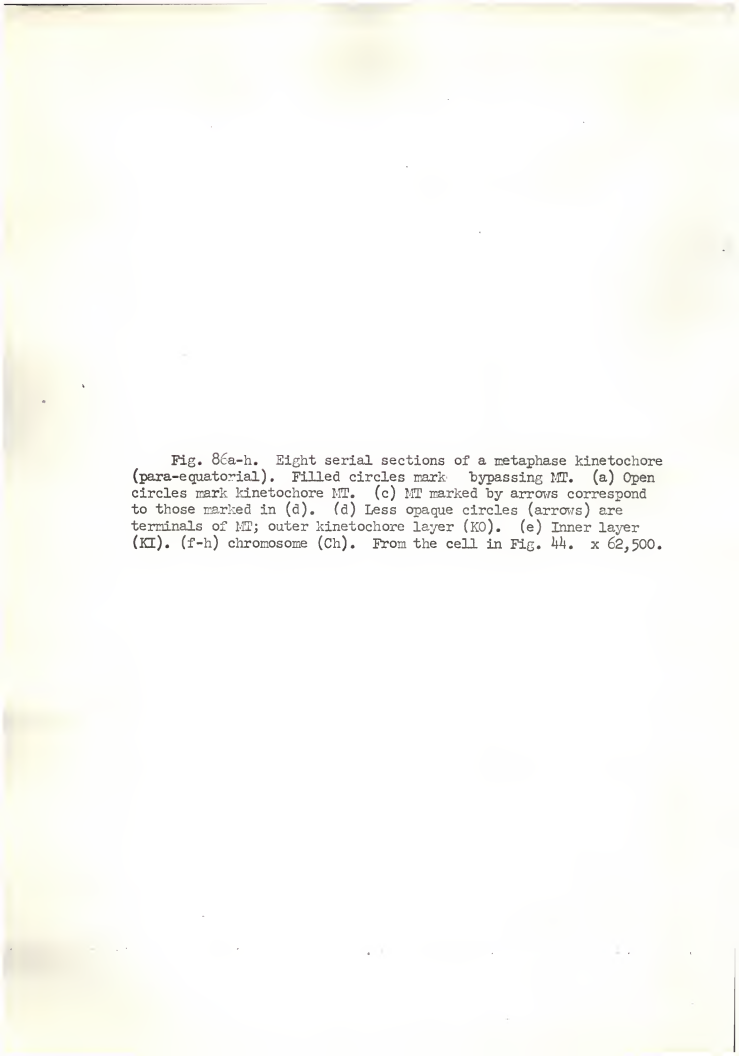

Fig. 86a-h. Eight serial sections of a metaphase kinetochore (para-equatorial). Filled circles mark bypassing MT. (a) Open circles mark kinetochore MT. (c) MT marked by arrows correspond to those marked in (d). (d) Less opaque circles (arrows) are terminals of MT; outer kinetochore layer (KO). (e) Inner layer (KI). (f-h) chromosome (Ch). From the cell in Fig. 44. x 62,500.

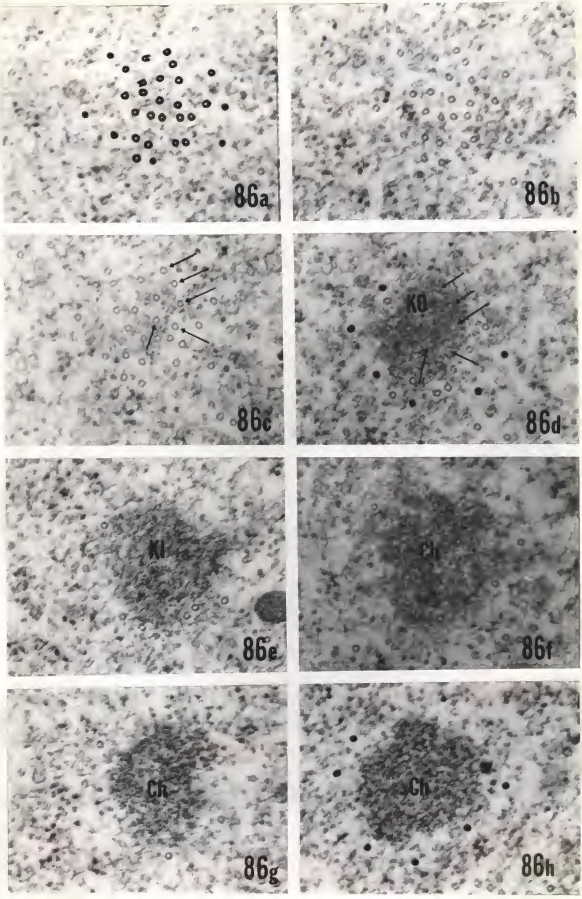
86a
86b
86c
Kd
86d
Kl
86e
Ch
86f
Ch
86g
Ch
86h

Fig. 87a, b. Two serial sections of two metaphase kinetochores (para-equatorial). Filled circles mark bypassing MT. (a) Open circles mark kinetochore MT. MT marked by arrows are the same marked in (b). (b) Arrows mark terminals of MT in outer layer. From the same cell as Fig. 87. x 50,000.

Fig. 88. Metaphase kinetochore. Note electron dense inner layer (large arrow) within less dense outer layper; intrachromosomal MT and granule within clear space (circle); other chromosomal granules (small arrows). From the same cell as Fig. 87. x 50,000.

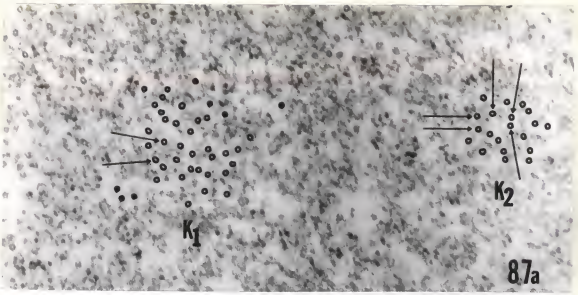
K1
K2
87a

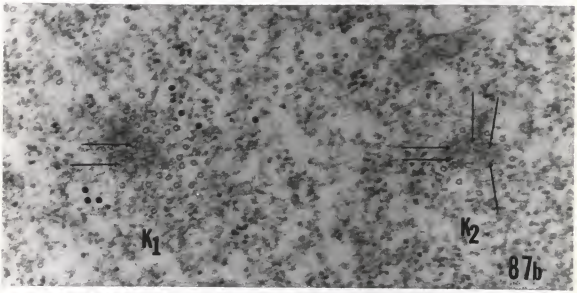
K1
K2
87b

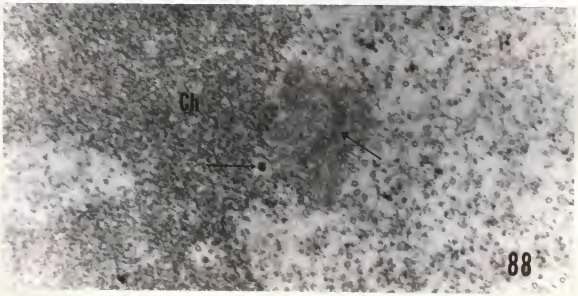
Ch
88

Fig. 89. Para-equatorial section of metaphase cell. Note intrachromosomal MT within clear circle (arrow). From the same cell as Fig. 87. x 62,500.

Fig. 90. Para-equatorial section of metaphase cell. Bundle of kinetochore MT. Note "cross-bridges" (large arrows) and "arms" (small arrows). From the same cell as Fig. 87. x 75,000.

Fig. 91a, b. Two serial sections of mid-anaphase kinetochore (para-equatorial). From the cell in Fig. 50. x 75,000.

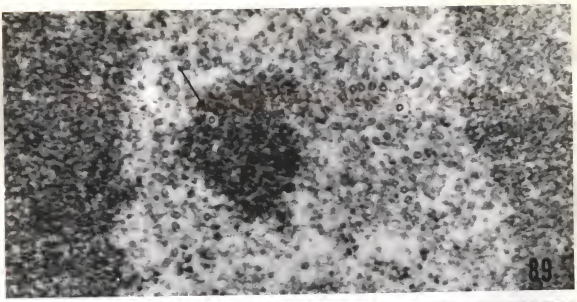
89

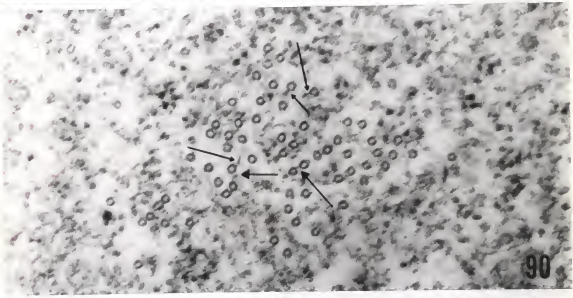
90

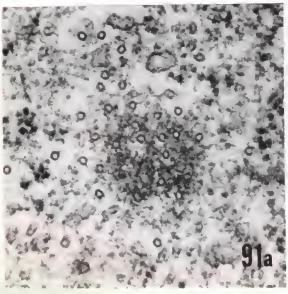
91a

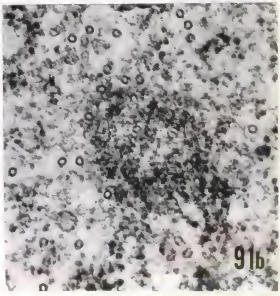
91b

Fig. 92. Kinetochores in c-mitosis. Two chromosomes (Ch_1, Ch_2) in longitudinal section. K_1, K_2, the sister kinetochores of Ch_1. x 50,000. Treatment A.

Fig. 93. Kinetochore in c-mitosis. Grazing section of kinetochore (K), which is seen in face-view in the depression of the primary constriction. Portions of the two arms of the chromatid (Chd). x 50,000. Treatment A.

Fig. 94. Kinetochores in c-mitosis. Sister kinetochores (K_1, K_2) of transversely sectioned chromosome (Ch). Note two centrioles (C). x 50,000. Treatment A.

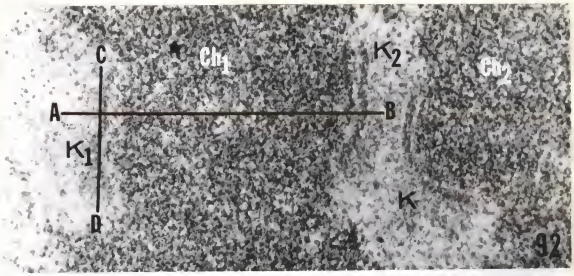
C
Ch1
K2
Ch2
A
B
K1
D
K
92

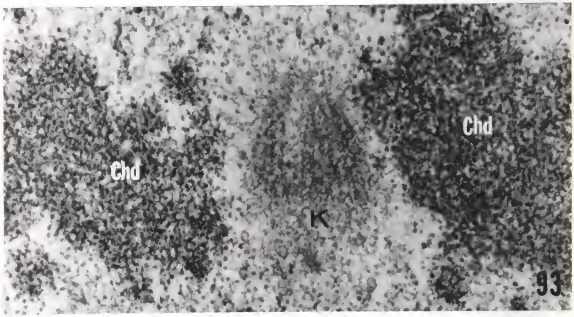
Chd
Chd
K
93

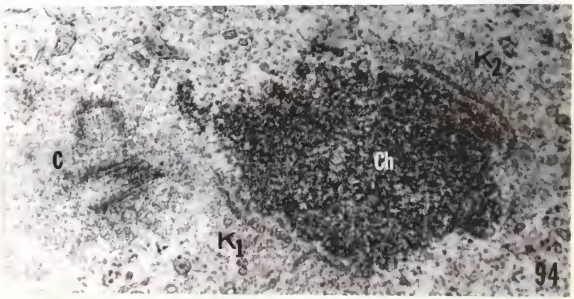
K2
C
Ch
K1
94

Fig. 95a-c. Kinetochores in c-mitosis. Three serial sections (a, b, adjacent) of sister kinetochores (K_1, K_2) with strange profiles. From the same cell as Fig. 94. x 75,000. Treatment A.

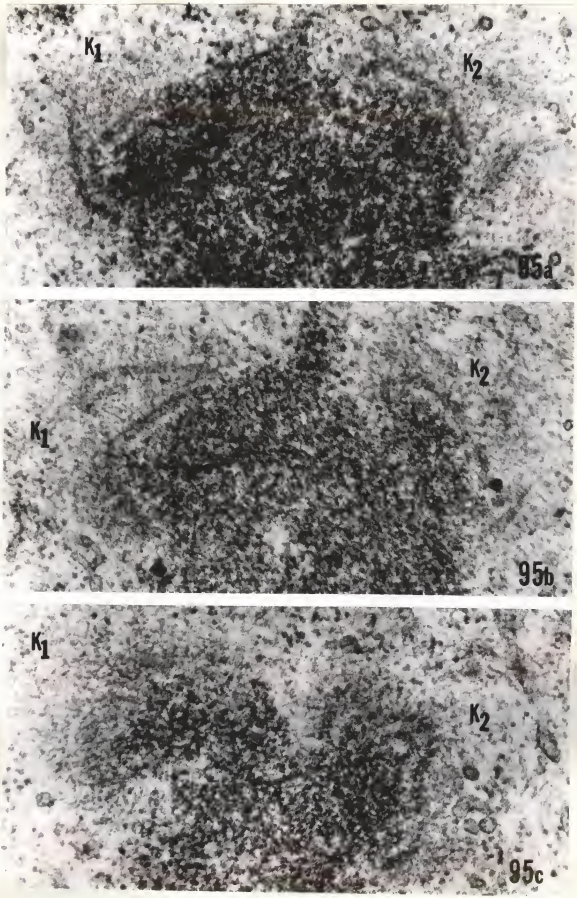
K1
K2
95a
K2
K1
95b
K1
K2
95c

Fig. 96. Kinetochores in c-mitosis. K_1 obliquely, K_2 transversely sectioned, K grazed. From the same cell as Figs. 92 and 93. x 50,000. Treatment A.

Fig. 97. Kinetochore in c-mitosis. Approximately median section. Note doubleness (white arrows), "knots" (black arrows). From the cell shown in Fig. 66. x 100,000.

Fig. 98. Kinetochores in c-mitosis. Sister kinetochores (K_1, K_2) in primary constriction. Note doubleness of K_2. From the cell shown in Fig. 66. x 67,500.

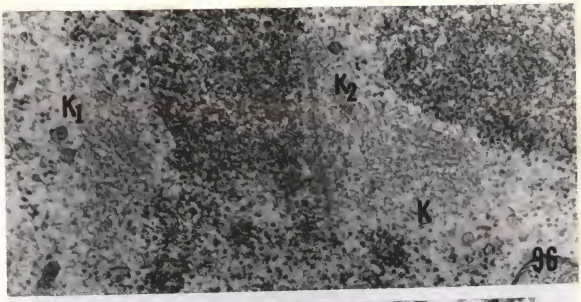
K1
K2
K
96

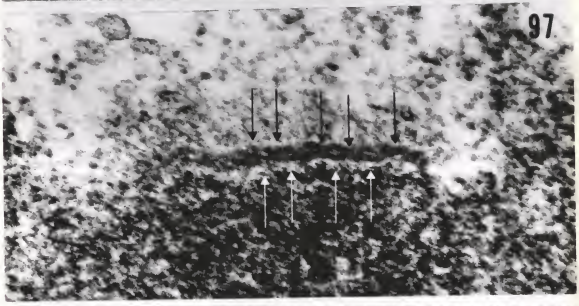
97

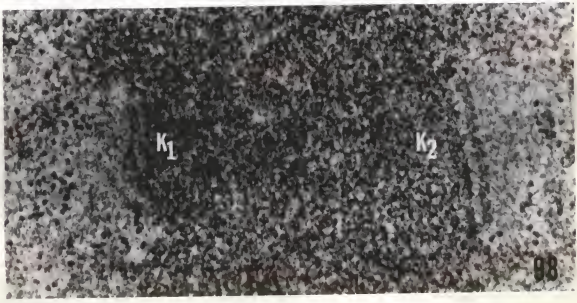
K1
K2
98

Fig. 99. Dicentric bridge in an untreated anaphase cell. The bridge does not appear continuous in this section. Note slight lagging of one of the daughter X chromosomes (X_2), its normal kinetochore (K_2), and the nucleolus organizer (NO). x 11,500. Inset: Phase contrast micrograph of the cell in plastic. Note attenuation of bridge; fragments (arrow), and the X chromosome (X_2); (x 1,280).

Fig. 100. Dicentric bridge in an anaphase cell (serial section of the cell in Fig. 99). Note normal kinetochore (K_2) of bridged chromosome. x 15,750.

Fig. 101. Dicentric bridge in an untreated anaphase cell. Note normal kinetochore (K_2) of bridged chromosome. x 11,500. Inset: Phase contrast micrograph of the cell in plastic. Arrow marks location of fragments (x 1,280).

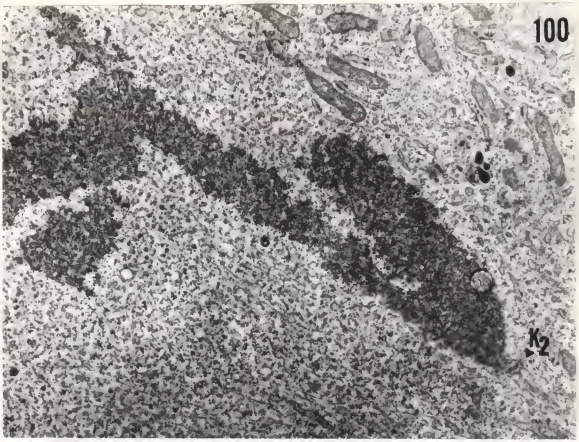
100
K2

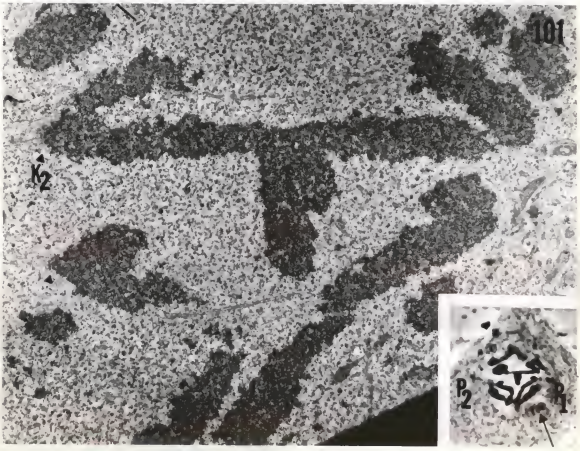
101
K2
P2
P1

Fig. 102a, b. Kinetochores of lagging chromosomes in untreated anaphase cell. (a) Chromosome no. 1(see inset). (b) Chromosome X_2. Note bypassing MT (large arrows), kinetochore MT (small arrows). Fuzzy kinetochore material is indicated by arrowheads. Dark spot left of center in (b) is staining artifact. x 50,000. Inset: Phase contrast micrograph of the cell in plastic. Note position of three laggards (no. 1, no. 2, X_2); (x 1,280).

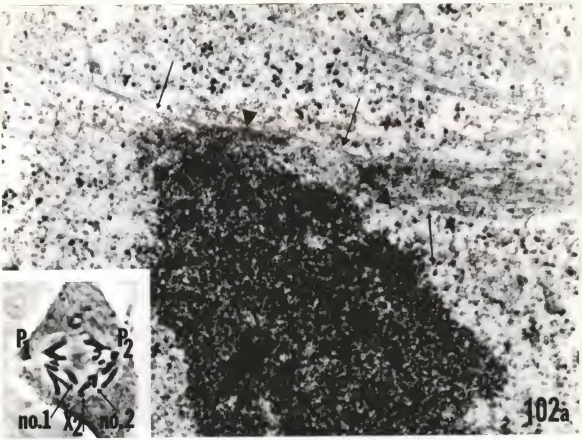
P1
P2
no.1
no.2
102a

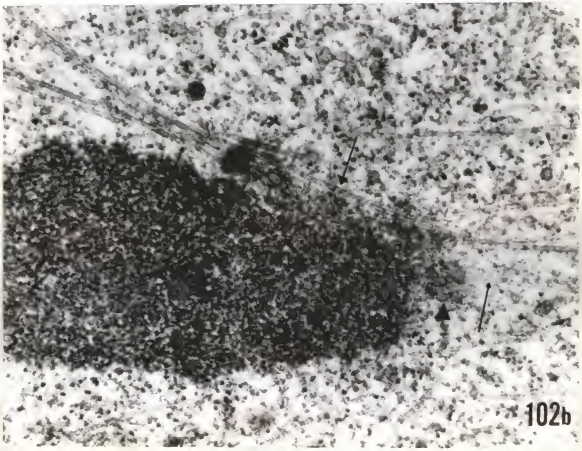
102b

Fig. 103a, b. Kinetochore and MT of a non-lagging chromosome in the same cell as Fig. 102. Note curved and disoriented MT (arrows), kinetochore (K). x 50,000.


K

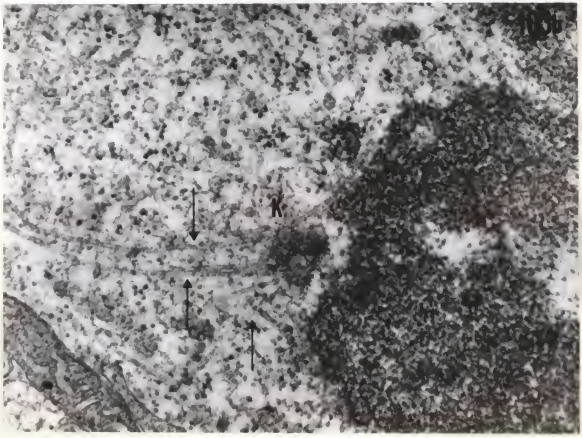
K

Fig. 104. Four centrioles in an untreated interphase cell. x 30,000.

Fig. 105a-c. Abnormal centrioles in an untreated cell in mid-prophase. (a) Centriole pairs (C_1, C_2) on opposite sides of the nucleus. x 7,750. (b) Higher magnification of the centriole seen at C_1 in (a). Note paucity of MT. x 30,000. (c) Serial section of centrioles at C_2 in (a). Note paucity of MT. x 30,000.

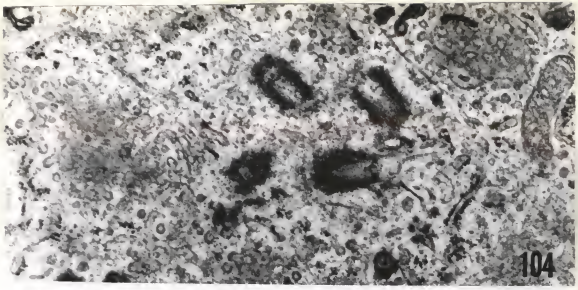
104

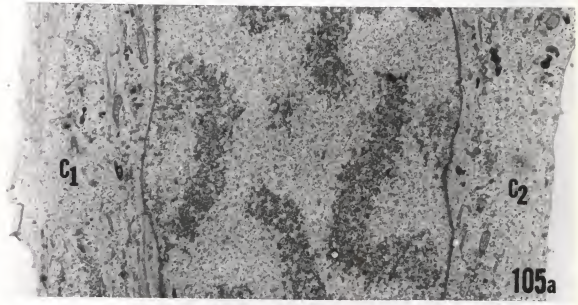
C1
C2
105a

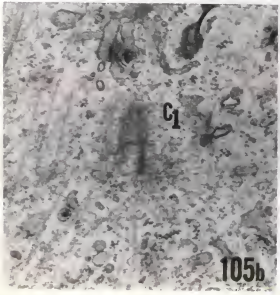
C1
105b

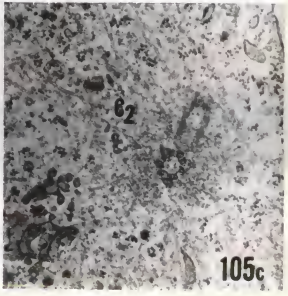
C2
105c

Fig. 106a, b. Abnormal centrioles in an untreated cell in late prometaphase. Two serial sections. Three centrioles (C_1, C_2, C_3) are visible. Note cup-shaped C_1. MT converge on osmiophilic masses left and right of C_1. From the cell in Fig. 29, P_2. x 57,500.

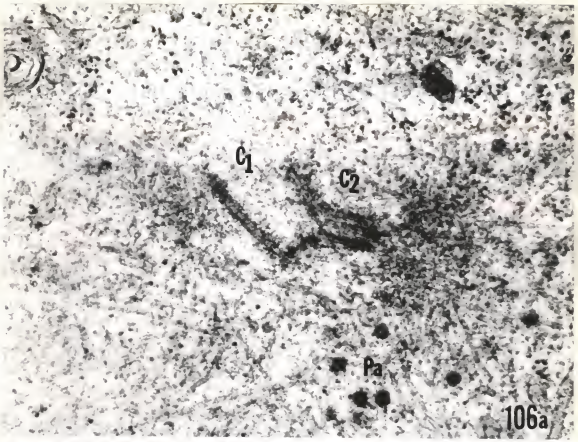
C1
C2
Pa
106a

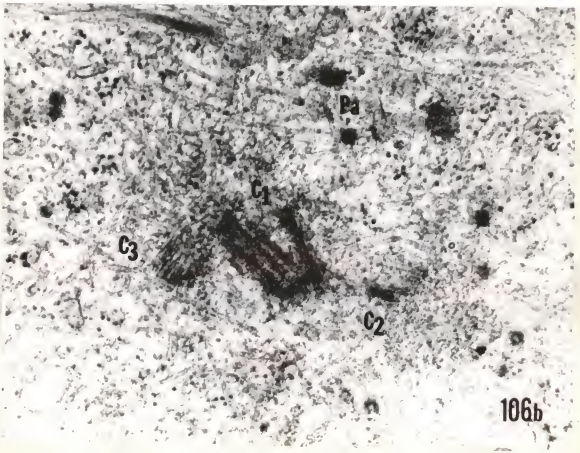
Pa
C1
C3
C2
106b

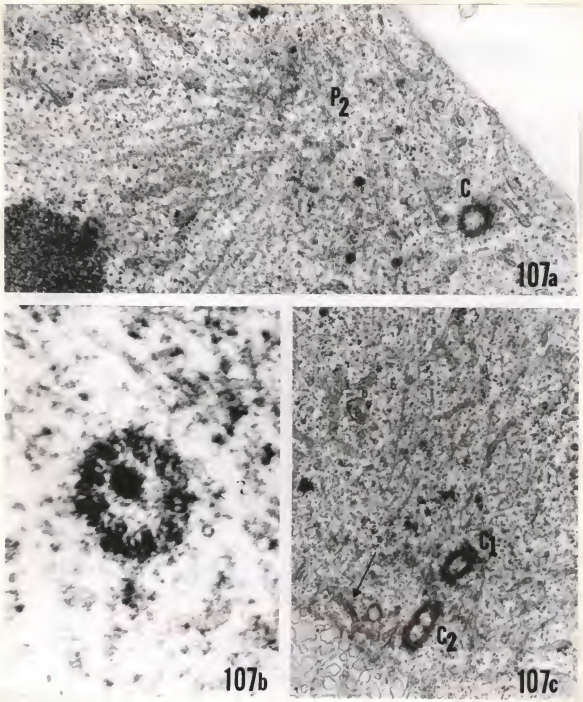

Fig. 107a-c. Abnormal centrioles in an untreated anaphase cell. (a) Pole no. 2 of the cell in Fig. 102. The centriole (C) shown is one of a pair. Note MT converging near P_2, not C. x 30,000. (b) Serial section of the centriole shown in (a). Note particle in centriole lumen. x 137,500. (c) Pole no. 1 of the same cell. Note strange appearance of C_2, possibly a third centriole (arrow). x 22,500.

Fig. 108a-f. Streptonigrin-induced aberrations. Phase contrast micrographs. (a) Aberrant "metaphase". Chromosomes scattered in the spindle, sister chromatids twisted. (b) Very early anaphase. Chromosomes not aligned on the equator. Sister chromatids bifurcated in the stretched centromere regions. (c) Late anaphase. Dicentric bridges (center), acentric fragments (arrow). (d) Late anaphase. Two dicentric bridges (center), acentric fragments (arrow). (e) Late anaphase. Two prominent bridges. Lagging daughter chromosomes connected by very thin bridge (center of spindle). Acentric fragments (arrows). (f) Late anaphase - telophase. Three thin bridges (center), two groups of acentric fragments (arrows). (a), (b), (c), (e), and (f): 0.05 µg/ml SN; (d): 0.01 µg/ml SN; (all x 1,280).

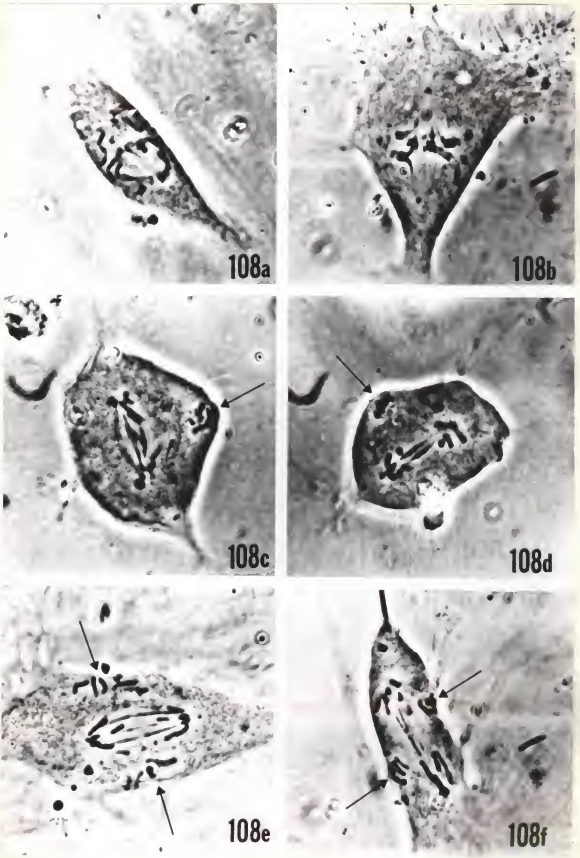
108a
108b
108c
108d
108e
108f

Fig. 109. Streptonigrin-treated cell in early anaphase. Chromatin strand connecting the kinetochore regions of daughter chromosomes (arrows). Note profile of kinetochore (K) in a pocket of the adjacent chromosome. From the cell in Fig. 108b. x 22,500.

Fig. 110a, b. Streptonigrin-treated cell in late anaphase. (a) Portion of a dicentric chromosome with kinetochore (K_2), dense chromatin strand (arrows). One other kinetochore is visible (K). x 22,500. (b) Chromatin strand of a similar bridge at higher magnification. Note difference in coiling between strand (marked by the two lines) and peripheral fibers. x 157,500. Both from the cell in Fig. 108f.

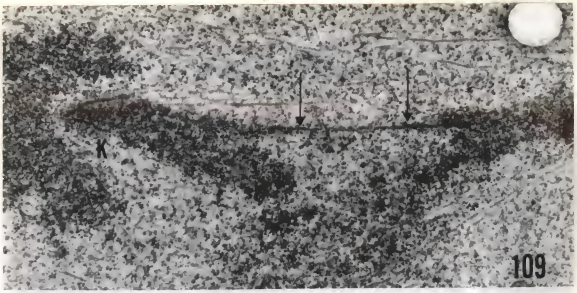
K
109

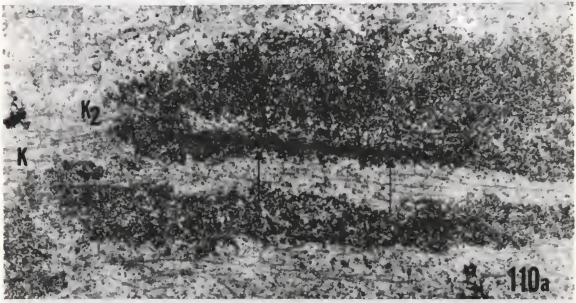
K2
K
110a

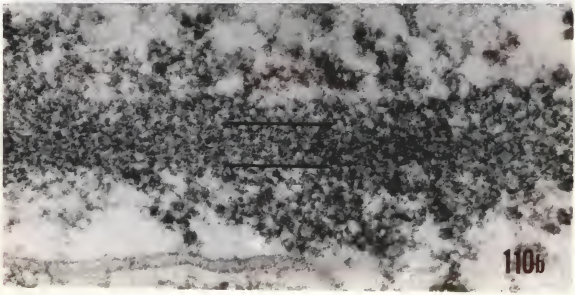
110b

Fig. 111a-c. Streptonigrin-treated cell in late anaphase. (a) Kinetochore (K) and strand (arrows) of a dicentric chromosome. x 22,500. (b) Telomeres of two long daughter chromosomes (Ch_1, Ch_2). Note patches of more densely packed fibers (arrows). x 22,500. (c) Loosely coiled chromosome with patches of more densely packed fibers (arrows). x 40,000. All from the cell in Fig. 108c.

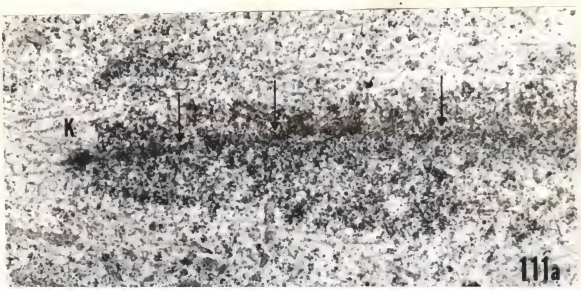
K
111a

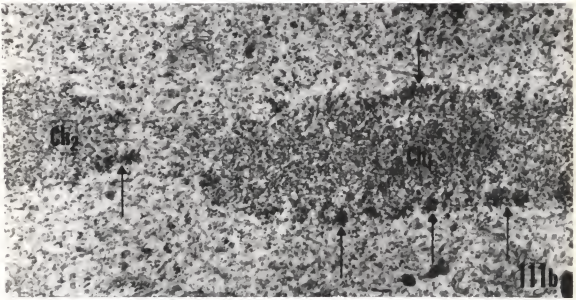
Ch2
Ch1
111b

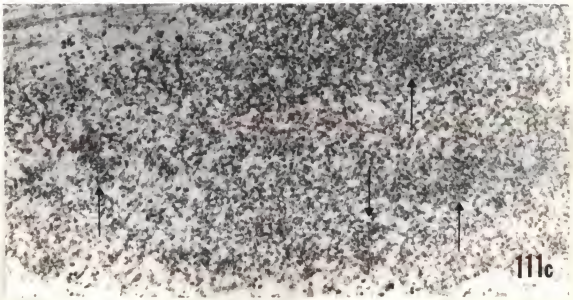
111c

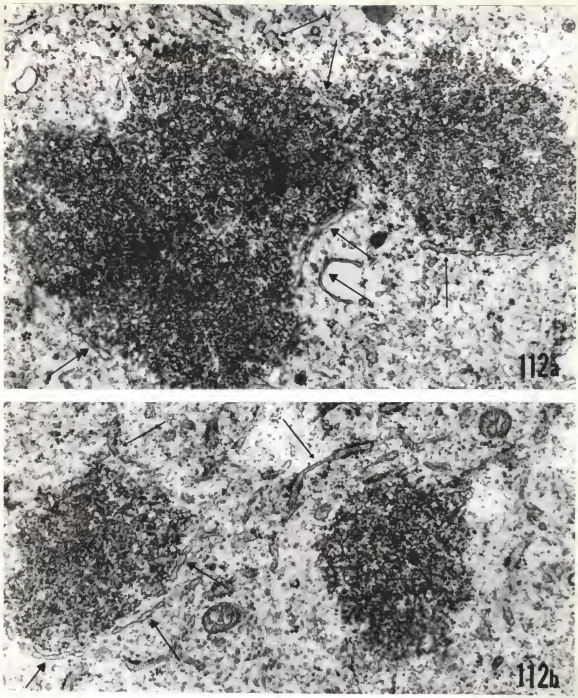

Fig. 112a, b. Streptonigrin-treated cells in late anaphase. Reconstruction of the NE. (a) Portion of a polar group of chromosomes. Note close relationship of membrane cisternae (large arrows) and RER (small arrows) with chromatin. From the cell in Fig. 108d. x 30,000. (b) Portions of two chromosomes near a pole. Note membrane cisternae apposed to chromosome (large arrows), RER in proximity to chromosomes (small arrows). From the cell in Fig. 108f. x 30,000.

Fig. 113. Streptonigrin-treated cell in late anaphase. Note position of the kinetochores (K) relative to the pole (which was just beyond the left margin). From the cell in Fig. 108d. x 30,000.

Fig. 114. Streptonigrin-treated cell in late telophase. Portion of the nucleus shown in Fig. 116. Note nuclear pocket near left margin. Osmiophilic patches (arrowheads) are presumably remnants of kinetochores. Another kinetochore (K) within the nucleus; note its associated MT (arrows). x 50,000.

Fig. 115. Streptonigrin-treated cell in late telophase. Nuclear pocket with remnant of kinetochore (black arrow). A MT penetrating into the nucleus (white arrow). x 75,000.

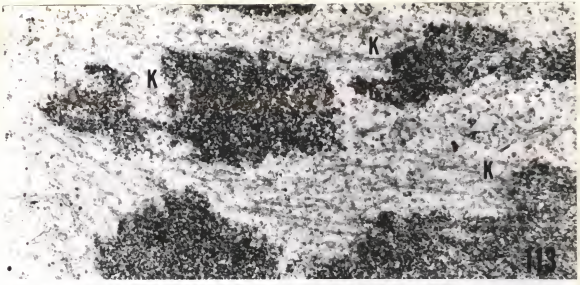
K
K
K
113

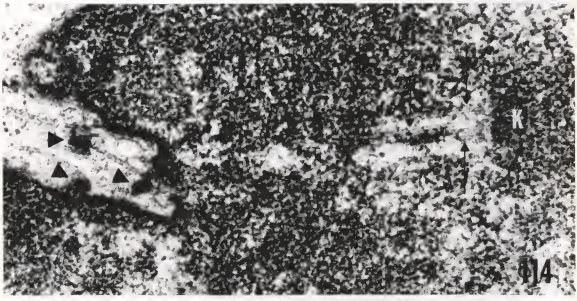
K
114

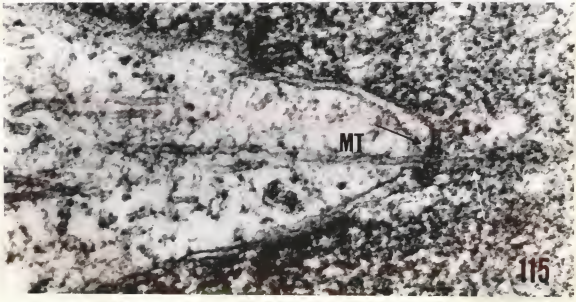
MT
115

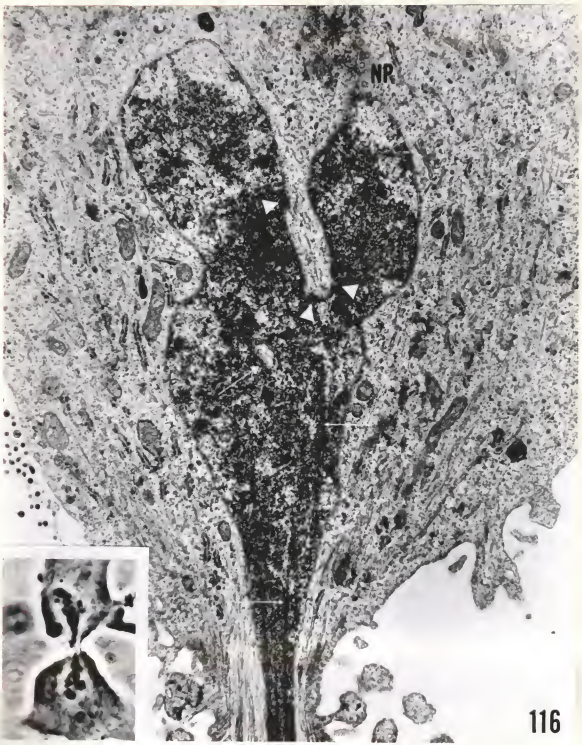

Fig. 116. Streptonigrin-treated cell in late telophase. Nucleus of the upper daughter cell in the inset. Note nuclear pore complexes (NP), kinetochores (arrowheads), nuclear pocket (also at the large arrow), intranuclear MT (small arrows). x 15,750. Inset: Phase contrast micrograph of the cell in plastic (x 1,280).

Fig. 117a, b. Streptonigrin-treated cell in late telophase. (a) Nuclear pockets; piece of RER trapped in the nucleus (arrow). x 62,500. (b) Ribosome-like particles on outer and inner membrane of NE (arrows). x 75,000. Both from the cell in Fig. 116.

Fig. 118. Streptonigrin-treated cell in late cytokinesis. Portion of the nuclear bridge (arrows) near the nucleus (N) of one daughter cell. x 15,750.

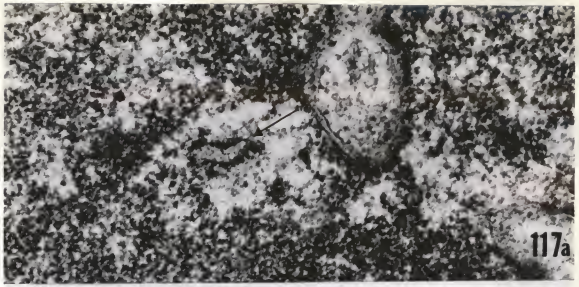
117a

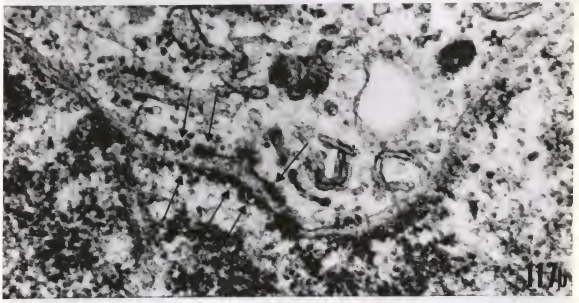
117b

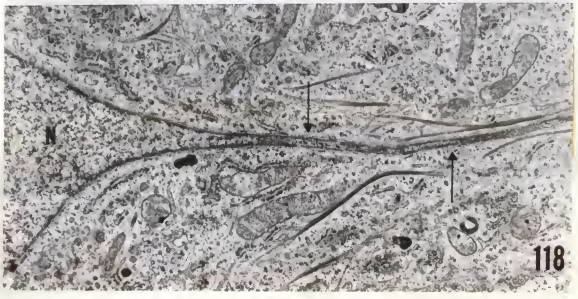
N
118

Fig. 119a, b. Streptonigrin-treated cell in late cytokinesis. (a) Drop-shaped nuclear bleb (near left margin) and fine nuclear bridge (arrows). Note midbody (MB), MT. x 7,750. (b) Micronuclei (MN) with intact NE (arrows). Note main nucleus (N). x 40,000. Both from the same cell.


MT
MB
119a


N
M
M
119b

DISCUSSION

The phase contrast micrographs taken prior to sectioning of selected cells were extremely helpful in determining mitotic stages. Equally important, they facilitated the task of locating individual chromosomes on thin sections, thus safeguarding against utterly false conclusions. Consider, for example, Figure 27. From the electron micrograph it would appear there is one long chromosome with four kinetochores at the equator of the spindle. Phase contrast micrographs at different levels of focus clearly revealed two different chromosomes.

Not only the combination of light and electron microscopy, but also the rat kangaroo cells themselves were an asset in this study. The low chromosome number, the individuality of the chromosomes, and the fact that the axis of the mitotic spindle in these cells is always more or less parallel to the growth surface, all allowed a more detailed study of mitosis than has ever been published for animal cells.

Centrioles

Structurally, the centrioles of PtK_2 cells, whether untreated, colcemid-, cold-, or SN-treated (Figures 4, 9, 56, 77, and 94), are similar to those in other cells and organisms (e.g., Brinkley and Stubblefield 1970, de Harven 1968, Erlandson and de Harven 1971, Robbins et al. 1968). The nine tubular triplets are embedded in an osmiophilic matrix, which may be differentiated into ill-defined structures (Figure 9). This matrix appears to be continuous with the extensive, slightly less osmiophilic material at the distal end

(Figures 56 and 77). At the proximal end the centriole is differentiated into the typical cartwheel (Figure 9). Satellites and an intracentriolar vesicle occur (Figures 4, 9, and 56), but I have been unable to follow possible changes during the cell cycle, or to assess the effect of cold, colcemid, or SN on these structures. The osmiophilic, globular particles found near the centrioles at all stages of mitosis are a mystery. They have also been observed by Brinkley (personal communication). The possibility that they are virus particles lies at hand, but is not confirmed. One is tempted to speculate that their consistent association with the centrioles assures distribution to daughter cells.

Centriole duplication follows the well-known pattern (Brinkley and Stubblefield 1970, Erlandson and de Harven 1971, Murray et al. 1965). Daughter centrioles arise at approximately a right angle to parent centrioles (Figure 8). I have not obtained a sufficient number of favorable sections of this stage to be able to confirm that daughter centrioles are formed at the proximal end (see Brinkley and Stubblefield 1970). However, centrioles at the poles of the mitotic spindle are oriented so that the proximal ends with the cartwheel point away from each other (Figures 20, 56, and 77). Unless rotation and dislocation occur following duplication, this configuration must reflect the original parent-daughter association. It is interesting to note here that the orthogonal arrangement is not the case in interphase cells with supernumerary centrioles (Figure 104). Sections of colcemid-treated cells (Figure 63) confirmed the observation by Brinkley et al. (1967) that this drug does not inhibit duplication of centrioles. The same is true for the spindle poison vincristine (Journey et al. 1968).

Whether centrioles also duplicate during cold treatment could only be ascertained by direct observation or cinemicrography of living cells. I have observed parent-daughter pairs in a cold-treated cell in early prophase. In this case duplication could have occurred prior to treatment and the cell may have been completely arrested by cold.

No other organelle in cells of higher animals can match the esthetic appeal of centrioles. Their orderly, symmetrical structure is certainly in part the cause for much of the attention they have received since the early electron microscopic studies of Burgos and Fawcett (1956) and de Harven and Bernhard (1956). In recent years, however, the interest provoked by these intriguing organelles has led to unwarranted speculation about their function (Brinkley and Stubblefield 1970, Stubblefield and Brinkley 1967; see also discussions by Pickett-Heaps 1969, 1971).

One such hypothetical function is the generation of continuous spindle MT (Brinkley and Stubblefield 1970). It is clear that ultrastructural studies can contribute only circumstantial evidence for this hypothesis. In prophase cells, the centrioles appear to be the focus of the increasing number of MT (Figure 11). Some of these will undoubtedly become astral MT, others probably continuous and, possibly, kinetochore MT. Except for the relatively rare skew MT, all the MT of the fully formed spindle converge towards the centrioles (e.g., Figures 29 and 45). Several investigators have claimed to have observed MT directly connected to the tubules of the centrioles (Krishan and Buck 1965), or inserted into the centriole wall between the triplets (Brinkley and Stubblefield 1970, Gall 1961). I have examined these published electron micrographs and found them totally unconvincing.

Furthermore, I have examined numerous of my own micrographs of centrioles at all stages of mitosis. In reasonably thin sections there is no evidence whatsoever for direct connections between MT and centrioles. Rare images where this seems to be the case can be explained by lack of resolution or superposition in rather thick sections. If the hypothesis were correct, one could reasonably expect such MT-centriole associations to be frequent and unambiguous. The fact that even the most ardent proponents of the hypothesis cannot claim this speaks for itself.

Having dispensed with a popular myth we now can direct our attention to a probably more important polar constituent, the osmiophilic material surrounding and partly enveloping the distal ends of the centrioles (e.g., Figures 45 and 56). The possibility that this material is absent or reduced in amount at least during part of the interphase (e.g., Figure 3) merits further investigation. It is certainly present during all stages of mitosis, and it seems to be arranged mainly around one of the centrioles of a pair, probably the parent (Figures 56 and 77). I have been unable to observe changes related to the mitotic cycle, as reported for HeLa cells by Robbins et al. (1968). The material also occurs in colcemid-, cold-, and SN-treated cells (Figures 63 and 77). Spindle MT penetrate into this material in a rather chaotic fashion and apparently terminate there (Figure 56).

Pickett-Heaps (1969) suggested that the microtubule-organizing-center (MTOC) of animal cells could be in the osmiophilic material, rather than the centrioles themselves. He did not explicitly discuss the possibility that the MTOC, or some other component of the

osmiophilic material, could also be the pole-determinant, but the two functions are obviously related. A rather diffuse, morphologically less well-defined polar determinant and MTOC could apply to acentriolar mitosis in higher plants and other organisms as well.

The concept of MTOC as stated above is amenable to scrutiny in animal cells. Ultrastructural investigations of the following possibilities would yield significant information: (1) The number of mitotic poles is correlated with the number of single centrioles or pairs of centrioles regardless of the presence or absence of osmiophilic material. (2) The number of poles is correlated with the number of masses of osmiophilic material, regardless of the number of centrioles present. Light microscopic observations have produced some evidence against point (1). Normal bipolar divisions are more frequent than multipolar divisions in somatic hybrid cells (e.g., Yamanaka and Okada 1968), and in spermatocytes of certain Diptera mitosis can take place in cells lacking centrioles (Dietz 1959, 1966). Some of the centriole aberrations I observed provide additional information. For instance, the centriole shown in Figure 107a is not at the spindle pole. In a preliminary study on the effect of the alkylating agent TEPA (triethylenephosphoramide) I have observed a solitary centriole in the interzone of a tripolar anaphase. Osmiophilic material was associated with this centriole and some MT converged at this site, but it was not a functional mitotic pole. On the other hand, both osmiophilic masses in Figure 106 are foci of MT. It appears that the presence of a centriole in a mitotic cell is not identical with the formation of a pole. Whether the same applies to osmiophilic masses remains to be seen. Centriole-free divisions as in dipteran spermatocytes would be the system of choice to investigate this.

In the view of Brinkley and Stubblefield (1970) centriole migration is a consequence of the generation of MT, i.e., the centrioles "propel themselves to the opposite mitotic poles by pushing against each other through the spindle which they generate." The same concept has been adopted by Friedländer and Wahrman (1970) and McIntosh et al. (1969). This idea is plausible, for no matter what kind of pole-determinants we propose, we are faced with the problem how they reach opposite poles. Centriole migration does not occur in colcemid-treated cells (Figure 63; see also Brinkley et al. 1967). I have seen a few MT around centrioles in interphase cells treated with 0.25 µg/ml colcemid, but not in mitotic cells. It would be very interesting to know if centriole migration occurs in cold-treated cells where almost all of the MT present are of the kinetochore type (Figure 75; see also Brinkley and Cartwright 1970). This could only be investigated by observing living cells, for although all stages of mitosis are found in unsynchronized populations of cold-treated cells, this may just reflect the state prior to, not the processes occurring during treatment. What casts some doubt on this concept of pushing is the paucity and disorientation of MT in very early prophase (Figures 8 and 9). This is even more striking in Figure 105, where the centrioles have apparently migrated to opposite poles prematurely, before a true spindle was formed. Alternative explanations of centriole migration are difficult to conceive. Additional information, preferably from simpler systems, is certainly necessary.

Microtubules

Microtubules in PtK_2 cells have the usual dimension, i.e., a diameter of 200-250 A. Preparations with long, straight MT can be

obtained (e.g., Figures 11b, 28, and 42). Wavy MT occur most often between, or near, chromosomes (Figures 20, 25, 27, and 33). This might well be an artifact, for as Jensen and Bajer (1969) demonstrated in Haemanthus endosperm, shrinkage of chromosomes during dehydration can cause adjacent MT to become wavy.

I do not think that skew MT are an artifact (e.g., Figures 25, 27, 28, 42, and 47). One is tempted to speculate that the number of skew and otherwise "maloriented" MT decreases from early prometaphase to metaphase, thereby reflecting the organization of the mitotic spindle. To substantiate such speculation would require a thorough analysis of a great number of sections of several cells. For lack of numerical data we must content ourselves with the explanation that skew MT are part of the normal spindle and that they do not interfere with orderly chromosome movement.

Microtubules appear as hollow cylinders whose lumen has the same electron density as the cytoplasmic matrix (Figure 90). The walls appear as dark, more or less sharp lines or circles in untreated cells (Figures 84 and 90). In cold-treated cells the MT are coated by an amorphous or finely granular, moderately osmiophilic substance (Figures 73 and 75). In dividing amebae (Chaos) exposed to cold the MA is completely disorganized, but MT reappear after only a few minutes recovery at normal temperature (Roth 1967). These MT are not coated by any material. On the other hand, fixatives containing divalent cations preserve a fine material on the surface of MT in the MA of the same organism (Roth and Daniels 1962). Amebae fixed in OsO_4 alone contain no MT, but finely fibrillar, linearly oriented elements in the spindle region. Kane and Forer (1965) observed no MT, but large numbers of

granules of approximately the same size in isolated MA of sea urchins stored for longer periods of time.

Considering these observations one can hypothesize that the substance coating MT in cold-treated PtK_2 cells is microtubular material in a dispersed state, but still retaining affinity for persisting MT. The latter could serve as nucleating centers for rapid polymerization during recovery from cold. The necessity of nucleating centers for polymerization of free subunits has been demonstrated by Stephens (1969) with flagellar outer fibers, but a similar experiment with spindle MT has not as yet been reported. But it is clear that repolymerization of MT, as judged by reappearance of birefringence, occurs within seconds or minutes after exposure to cold, depending on the duration of the treatment (Inoué 1964, Inoué et al. 1970).

Brinkley et al. (1967) found persisting MT in Chinese hamster cells arrested by exposure to 0.06 µg/ml colcemid. These MT were of the kinetochore type; continuous MT were absent. A normal metaphase configuration was formed after 15-20 min recovery. In contrast to this, I found no MT in PtK_2 cells after 1 hr recovery following a 2 hr exposure to 0.05 µg/ml colcemid (e.g., Figures 63 and 64). This indicates a distinct difference in sensitivity.

The microfibrils observed in PtK_2 cells exposed to 0.25 µg/ml colcemid may be significant in the context of MT depolymerization. In my opinion these fibrils are not identical with microfibrils that are numerous mainly near the growth surface in untreated cells. Similar microfibrils have been reported in cells treated with vincristine by Journey et al. (1968). Nathaniel et al. (1968) observed 35-50 A fibrils in great quantity in melanocytes of Harding-Passey tumor treated with

colchicine. Here, then, are three instances where great numbers of microfibrils were observed in cells exposed to spindle poisons. Perhaps these fibrils represent a different aggregation state of MT subunits induced by the experimental conditions. Naturally, the correlation observed may be fortuitous. Further investigations, undoubtedly necessary, will have to aim at demonstrating a negative correlation between appearance and disappearance of microfibrils and MT.

There is evidence from immunological (Went 1960) and biochemical studies (e.g., Sisken and Wilkes 1967, Wilt et al. 1967) that the major proteins of the MA, among them MT proteins, are synthesized before the onset of division. The formation of MT in the cytoplasm during prophase can be explained as an assembly of preexisting subunits (see also Roth 1964, Nicklas 1971), possibly directed by organizing centers (Inoué 1964, Inoué and Sato 1967; the MTOC proposed by Pickett-Heaps 1969, 1971). Purely ultrastructural studies contribute little to the solution of this problem.

If there is indeed a pool of MT subunits during prophase, the absence of MT from the nucleus strongly suggests the NE is a real barrier to these subunits. In all the mammalian cells studied so far no MT are present within the nucleus during prophase (e.g., Krishan and Buck 1965, Murray et al. 1965, Robbins and Gonatas 1964). At the time the NE begins to break down near the centrioles, MT are numerous on the outside, but very sparse on the inside of the envelope in PtK_2 cells (e.g., Figure 10b). This observation leaves no doubt that the NE is a barrier to both subunits and assembled MT. In other organisms, however, the spindle is intranuclear, and the NE apparently does not act as a barrier (e.g., Aldrich 1969).

Electron micrographs such as Figures 18 and 19 demonstrate yet another aspect of spindle formation: MT within the "nucleus" are far more numerous near centrioles than on the opposite side. This could be interpreted as a "growing process" away from the centrioles, possibly concomitant with the diffusion of MT subunits into the "nucleus." As the spindle develops further and the centrioles arrive at opposite poles, the distribution of MT becomes more uniform (Figures 20, 26, and 29). The apparent paucity of continuous MT compared to kinetochore MT in fully developed spindles (Figures 29, 42, and 47) is probably imaginary. Kinetochore MT, arranged in bundles, are more conspicuous than the dispersed continuous MT.

The absence of MT from the nucleus during prophase has a parallel in telophase. Microtubules do not occur within the nucleus after the NE is completely reconstructed (Figure 60). The presence of MT in abnormal daughter nuclei of SN-treated cells (Figures 114-116) does not contradict this observation, because in these cases the NE is incomplete. It is not clear, however, in what way elimination of MT enclosed in the chromosomal mass in late anaphase (Figure 52) is accomplished. Robbins and Gonatas (1964) observed incompatibility of MT and complete NE in HeLa cells, but showed possible exceptions, i.e., MT apparently penetrating the NE. The authors conceded, however, that this could have been a false impression created by superposition.

I have not studied MT in the midbody in detail. It is possible that most of the "continuous" MT terminate in this body, or near it, but Figure 55a strongly suggests that at least some MT pass from one half-spindle into the other. It is interesting to note the abundance of MT converging in the midbody of cells in late cytokinesis, after the

spindle proper has been disorganized (Figures 61 and 62). Apparently these MT are more stable than others.

Chromosomes

Aberrations

The frequency of abnormal metaphase cells in the controls is obviously exaggerated (Table 1). Many late prometaphase cells with maloriented chromosomes (e.g., Figure 29) were scored as aberrant metaphases, but most of these cells would probably have divided normally, otherwise the frequency of aberrations in anaphase cells would have been similar to that in metaphase cells. Nevertheless, the frequency of aberrations may reflect instabilities of the cell line, or it may be due to the presence in the culture of a biological clastogen (virus or other microorganisms). Walen (1965) reported sister chromatid exchanges in the original culture of rat kangaroo cells. Similarly, Levan (1970) described changes of chromosome number and structure in the PtK_1 line derived from a female rat kangaroo. He interpreted these changes to reflect adaptation of the cells to the *in vitro* environment. Heneen (1970) studied frequency and types of aberrations in untreated PtK_1 cells. Many of these were similar to aberrations I observed in the controls.

The lower of the two concentrations of SN used (0.01 µg/ml) had little mitodepressive effect (Table 2), but induced almost 50% aberrations (Table 3). In contrast, 0.05 µg/ml SN had a great mitodepressive effect (Table 2), which accounts for the small sample of cells examined for aberrations (Table 3). These results confirm the great potency of SN as a clastogen.

The question whether the SN-treated abnormal cells represented the first or second generation after treatment cannot be answered. The 48 hr recovery period was long enough for one round of divisions, but the mitodepressive and general cytotoxic effects most likely altered the division cycle. However, it is very unlikely that any of the aberrations were induced in G_2. Indeed, no subchromatid aberrations were observed.

Fine Structure

The analysis of thin sections of dicentric bridges revealed little about the composition of the chromosomes involved. A comparison of the number of fibers in dicentrics attenuated to a variable degree might have provided some insight into the coiling or lateral association of the fibers, but this was not feasible.

Electron micrographs such as Figures 27 and 30b demonstrate that in thin sections individual chromosomes do not always appear physically separated. This posed a certain problem for the analysis of dicentric bridges such as shown in Figures 99-101. In some of the serial sections (e.g., Figure 100) the impression was not one of two truely linked chromosomes, but of long chromosomes whose telomeric ends were twisted around each other. The attenuation of the bridge (Figure 99) and the presence of acentric fragments (Figures 99 and 101), however, were evidence for a real exchange.

In the phase contrast microscope the chromosomes in many of the cells treated with 0.05 µg/ml SN appear fainter and more slender than normal chromosomes. Examination of thin sections of these chromosomes revealed generally looser, but also more irregular packing of fibers (Figure 111). Most likely, these chromosomes condensed during the

recovery period, not during exposure to SN. It therefore appears that high concentrations of SN alter the bonding properties of the molecules involved in coiling of chromatin.

Interesting is that high concentrations of colcemid produce a similar effect (Figures 65 and 66). Considering the short duration of the treatment (15 min) it is more likely that colcemid dispersed already condensed chromosomes rather than inhibiting the process of condensation. Morphological alterations of chromatin in mitotic grasshopper neuroblasts by colchicine was reported by Gaulden et al. (1970). Colcemid and colchicine are widely used, often at concentrations similar to those altering chromosome structure, for the accumulation of metaphase cells destined to yield a great number of chromosomes for ultrastructural studies (e.g., Abuelo and Moore 1969). The implications are clear: not only do we have to consider artifacts produced in whole-mounted chromosomes by the preparation techniques, but the preceding colcemid or colchicine treatment may have completely altered the ultrastructure of the chromosomes.

Remarkable is the appearance of centromere granules in chromosomes of cells that were probably in late prophase or in prometaphase at the time of treatment (Figure 65). I could not definitely determine whether there are one or two granules per chromatid. The structure and position of these granules is very similar to those observed by Stubblefield and Wray (1971) in whole-mounted Chinese hamster chromosomes. In the latter case, however, the possibility of an artifact produced by colcemid is slight, because at the concentration used (0.06 µg/ml for 4 hr) the drug does not even disperse all the MT (Brinkley et al. 1967).

To my knowledge chromatin strands connecting daughter chromosomes in early anaphase (Figures 46-48, and 109) have not been previously reported. In random sections of mitotic cells these strands, as well as the cells themselves at this stage, can easily escape detection. Nevertheless, it remains to be proven that this is a universal phenomenon or that it is restricted to rat kangaroo cells. The densely fibrillar structure of the strands is most easily explained as a consequence of stretching. Attenuation could produce parallel alignment of the fibers involved, which would allow tighter packing than is possible for coiled fibers. This explanation is supported by similarly packed fibers in dicentric bridges, where stretching certainly occurs (Figures 110 and 111a).

DuPraw (1965, 1968) proposed with his folded-fiber model of chromosomes that sister chromatids at metaphase are held together by short segments of unreplicated DNA in the centromere region. Immediately preceding anaphase separation these segments would be replicated. Numerous autoradiographic studies have demonstrated late-labeling centromere regions in chromosomes of various cell lines (see DuPraw 1968 for references), but the short burst of DNA synthesis prior to anaphase, expected according to DuPraw's model, has not been proven.

Be this as it may, the fact is that sister chromatids in whole-mount preparations are connected in the centromere region by chromosomal fibers (e.g., Abuelo and Moore 1969, DuPraw 1968, Stubblefield and Wray 1971). It is possible that the chromatin strands I observed in early anaphase cells are a consequence of the physical separation of these connections. Logically, the strands can be detected in thin sections only when the centromere regions are stretched, because in the

relaxed state they blend in with the other fibers. This could explain the occurrence of similar strands of more or less parallel fibers in stretched prometaphase chromosomes (Figures 31 and 36). The significance of chromatid connections for stable metaphase orientation of chromosomes is clear, assuming that orientation stability depends on a balance of pulling forces acting on sister kinetochores oriented towards opposite poles. This theory was proposed by Östergren (1951) for meiosis, and experiments by Henderson and Koch (1970), Nicklas (1967), and Nicklas and Koch (1969) with grasshopper spermatocytes strongly support it. Connections between sister chromatids prevent premature separation, which would lead to unipolar attachment of chromatids and, consequently, unstable orientation followed by haphazard chromosome distribution.

The surprisingly frequent occurrence of very fine nuclear bridges in SN-treated cells in cytokinesis indicates that not all the dicentric bridges rupture during anaphase (Figures 118 and 119a). Acentric fragments form micronuclei if included in daughter cells (Figure 119b). In one case examined in the electron microscope, however, I found an "elimination body," consisting of a polymorphic micronucleus and very little cytoplasm, in the cleavage furrow between daughter cells. This body possibly contained acentric fragments that were lying near the equator at the periphery of the cell in metaphase, as shown in Figures 108c and 108e.

Osmiophilic granules in chromosomes of PtK_2 cells have been reported by Brinkley and Shaw (1970). I have found these granules in interphase and all stages of mitosis. They are more clearly visible, possibly more numerous, in cold-treated than in control cells (Figure 71).

Their significance is not at all clear. In size they are distinctly different (approximately 300-500 A in diameter) from ribosomes and the granular component of the nucleolus.

Kinetochores

Structural Changes During Mitosis

The term "maturation" suggested by Jokelainen (1968) best describes the structural differentiation of kinetochores from prometa- to metaphase. By definition a mature kinetochore appears in thin sections as the typical triple-banded structure at the surface of metaphase chromosomes.

Kinetochores appear "out of nowhere" at the primary constriction of chromosomes (Figures 10, 11a, 15-17). I could not detect any relationship between primary constrictions and NE, which nevertheless does not rule out the possibility that other points of attachment determine the coiling pattern of chromosomes (see Comings 1968, Comings and Okada 1970a, b). In stages of prophase earlier than illustrated in Figure 10 kinetochores are not visible as such, but their future position is indicated by a slight constriction on the loosely coiled chromosomes. From mid- to late prophase the electron density of kinetochores increases slightly, making their detection easier. In any event, however, the chromosomes always stain much more intensely than the kinetochores (e.g., Figure 16).

Radical changes in kinetochore structure occur during prometaphase. These changes first involve the kinetochores of chromosomes near the centrioles, i.e., in the region where the NE breaks down first (Figure 23). In cells such as the one shown in Figure 19 one

therefore finds immature prophase kinetochores on the chromosomes in the center of the "nucleus," and more mature kinetochores near the two poles. I could not establish a clear-cut correlation between attachment of kinetochores to MT and the appearance of the three bands typical for mature kinetochores. On the contrary, kinetochores not attached to MT often exhibit more distinct bands than attached kinetochores (e.g., Figure 23). However, it is possible that attached kinetochores are triple-banded, but since they are drawn out into a cone or more odd structure (Figures 23, 24, and 36) they would necessarily be cut obliquely by any but ideal median sections and consequently the bands would be less distinct. In fact, Figure 23 indicates that these kinetochores are banded. Much of the foregoing also applies to structural differences between sister kinetochores of maloriented chromosomes in late prometaphase (Figures 20, 37, and 38).

Figure 120, illustrating asynchronous maturation during prometaphase of sister kinetochores of a maloriented chromosome, is based on the above mentioned assumption and observations. Kinetochore no. 1 possibly had a structure similar to that of kinetochore no. 2 in Figure 120b at a stage preceding that shown in Figure 120a. The transition of kinetochore no. 2 from Figure 120a to Figure 120b is hypothetical. This kinetochore matured later than its sister oriented towards the near pole and attached to MT very early. A similar sequence can be postulated for equatorial chromosomes with one unobstructed and one obstructed kinetochore. If both kinetochores of an equatorial chromosome are unobstructed they mature synchronously (e.g., Figure 25).

It appears that the outer layer is formed within the finely fibrillar material of prophase and immature prometaphase kinetochores

Fig. 120. Diagrammatic representation of kinetochore maturation during prometaphase. (a) The chromosome lies near one pole. The kinetochore oriented towards this pole (K_1) is drawn out to a cone and attached to MT. The outer layer has possibly formed. The kinetochore oriented towards the far pole (K_2) is less mature. As yet none of the layers has formed and the kinetochore is not attached to MT. Compare with Fig. 24. (b) The outer layer of K_2 is forming, but the kinetochore is still not attached to MT. K_1 is unchanged. The chromosome is still near the same pole. Compare with Figs. 23 and 37. (c) K_2 has reached the stage of maturity corresponding to K_1 in (a); it is attached to MT. The inner layer of K_1 is forming. Both kinetochores are stretched and the chromosome is moving towards the equator (to the left). Compare with Fig. 40. (d) Both kinetochores are nearly mature, showing three layers. Both are also stretched. The chromosome has attained stable bipolar orientation at the equator. Compare with Fig. 34.

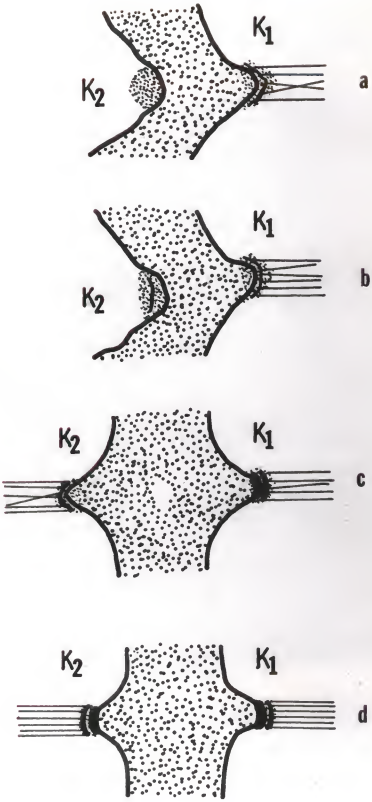

120

(Figures 23 and 33). This material is gradually reduced in extent, but some of it remains present in mature kinetochores as the corona and the middle layer (Figures 42, 46, 78, and 84). The inner layer, at the surface of the chromosome, appears last (Figures 33-35).

Kinetochore maturation as described herein essentially agrees with the observations of Jokelainen (1965). However, his conclusions that sister kinetochores always mature asynchronously does not apply to PtK_2 cells. A better knowledge of the position of chromosomes in the spindle and the orientation of sister kinetochores allowed detection of subtle differences between kinetochores of maloriented chromosomes, as well as obstructed and unobstructed kinetochores of equatorial chromosomes.

There is virtually no change in kinetochore structure from metaphase to mid-anaphase (Figures 42, 43, 45-49). "Dedifferentiation" of kinetochores begins in late anaphase (Figures 52 and 53). The triple-layered profiles appear less distinct. Concomitantly the number of kinetochore MT is reduced. During telophase, the reforming NE separates the remnants of inner and outer layers (Figures 59 and 60). The former is lost in the cytoplasm, while the latter comes to lie closely apposed to the inner membrane of the NE (see also Figures 115 and 116). The most convincing evidence for this conclusion came from an aberrant cell similar to the one in Figure 116, but from a TEPA-treated culture. The inner layers of several kinetochores, also situated in deep invaginations of the NE on the polar side, appeared as very electron dense bumps on the inner membrane of the NE. On the outside of the outer membrane, opposite these bumps, remnants of the less opaque outer layers with MT still attached were visible.

The Fine Structure of Mature Kinetochores

Several arguments based on published observations and electron micrographs speak against the filament model of mammalian kinetochores proposed by Brinkley and Stubblefield (1966, 1970). First, the kinetochores in colcemid-treated Chinese hamster cells, on which the original paper was almost exclusively based (Brinkley and Stubblefield 1966), are structurally different from kinetochores of normal metaphase chromosomes. The inner kinetochore layer is absent in c-mitotic cells, but it is present on metaphase chromosomes in cells recovering from colcemid (Brinkley et al. 1967). Secondly, random sections of mitotic cells, particularly if embedded as a pellet (as were the cells used by Brinkley and Stubblefield 1966), should yield at least some cross sections of kinetochore filaments. Such profiles have never been presented. Thirdly, the difference in electron density between outer and inner bands of normal metaphase kinetochores, observed by a number of investigators (e.g., Barnicot and Huxley 1965, Luykx 1965a), suggests the two bands do not represent identical filaments. Fourthly, Jokelainen (1967) and McIntosh and Landis (1971) have published electron micrographs of para-equatorial sections of metaphase cells showing circular kinetochores. Krishan (1968) also presented a micrograph showing a circular kinetochore in a telophase cell after recovery from vinblastine. Finally, kinetochores in a variety of cells treated with the spindle poisons vincristine and vinblastine are virtually identical with kinetochores in colcemid-treated Chinese hamster cells, and equally different from normal metaphase kinetochores (George et al. 1965, Journey et al. 1968, Journey and Whaley 1970, Krishan 1968).

Extending their model to PtK_1 rat kangaroo cells, Brinkley and Stubblefield (1970) interpreted the outer and inner bands of metaphase kinetochores as representing the two kinetochore filaments. My observations on paraxial (e.g., Figures 78-85) and para-equatorial (Figures 86, 87, and 91) serial sections leave no doubt that mature kinetochores in PtK_2 cells are trilaminar, roughly circular plates at the surface of chromosomes. I have not seen any filaments in para-equatorial sections. Furthermore, kinetochore MT are arranged in bundles, not in "sheets," as would be expected were they connected to filaments.

My view of mature kinetochores essentially agrees with the model of Jokelainen (1967), except for one important aspect: kinetochore plates are very seldom, if ever, flat. Rather, they are undulated (Figures 42 and 82), concave (Figure 85), or convex (Figures 46, 47, and 84) discs. Figure 121a-c diagrammatically represents three-dimensional reconstructions of kinetochores of various shapes. The shape of a kinetochore is certainly determined by the curvature of the chromosomal surface at this locus. It is also possible that both the shape of the kinetochore and the curvature of the chromosome are influenced by the differential pulling action of the attached MT.

Ultrathin paraxial sections (Figures 82 and 84) strongly suggest that kinetochore MT terminate in the outer layer. Even more convincing are para-equatorial sections (Figures 86 and 87). Nebel and Coulon (1962) and Luykx (1965a) concluded from their micrographs that kinetochore MT terminate in the inner layer. These observations, however, were severely hampered by inadequate preservation of fine structure. Jokelainen (1967) also concluded that kinetochore MT are anchored in

Fig. 121. Diagrammatic representation of the three-dimensional structure of kinetochores. (a) Mature metaphase kinetochore (compare with Figs. 78, 82, and 86). (b) and (c) anaphase kinetochores (compare with Figs. 46-49). (d) Sister kinetochores of a telocentric chromosome in a colcemid-treated cell (compare with Fig. 95). (e) Sister kinetochores of a metacentric or submetacentric chromosome in a colcemid-treated cell (compare with Figs. 92-94, 96-98).

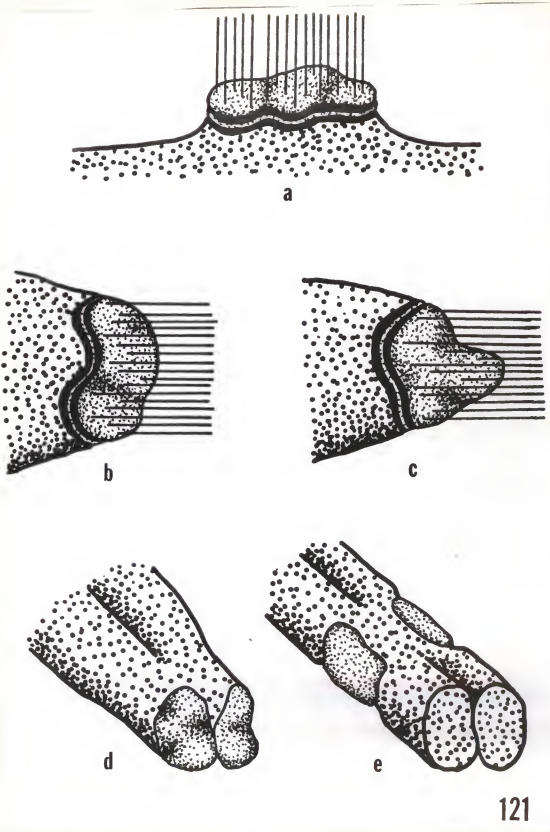

121

the inner layer or, possibly, even deeper in the chromosome. But his sections were more than 750 A thick and the apparent deep penetration of MT could well be ascribed to a superposition effect. In the micrograph of an early anaphase kinetochore published by Robbins and Gonatas (1964, Figure 19) the MT seem to terminate in the outer layer. Intuitively one would expect a certain uniformity regarding MT attachment in cells of different organisms, especially among mammals. I believe that a careful and detailed reexamination of the cases apparently contradicting my conclusions would reveal this uniformity.

The purpose of the colcemid treatments was to check the possibility that kinetochores of PtK_2 cells under these conditions are different from kinetochores in similarly treated Chinese hamster cells. This was not the case (Figures 92, 94, and 96-98). The inner layer is lacking and the outer layer structurally resembles that in c-mitotic Chinese hamster cells, as well as cells treated with vincristine and vinblastine (George et al. 1965, Journey et al. 1968, Journey and Whaley 1970, Krishan 1968). Grazing sections of chromosomes yielded images compatible with the idea that the outer layer is a circular or oval plate in a depression of the chromatid (Figures 93, 96, and 121e). Similar images were obtained by Journey (personal communication) from vincristine-treated Chinese hamster cells.

Kinetochore profiles in transverse sections of chromosomes in colcemid-treated PtK_2 cells (Figures 92, 94, 97, and 98) suggest the plate-like outer layer is bilaminar. This substructure is not discernible in normal, mature kinetochores (e.g., Figures 82 and 84), but it can be seen in immature prometaphase kinetochores (e.g., Figures 23c and 41). To me these observations indicate that immature

prometaphase kinetochores and kinetochores in colcemid-treated cells are less condensed than mature kinetochores. The generally greater diameter of kinetochores and the more extensive matrix in c-mitotic compared to untreated metaphase cells further supports this interpretation.

Intuitively one expects a larger plate to be more easily bent than a smaller one, particularly if it is also less rigid, as might be the case with the less condensed outer kinetochore layer in c-mitotic cells. With this in mind we can explain the strange kinetochore profiles in Figure 95. They represent oblique sections of the highly undulated outer layer (Figure 121d). Undulations are more likely to occur on telocentric chromosomes, or on submetacentric chromosomes bent at a sharp angle in the kinetochore region. Either of these possibilities could apply to Figure 95. The near-circular kinetochore profiles observed by Journey and Whaley (1970) in vincristine-treated HeLa and Chinese hamster cells could be the result of superficial sections through cap-shaped kinetochores such as K in Figure 92, or they represent near-terminal sections of subtelocentric or telocentric chromosomes (as in Figure 121d).

Brinkley and Stubblefield (1966) observed 50-80 A fibrils apparently looping out from the main band of kinetochores in Chinese hamster cells recovering from colcemid. I have not observed such loops in colcemid-treated PtK_2 cells, but the matrix in which the outer kinetochore layer is embedded does contain fibrils (e.g., Figure 94). The fibrils observed by Brinkley and Stubblefield (1966) are possibly also part of the matrix, or they could be characteristic for cells in which the kinetochore recondenses and the number of kinetochore MT increases during recovery from colcemid.

I more or less expected the kinetochores in cold-treated cells to resemble those in colcemid-treated cells. This was not the case (compare Figure 75 with Figure 92). One significant difference was the presence of kinetochore MT in cold-treated and their complete absence in colcemid-treated cells. As already explained in the section on kinetochore maturation, it is not clear if a relationship exists between microtubular attachment and the appearance of triple-layered kinetochores. Observations on cold-treated cells might suggest such a relationship, but in colcemid-treated Chinese hamster cells the inner layer of kinetochores attached to persisting MT is apparently also lacking (Brinkley and Stubblefield 1966).

Definite conclusions regarding the molecular composition of kinetochores are not possible without extensive cytochemical studies. The fact that the outer layer stains differently than the inner layer suggests a different molecular composition. I tentatively conclude that the outer layer is not made of chromatin, and that the inner layer consists of tightly packed chromatin fibers. This rules out covalent bonds between the two layers. The outer layer possibly consists of protein. Since kinetochore MT are attached to the outer layer, the implications are clear: the bonds between MT and the outer layer on one hand, and outer and inner layers on the other hand must be very strong, in fact stronger than the bonds maintaining chromosomal fibers in a coiled state. This is borne out by the observations that kinetochores of dicentric chromosomes subjected to considerable pull (Figures 101, 110a, 111a, and 113) are structurally normal. Also, centrifugation forces sufficient to uncoil chromosomes do not rupture spindle attachments (Shimamura 1940). How this strong bonding is achieved

remains unexplained, but the matrix persisting as the corona and middle layer of mature kinetochores may play an important role.

Kinetochore-Microtubule Interactions

Kinetochores are involved in two important processes during prometaphase: Chromosome orientation and congression. A third possible function, assembly and orientation of MT, is central to most models of mitosis (Dietz 1969, Inoué 1964, Luykx 1970, McIntosh et al. 1969), but the available evidence is not entirely conclusive (for detailed discussions see Luykx 1970, Nicklas 1971). Neither light microscopic nor ultrastructural studies alone can answer the questions remaining. A cinemicrographic and electron microscopic analysis of the effect of UV microbeam irradiation and spindle poisons is more likely to yield significant data. The electron micrographs of PtK_2 cells in very early prometaphase (Figures 18a and 19) can be interpreted as supporting either the idea that kinetochores organize MT or that they attach to existing MT. Counts of the number of MT before and after kinetochore attachment, as presented by Manton et al. (1969a, b) for the diatom Lithodesmium, might provide clues, but spindle formation in PtK_2 cells is more complex.

Chromosome orientation has been extensively investigated in the first meiotic division in spermatocytes (e.g., Nicklas 1967). There, spindle attachments of chromosomes are often broken naturally, or can be broken experimentally, and subsequently reorientation of chromosomes and reattachment occur (see also Nicklas and Koch 1969). This is necessary for stable bipolar orientation of bivalents initially attached to one pole only (maloriented bivalents). No similar data are available for mitosis. Most of the current models of mitosis, which,

of course, are also designed to explain meiosis, picture the chromosomes as orienting within the more or less completely formed central spindle (Dietz 1969, Luykx 1970, McIntosh et al. 1969). The MT growing out from the kinetochores are supposed to interact with the already present "continuous" MT of the central spindle. Whether this is indeed so in the cells considered by the authors remains to be proven, because no ultrastructural studies of prometaphase have been presented. In PtK_2 cells the above is certainly not the case, as demonstrated by Figure 23, and similar micrographs not included. These pictures clearly show that MT do not grow out from, or attach to, both kinetochores simultaneously, and that chromosomes may connect to a pole as soon as the nuclear envelope breaks down, regardless of whether the central spindle is fully formed or not.

Östergren (1951) postulated a pulling theory of chromosome orientation and congression for meiosis. Briefly, this theory proposes that bipolar orientation of bivalents is the consequence of kinetochore polarity. This polarity allows each kinetochore to connect only to that pole towards which it is oriented. Prometaphase movements are caused by random activity of kinetochores. Ultimately, the kinetochores exert a pull and the equatorial position of chromosomes at late prometaphase and metaphase is the result of balanced tension on kinetochores oriented towards opposite poles.

The following reconstruction of events leading to chromosome orientation and congression in PtK_2 cells fits this theory well, if it is modified to account for differences between meiotic chromosomes (bivalents) and mitotic chromosomes (pairs of sister chromatids). As soon as the nuclear envelope breaks down near the centrioles, the

chromosomes near this site become attached to MT by one kinetochore. Kinetochores are polarized in the sense that the outer, but not the inner layer, can connect with MT. Therefore, attachment is possible only to MT approaching from the side the kinetochore faces. Even if a kinetochore could theoretically attach to MT approaching from the opposite side ("from the back"), these MT would have to be bent at an impossible angle. Consequently, for the meta- and submetacentric chromosomes the initial unipolar attachment immediately establishes bipolar orientation, especially if combined with tension. Therefore, when one kinetochore is attached, the other has no choice but to attach to the opposite pole. Telocentric chromosomes are more likely to attach with both kinetochores to the same pole. In fact, the only chromosome I observed displaying this configuration was a telocentric chromosome in a TEPA-treated cell in mid-prometaphase. Bajer and Molè-Bajer (1969), however, published a micrograph showing a metacentric chromosome apparently attached to the same pole with both kinetochores. Such observations are rare and, though almost certainly due in part to neglect by many investigators, may reflect the rarity of the event. For comparison, in crane fly meiosis ten per cent of the bivalents show unipolar orientation in early prometaphase (Bauer et al. 1961).

If the two poles are still close together at the time the first attachments are established, one might expect some kinetochores to connect to both poles. I have never observed this, but Bajer and Molè-Bajer (1969) reported such a case for Haemanthus endosperm.

It is possible that early unipolar attachments involving only one kinetochore are maintained during migration of the centrioles and formation of the definitive spindle axis, with the result that some

chromosomes lie close to one pole in mid- and late prometaphase (e.g., Figures 26-29). Also, these unipolar attachments may be followed by movement of the chromosome involved towards the near pole. At some point, however, the sister kinetochore oriented towards the far pole also becomes attached, and this is followed by movement towards the far pole (Figure 120c). Figure 40 possibly illustrates the "return point," i.e., two chromosomes just beginning to move towards the equator. Once the tension exerted on sister kinetochores is balanced, the chromosomes remain stably in an equatorial position.

Chromosomes lying farther from the poles at the time the nuclear envelope breaks down become attached later than the chromosomes lying close. Whether this is so because of the greater distance from the probable pool of MT subunits around the centrioles, or because they are shielded from the poles by other chromosomes and therefore cannot form connections until after reshuffling due to movements of already attached chromosomes has occurred, remains an open question. Nevertheless, the chance that the kinetochores of these chromosomes attach to opposite poles simultaneously is greater, because the spindle axis is established. For example, the chromosome in Figure 24 could have attached earlier than the chromosome in Figure 25. Consequently the latter shows bipolar orientation and attachment, whereas the former shows bipolar orientation, but unipolar attachment. Equatorial chromosomes immediately attached to both poles can be expected to be stabilized by tension and to move very little during prometaphase. However, if one sister kinetochore of an equatorial chromosome is obstructed, unipolar attachment would precede bipolar attachment. Again, the latter could occur only after reshuffling has cleared the

field between the previously unattached kinetochore and its pole. As a consequence of unipolar attachment the chromosome should travel towards the pole to which it is attached. This is probably not so, otherwise many more chromosomes could be found near the poles. Possible explanations are connections between non-sister kinetochores (perhaps between the kinetochores of chromosomes no. 1 and 2 in Figure 33; see also Bajer 1970, Luykx 1965b), or simply physical hindrance. In fact, neighbor chromosomes can lie so close to each other that a separation is not detectable in thin sections (Figure 27).

Chromosomes without definite attachment to either pole (Figure 39) may simply drift in the spindle or remain stationary until one or both of its kinetochores become attached. Their subsequent behavior would depend on the nature of the attachments.

If my interpretation is correct, detachment, reorientation, and reattachment should occur less frequently for mitotic than for meiotic chromosomes. This awaits experimental verification. Not only does the above account agree with Östergren's theory (1951), but Nicklas (1967) clearly demonstrated that in grasshopper spermatocytes kinetochore position after detachment by micromanipulation determines to which pole the kinetochore will orient and attach. Finally, stabilization of chromosomes by tension was beautifully demonstrated by Henderson and Koch (1970), Henderson et al. (1970), and Nicklas and Koch (1969).

The hypothetical points of my interpretation can be tested experimentally. Time-lapse cinemicrographic records of the prometaphase behavior of selected chromosomes followed by an ultrastructural analysis of kinetochore structure and attachments to MT could easily reveal which of my assumptions are true or false.

Nuclear Envelope

Fragmentation and reconstruction of the nuclear envelope (NE) in PtK_2 cells are similar in many ways to the processes in other mammalian cells. However, I have neither observed stacking of NE fragments as reported for rat lymphocytes (Murray et al. 1965) and rat hepatoma cells (Chang and Gibley 1968), nor "polar caps" consisting of numerous cisternae and vesicles as in HeLa cells in metaphase (Robbins and Gonatas 1964). There are no membrane elements at metaphase and early anaphase that could be identified as fragments of the NE (Figures 42, 43, 45, and 47). Cisternae possibly representing elements of the reforming NE occur only in late anaphase at the periphery of the spindle (Figure 51a). In very late anaphase and early telophase such cisternae can be clearly identified as portions of the NE mainly because of their association with the chromosomal mass (Figures 52 and 57).

Comings and Okada (1970a) have described associations of NE fragments with meta- and anaphase chromosomes as seen in whole mounts. Their observations can be criticized for two reasons: (1) Most of the preparations were made from colcemid-arrested cells, and (2) anaphase was simply judged according to time after colcemid reversal. According to the authors, however, the results agreed with Comings' hypothesis (1968; also Comings and Kakefuda 1968, Comings and Okada 1970b, c) that persisting chromosomal attachments to the NE account for reproducible patterns of DNA replication and chromosome folding. This is a tempting hypothesis, but evidence is rather scarce and unconvincing. In PtK_2 cells the reconstruction of the NE seems to be related spatially to the chromosomal mass as a whole, rather than to specific sites of individual chromosomes (Figures 52 and 57).

The possibility that endoplasmic reticulum (ER) is involved in the reconstruction of the NE was raised by Porter and Machado (1960), based on studies of mitosis in onion root tip cells. Bajer and Molè-Bajer (1969; Haemanthus endosperm cells) and Robbins and Gonatas (1964; HeLa cells) agreed that this is a likely possibility. My own observations support this concept (Figures 51a, 52, 112, and 117). Quite frequently, cisternae with ribosomes can be seen apposed to the chromosomal mass (Figure 52). Other cisternae, in a similar association with chromatin, appear continuous with rough ER.

The serial sections yielded numerous oblique views of NE fragments in prometaphase, thus providing a better insight into the fate of nuclear pore complexes. There is no doubt that the pores disappear (Figure 21). Remarkable is their reappearance on very small cisternae associated with chromatin in late anaphase (Figure 50). One gets the impression that pores are reformed almost immediately upon contact of cisternae with chromatin, but the process is shrouded in mystery.

CONCLUSIONS

Knowing the question is knowing half the answer. Applied to science this means if we are able to state a problem and to formulate a hypothesis, we are able to design experiments with the aim to gather evidence for or against the hypothesis, or to reach new ideas. Instead of collecting data more or less at random we could then proceed in an organized fashion to solve a particular problem.

From the preceding chapters it is clear that not all my expectations stated in the preface were fulfilled. The study of chromosomal ultrastructure took second place to the investigation of mitosis. Biophysical and biochemical studies are more likely to provide a better understanding of such interesting and important problems as polynemy or uninemy and the orderly coiling of chromosomes, than ultrastructural studies alone.

My observations on prometaphase and early anaphase of mitosis, previously neglected by most investigators, have revealed interesting new data. But again, electron microscopy alone, although a powerful tool, has its limits. I am firmly convinced, however, that a concerted and organized effort combining *in vivo* observation, particularly polarization microscopy and cinemicrography, with electron microscopy will clarify many of the still mysterious aspects of mitosis.

REFERENCES

Abuelo, J. G., and D. E. Moore. 1969. The human chromosome. Electron microscopic observations on chromatin fiber organization. J. Cell Biol. 41: 73-90.

Aikawa, M., and R. L. Beaudoin. 1968. Studies on nuclear division of a malarial parasite under pyrimethamine treatment. J. Cell Biol. 39: 749-754.

Aldrich, H. C. 1967. The ultrastructure of meiosis in three species of Physarum. Mycologia 59: 127-148.

Aldrich, H. C. 1969. The ultrastructure of mitosis in myxamoebae and plasmodia of Physarum flavicomum. Amer. J. Bot. 56: 290-299.

Anonymous. 1967. American Type Culture Collection Cell Repository. Registry of animal cell lines certified by the cell culture collection committee, suppl. 2.

Bacq, Z. M., and P. Alexander (eds.). 1955. Radiobiology Symposium 1954. Academic Press, New York. 362 p.

Bajer, A. 1958. Cine-micrographic studies on chromosome movements in β-irradiated cells. Chromosoma 9: 319-331.

Bajer, A. 1963. Observations on dicentrics in living cells. Chromosoma 14: 18-30.

Bajer, A. 1964. Cine-micrographic studies on dicentric chromosomes. Chromosoma 15: 630-651.

Bajer, A. 1965. Subchromatid structure of chromosomes in the living state. Chromosoma 17: 291-302.

Bajer, A. 1968. Behavior and fine structure of spindle fibers during mitosis in endosperm. Chromosoma 25: 249-281.

Bajer, A. 1969. Effects of UV microbeam irradiation on chromosome movements and spindle fine structure (with film demonstration). Biophys. J. 9: A-151.

Bajer, A. 1970. See Luykx, 1970, p. 54.

Bajer, A. and R. D. Allen. 1966. Structure and organization of the living mitotic spindle of Haemanthus endosperm. Science 151: 572-574.

Bajer, A., and J. Molè-Bajer. 1961. UV microbeam irradiation of chromosomes during mitosis in endosperm. Exp. Cell Res. 25: 251-267.

Bajer, A., and J. Molè-Bajer. 1963. Cine analysis of some aspects of mitosis in endosperm, p. 357-409. In G. G. Rose (ed.) Cinemicrography in Cell Biology. Academic Press, New York.

Bajer, A., and J. Molè-Bajer. 1969. Formation of spindle fibers, kinetochore orientation, and behavior of the nuclear envelope during mitosis in endosperm. Fine structural and in vitro studies. Chromosoma 27: 448-484.

Barnicot, N. A. 1966. A note on the structure of spindle fibers. J. Cell Sci. 1: 217-222.

Barnicot, N. A., and H. E. Huxley. 1965. Electron microscope observations on mitotic chromosomes. Quart. J. Microscop. Sci. 106: 197-214.

Bauer, H., R. Dietz, and C. Röbbelen. 1961. Die Spermatocytenteilungen der Tipuliden. III. Mitteilung. Das Bewegungsverhalten der Chromosomen in Translokationsheterozygoten von Tipula oleracea. Chromosoma 12: 116-189.

Behnke, O., and A. Forer. 1966. Some aspects of microtubules in spermatocyte meiosis in a crane fly (Nephrotoma suturalis Loew): intranuclear and intrachromosomal microtubules. C. R. Trav. Lab. Carlsberg 35: 437-455.

Bělař, K. 1929. Beiträge zur Kausalanalyse der Mitose. II. Untersuchungen an den Spermatocyten von Chorthippus (Stenobothrus) lineatus Panz. Wilhelm Roux Arch. Entwicklungsmech. Organ. 118: 359-484.

Bernhard, W., and E. de Harven. 1960. L'ultrastructure du centriole et d'autres elements de l'appareil achromatique. Proc. 4th Int. Conf. Electr. Microscop. 2: 217-227.

Bessis, M., J. Breton-Gorius, and J. P. Thiéry. 1958. Centriole, corps de Golgi et aster des leucocytes. Étude au microscope électonique. Rev. Hématol. 13: 363-386.

Biesele, J. J. 1962. Experimental and therapeutic modification of mitosis. Cancer Res. 22: 779-787.

Bloom, W., R. E. Zirkle, and R. B. Uretz. 1955. Irradiation of parts of individual cells. III. Effects of chromosomal and extrachromosomal irradiation on chromosome movements. Ann. N. Y. Acad. Sci. 59: 503-513.

Borisy, G. G., and E. W. Taylor. 1967a. The mechanism of action of colchicine. Colchicine binding to sea urchin eggs and the mitotic apparatus. J. Cell Biol. 34: 535-548.

Borisy, G. G., and E. W. Taylor. 1967b. The mechanism of action of colchicine. Binding of colchicine-3H to cellular protein. J. Cell Biol. 34: 525-533.

Brandham, P. E. 1970. Chromosome behaviour in the Aloineae. III. Correlations between spontaneous chromatid and sub-chromatid aberrations. Chromosoma 31: 1-17.

Brinkley, B. R., and J. Cartwright, Jr. 1970. Organization of microtubules in the mitotic spindle: differential effects of cold shock on microtubule stability. J. Cell Biol. 47: 25a.

Brinkley, B. R., and R. M. Humphrey. 1969. Evidence for subchromatid organization in marsupial chromosomes. I. Light and electron microscopy of X-ray-induced side-arm bridges. J. Cell Biol. 42: 827-836.

Brinkley, R. R., P. Murphy, and L. C. Richardson. 1967. Procedure for embedding in situ selected cells cultured in vitro. J. Cell Biol. 35: 279-283.

Brinkley, B. R., and R. B. Nicklas. 1968. Ultrastructure of the meiotic spindle of grasshopper spermatocytes after chromosome micromanipulation. J. Cell Biol. 39: 16a-17a.

Brinkley, B. R., and M. W. Shaw. 1970. Ultrastructural aspects of chromosome damage, p. 313-345. In Genetic Concepts and Neoplasia. Williams and Wilkins, Baltimore.

Brinkley, B. R., and E. Stubblefield. 1966. The fine structure of the kinetochore of a mammalian cell in vitro. Chromosoma 19: 28-43.

Brinkley, B. R., and E. Stubblefield. 1970. Ultrastructure and interaction of the kinetochore and centriole in mitosis and meiosis, p. 119-185. In D. M. Prescott, L. Goldstein, and E. McConkey (eds.) Advances in Cell Biology, vol. 1. Appleton-Century-Crofts, New York.

Brinkley, B. R., E. Stubblefield, and T. C. Hsu. 1967. The effects of colcemid inhibition and reversal on the fine structure of the mitotic apparatus of Chinese hamster cells in vitro. J. Ultrstruct. Res. 19: 1-18.

Britten, R. J., and D. E. Kohne. 1968. Repeated sequences in DNA. Science 161: 529-540.

Buck, R. C. 1967. Mitosis and meiosis in Rhodnius prolixus: The fine structure of the spindle and diffuse kinetochore. J. Ultrastruct. Res. 18: 489-501.

Burgos, M. H., and D. W. Fawcett. 1956. An electron microscope study of spermatid differentiation in the toad, Bufo arenarum Hensel. J. Biophys. Biochem. Cytol. 2: 223-240.

Busch, H., and K. Smetana. 1970. The Nucleolus. Academic Press, New York. 626 p.

Byers, B., and D. H. Abramson. 1968. Cytokinesis in HeLa: post-telophase delay and microtubule-associated motility. Protoplasma 66: 413-435.

Carlson, J. G. 1938. Mitotic behavior of induced chromosomal fragments lacking spindle attachments in the neuroblasts of the grasshopper. Proc. Nat. Acad. Sci. 24: 500-507.

Carlson, J. G. 1954. Immediate effects on division, morphology, and viability of the cell, p. 763-824. In A. Hollaender (ed.) Radiation Biology, vol. 1 (pt. 2). McGraw-Hill, New York.

Carter, S. K., D. Rall, P. Schein, R. D. Davis, H. B. Wood, Jr., R. Engle, J. P. Davignon, J. M. Venditti, S. A. Schepartz, B. R. Murray, and C. G. Zubrod. 1968. Streptonigrin. NSC 45383. Clinical Brochure. Nat. Cancer Inst. Chemother. 20 p.

Casarett, A. P. 1968. Radiation Biology. Prentice-Hall, Englewood Cliffs. 368 p.

Chang, J. P., and C. W. Gibley, Jr. 1968. Ultrastructure of tumor cells during mitosis. Cancer Res. 28: 521-534.

Cohen, M. M. 1963. The specific effects of streptonigrin activity on human chromosomes in culture. Cytogenetics 2: 271-279.

Cohen, M. M., M. W. Shaw, and A. P. Craig. 1963. The effects of streptonigrin on cultured human leukocytes. Proc. Nat. Acad. Sci. 50: 16-24.

Comings, D. E. 1968. The rationale for an ordered arrangement of chromatin in the interphase nucleus. Amer. J. Human Genet. 20: 440-460.

Comings, D. E. 1971 Isolabelling and chromosome strandedness. Nature New Biol. 229: 24-25.

Comings, D. E., and T. Kakefuda. 1968. Initiation of deoxyribonucleic acid replication at the nuclear membrane in human cells. J. Mol. Biol. 33: 225-229.

Comings, D. E., and T. A. Okada. 1970a. Association of nuclear membrane fragments with metaphase and anaphase chromosomes as observed by whole mount electron microscopy. Exp. Cell Res. 63: 62-68.

Comings, D. E., and T. A. Okada. 1970b. Association of chromatin fibers with the annuli of the nuclear membrane. Exp. Cell Res. 62: 293-302.

Comings, D. E., and T. A. Okada. 1970c. Condensation of chromosomes onto the nuclear membrane during prophase. Exp. Cell Res. 63: 471-473.

De Harven, E. 1968. The centriole and the mitotic spindle, p. 197-227. In A. J. Dalton and F. Haguenau (eds.) The Nucleus. Academic Press, New York.

De Harven, E., and W. Bernhard. 1956. Etude au microscope electronique de l'ultrastructure du centriole chez les vértebrés. Z. Zellforsch. Mikroskop. Anat. 45: 378-398.

Deysson, G. 1968. Antimitotic substances. Int. Rev. Cytol. 24: 99-148.

Dietz, R. 1959. Centrosomenfreie Spindelpole in Tipuliden-Spermatocyten. Z. Naturforsch. 14b: 749-752.

Dietz, R. 1966. The dispensability of the centrioles in the spermatocyte divisions of Pales ferruginea (Nematocera), p. 161-166. In C. D. Darlington and K. R. Lewis (eds.) Chromosomes Today, vol. 1. Plenum Press, New York.

Dietz, R. 1969. Bau und Funktion des Spindelapparats. Naturwissenschaften 56: 237-248.

Dirksen, E. R. 1961. The presence of centrioles in artificially activated sea urchin eggs. J. Biophys. Biochem. Cytol. 11: 244-247.

Dirksen, E. R., and T. T. Crocker. 1966. Centriole replication in differentiating ciliated cells of mammalian respiratory epithelium. An electron microscopic study. J. Microscopie 5: 629-644.

DuPraw, E. J. 1965. Macromolecular organization of nuclei and chromosomes: A folded-fibre model based on whole-mount electron microscopy. Nature 206: 338-343.

DuPraw, E. J. 1968. Cell and Molecular Biology. Academic Press, New York. 739 p.

Dustin, P., Jr. 1963. New aspects of the pharmacology of antimitotic agents. Pharmacol. Rev. 15: 449-480.

Eigsti, O. J., and P. Dustin, Jr. 1955. Colchicine - in Agriculture Medicine, Biology, and Chemistry. Iowa State College Press, Ames. 470 p.

Erlandson, R. A., and E. de Harven. 1971. The ultrastructure of synchronized HeLa cells. J. Cell Sci. 8: 353-397.

Evans, H. J. 1962. Chromosome aberrations induced by ionizing radiations. Int. Rev. Cytol. 13: 221-321.

Evans, H. J. 1963. Chromosome aberrations and target theory, p. 8-40. In S. Wolff (ed.) Radiation-Induced Chromosome Aberrations. Columbia Univ. Press, New York.

Evans, H. J., and J. R. K. Savage. 1963. The relation between DNA synthesis and chromosome structure as resolved by X-ray damage. J. Cell Biol. 18: 525-540.

Flaks, B. 1971. Observations on the fine structure of the normal porcine liver. J. Anat. 108: 563-577.

Forer, A. 1966. Characterization of the mitotic traction system, and evidence that birefringent spindle fibers neither produce nor transmit force for chromosome movement. Chromosoma 19: 44-98.

Friedländer, M., and J. Wahrman. 1970. The spindle as a basal body distributor. A study in the meiosis of the male silkworm moth, Bombyx mori. J. Cell Sci. 7: 65-89.

Gachet, J., and J. P. Thiéry. 1964. Application de la méthode de tirage photographique avec rotations ou translations à l'étude de macromolécules (hémocyanine, hémoglobine, ferritine) et de structures biologiques (centrioles, fibres de flagelle, nucléocapsides virales). J. Microscopie 3: 253-268.

Gall, J. G. 1954. Lampbrush chromosomes from oocyte nuclei of the newt. J. Morphol. 94: 283-351.

Gall, J. G. 1961. Centriole replication. A study of spermatogenesis in the snail Viviparus. J. Biophys. Biochem. Cytol. 10: 163-193.

Gaulden, M. E., and J. G. Carlson. 1951. Cytological effects of colchicine on the grasshopper neuroblast in vitro with special reference to the origin of the spindle. Exp. Cell Res. 2: 416-433.

Gaulden, M. E., G. A. Mueller, and W. Drane. 1970. The effects of varying concentrations of colchicine on the progression of grasshopper neuroblasts into metaphase. J. Cell. Biol. 47: 69a.

Gelfant, S. 1963. Inhibition of cell division: a critical and experimental analysis. Int. Rev. Cytol. 14: 1-39.

George, P., L. J. Journey, and M. N. Goldstein. 1965. Effect of vincristine on the fine structure of HeLa cells during mitosis. J. Nat. Cancer Inst. 35: 355-375.

Gibbons, I. R., and A. V. Grimstone. 1960. On flagellar structure in certain flagellates. J. Biophys. Biochem. Cytol. 7: 697-716.

Hair, J. G. 1953. The origin of new chromosomes in Acroovron. Heredity 6 (suppl.): 215-233.

Harris, P. 1962. Some structural and functional aspects of the mitotic apparatus in sea urchin embryos. J. Cell Biol. 14: 475-487.

Harris, P. 1965. Some observations concerning metakinesis in sea urchin eggs. J. Cell Biol. 25 (1, pt. 2): 73-77.

Harris, P., and D. Mazia. 1962. The finer structure of the mitotic apparatus, p. 279-305. In R. J. C. Harris (ed.) The Interpretation of Ultrastructure. Academic Press, New York.

Heddle, J. A. 1969. The strandedness of chromosomes: Evidence from chromosomal aberrations. Can. J. Genet. Cytol. 11: 783-793.

Heddle, J. A., and D. J. Bodycote. 1970. On the formation of chromosomal aberrations. Mutation Res. 9: 117-126.

Henderson, S. A., and C. A. Koch. 1970. Co-orientation stability by physical tension: a demonstration with experimentally interlocked bivalents. Chromosoma 29: 207-216.

Henderson, S. A., R. B. Nicklas, and C. A. Koch. 1970. Temperature-induced orientation instability during meiosis: an experimental analysis. J. Cell Sci. 6: 323-350.

Heneen, W. K. 1970. In situ analysis of normal and abnormal patterns of the mitotic apparatus in cultured rat-kangaroo cells. Chromosoma 29: 88-117.

Hepler, P. K., and W. T. Jackson. 1968. Microtubules and early stages of cell-plate formation in the endosperm of Haemanthus katherinae Baker. J. Cell. Biol. 38: 437-446.

Hepler, P. K., J. R. McIntosh, and S. Cleland. 1970. Intermicrotubule bridges in mitotic spindle apparatus. J. Cell Biol. 45: 438-444.

Hollaender, A. 1954. Radiation Biology, vol. 1 (pt. 2). McGraw-Hill, New York.

Hollande, A. and J. Valentin. 1968. Infrastructure des centromères et déroulement de la pleuromitose chez les Hypermastigines. C. R. Acad. Sci. D, 266: 367-370.

Hsu, T. C., F. E. Arrighi, R. R. Klevecz, and B. R. Brinkley. 1965. The nucleoli in mitotic divisions of mammalian cells in vitro. J. Cell Biol. 26: 539-553.

Hsu, T. C., R. M. Humphrey, and C. E. Somers. 1964. Responses of Chinese hamster and L cells to 2'-deoxy-5-fluoro-uridine and thymidine. J. Nat. Cancer Inst. 32: 839-855.

Hu, F. 1971. Ultrastructural changes in the cell cycle of cultured melanoma cells. Anat. Rec. 170: 41-56.

Hughes-Schrader, S. 1948. Cytology of coccids (Coccoidea - Homoptera) Adv. Genet. 2: 127-203.

Humphrey, R. M., and B. R. Brinkley. 1969. Ultrastructural studies of radiation-induced chromosome damage. J. Cell Biol. 42: 745-753.

Inoué, S. 1952. The effect of colchicine on the microscopic and submicroscopic structure of the mitotic spindle. Exp. Cell Res. (suppl. 2): 305-314.

Inoué. S. 1960. On the physical properties of the mitotic spindle. Ann. N. Y. Acad. Sci. 90: 529-530.

Inoué, S. 1964. Organization and function of the mitotic spindle, p. 549-594. In R. D. Allen and N. Kamiya (eds.) Primitive Motile Systems in Cell Biology. Academic Press, New York.

Inoué, S., G. W. Ellis, E. D. Salmon, and J. W. Fuseler. 1970. Rapid measurement of spindle birefringence during controlled temperature shifts. J. Cell Biol. 47: 95a-96a.

Inoué, S., and H. Sato. 1967. Cell motility by labile association of molecules. The nature of mitotic spindle fibers and their role in chromosome movement. J. Gen. Physiol. 50 (6, pt. 2): 259-288.

Izutsu, K. 1961. As cited by Luykx, 1970.

Jagiello, G. 1967. Streptonigrin: effect on the first meiotic metaphase of the mouse egg. Science 157: 453-454.

Jensen, C., and A. Bajer. 1969. Effects of dehydration on the microtubules of the mitotic spindle. Studies in vitro and with the electron microscope. J. Ultrastruct. Res. 26: 367-386.

Jokelainen, P. T. 1965a. Fine structure aspects of kinetochores in dividing cells from fetal rat kidney. Anat. Rec. 151: 367.

Jokelainen, P. T. 1965b. The differentiation of sister kinetochores during metakinesis. J. Cell Biol. 27: 48a.

Jokelainen, P. T. 1967. The ultrastructure and spatial organization of the metaphase kinetochores in mitotic rat cells. J. Ultrastruct. Res. 19: 19-44.

Jokelainen, P. T. 1968. The effect of colchicine on the kinetochores and mitotic apparatus in the rat. J. Cell Biol. 39: 68a-69a.

Journey, L. J., J. Burdman, and P. George. 1968. Ultrastructural studies on tissue culture cells treated with vincristine (NSC-67574). Cancer Chemother. Rep. 52: 509-517.

Journey, L. J., and A. Whaley. 1970. Kinetochore ultrastructure in vincristine-treated mammalian cells. J. Cell Sci. 7: 49-54.

Kane, R. E., and A. Forer. 1965. The mitotic apparatus. Structural changes after isolation. J. Cell Biol. 25 (3, pt. 2): 31-39.

Kaufmann, B. P. 1954. Chromosome aberrations induced in animal cells by ionizing radiations, p. 627-711. In A. Hollaender (ed.) Radiation Biology, vol. 1 (pt. 2). McGraw-Hill, New York.

Kiefer, B., H. Sakai, A. J. Solari, and D. Mazia. 1966. The molecular unit of the microtubules of the mitotic apparatus. J. Mol. Biol. 20: 75-79.

Kihlman, B. A. 1964. The production of chromosomal aberrations by streptonigrin in Vicia faba. Mutation Res. 1: 54-62.

Kihlman, B. A. 1966. Actions of Chemicals on Dividing Cells. Prentice-Hall, New Jersey. 260 p.

Kihlman, B. A. 1970. Sub-chromatid exchanges and the strandedness of chromosomes. Hereditas 65: 171-186.

Koller, P. C. 1953. Dicentric chromosomes in a rat tumour induced by an aromatic nitrogen mustard. Heredity 6 (suppl.): 181-196.

Koopmans, A. 1958. Die Persistenz der Chromosomenspindelfaser. Naturwissenschaften 45: 66-67.

Koschel, K., G. Hartmann, W. Kersten, and H. Kersten. 1966. Die Wirkung des Chromomycins und einiger Anthracyclinantibiotica auf die DNA-abhängige Nucleinsäure-Synthese. Biochem. Z. 344: 76-86.

Krishan, A. 1968. Fine structure of the kinetochores in vinblastine sulfate-treated cells. J. Ultrastruct. Res. 23: 134-143.

Krishan, A., and R. C. Buck. 1965. Structure of the mitotic spindle in L strain fibroblasts. J. Cell Biol. 24: 433-444.

La Cour, L. F. 1953. The physiology of chromosome breakage and reunion in Hyacinthus. Heredity 6 (suppl.): 163-179.

Lambert, A. M. 1970. Etude de structures cinétiques en rapport avec la rupture de la membrane nucléaire, en début de méiose chez Mnium hornum L. Organisation des centromères. C. R. Acad. Sci. D, 270: 481-484.

Lampert, F. 1969. Feinstruktur und Trockengewicht menschlicher Chromosomen. Quantitative Elektronenmikroskopie. Naturwissenschaften 56: 629-633.

Lea, D. E. 1962. Actions of Radiations on Living Cells, 2nd ed. Cambridge Univ. Press, New York. 416 p.

Levan, A. 1938. The effect of colchicine on root mitoses in Allium. Hereditas 24: 471-486.

Levan, A. 1954. Colchicine-induced c-mitosis in two mouse ascites tumours. Hereditas 40: 1-64.

Levan, A. 1970. Contributions to the chromosomal characterization of the PTK 1 rat-kangaroo cell line. Hereditas 64: 85-96.

Levine, M., and M. Borthwick. 1963. The action of streptonigrin on bacterial DNA metabolism and on induction of phage production in lysogenic bacteria. Virology 21: 568-574.

Lima-de-Faria, A. 1950. The Feulgen test applied to centromeric chromomeres. Hereditas 36: 60-74.

Lima-de-Faria, A. 1956. The role of the kinetochore in chromosome organization. Hereditas 42: 85-160.

Lima-de-Faria, A. 1958. Recent advances in the study of the kinetochore. Int. Rev. Cytol. 7: 123-157.

Luykx, P. 1965a. The structure of the kinetochore in meiosis and mitosis in Urechis eggs. Exp. Cell Res. 39: 643-657.

Luykx, P. 1965b. Kinetochore-to-pole connections during prometaphase of the meiotic divisions in Urechis eggs. Exp. Cell Res. 39: 658-668.

Luykx, P. 1970. Cellular mechanisms of chromosome distribution. Int. Rev. Cytol., suppl. 2. Academic Press, New York. 173 p.

Malawista, S. E., H. Sato, and K. G. Bensch. 1968. Vinblastine and griseofulvine reversibly disrupt the living mitotic spindle. Science 160: 770-772.

Manton, I., K. Kowallik, and H. A. van Stosch. 1969a. Observations on the fine structure and development of the spindle at mitosis and meiosis in a marine centric diatom (Lithodesmium undulatum). I. Preliminary survey of mitosis in spermatogonia. J. Microscopy 89: 295-320.

Manton, I., K. Kowallik, and H. A. von Stosch. 1969b. Observations on the fine structure and development of the spindle at mitosis and meiosis in a marine centric diatom (Lithodesmium undulatum). II. The early meiotic stages in male gametogenesis. J. Cell Sci. 5: 271-298.

Manton, I., K. Kowallik, and H. A. van Stosch. 1970. Observations on the fine structure and development of the spindle at mitosis and meiosis in a marine centric diatom (Lithodesmium undulatum). III. The later stages of meiosis I in male gametogenesis. J. Cell Sci. 6: 131-157.

Markham, R., S. Frey, and G. J. Hills. 1963. Methods for the enhancement of image detail and accentuation of structure in electron microscopy. Virology 20: 88-102.

Mazia, D. 1961. Mitosis and the physiology of cell division, p. 77-412. In J. Brachet and A. E. Mirsky (eds.) The Cell, vol. 3. Academic Press, New York.

Mazia, D., P. J. Harris, and T. Bibring. 1960. The multiplicity of the mitotic centers and the time-course of their duplication and separation. J. Biophys. Biochem. Cytol. 7: 1-20.

McIntosh, J. R., P. K. Hepler, and D. G. Van Wie. 1969. Model for mitosis. Nature 224: 659-663.

McIntosh, J. R., S. C. Landis. 1971. The distribution of spindle microtubules during mitosis in cultured human cells. J. Cell Biol. 49: 468-497.

Metzner, R. 1894. As cited by Schrader, 1936.

Mizuno, N. S., and D. P. Gilboe. 1970. Binding of streptonigrin to DNA. Biochim. Biophys. Acta 224: 319-327.

Molè-Bajer, J. 1958. Cine-micrographic analysis of c-mitosis in endosperm. Chromosoma 9: 332-358.

Moor, H. 1967. Der Feinbau der Mikrotubuli in Hefe nach Gefrierätzung. Protoplasma 64: 89-103.

Murray, R. G., A. S. Murray, and A. Pizzo. 1965. The fine structure of mitosis in rat thymic lymphocytes. J. Cell Biol. 26: 601-619.

Nathaniel, E. J. H., N. B. Friedman, and H. Rychuk. 1968. Electron microscopic observations on cells of Harding-Passey melanoma following colchicine administration. Cancer Res. 28: 1031-1040.

Nebel, B. R., and E. M. Coulon. 1962. The fine structure of chromosomes in pigeon spermatocytes. Chromosoma 13: 272-291.

Nichols, W. W. 1970. Viruses and chromosomal abnormalities. Ann. New York Acad. Sci. 171: 478-485.

Nichols, W. W., A. Levan, and B. A. Kihlman. 1964. Chromosome breakage associated with viruses and DNA inhibitors, p. 255-271. In R. J. C. Harris (ed.) Cytogenetics of Cells in Culture. Academic Press, New York.

Nicklas, R. B. 1967. Chromosome micromanipulation. II. Induced reorientation and the experimental control of segregation in meiosis. Chromosoma 21: 17-50.

Nicklas, R. B. 1971. Mitosis. Adv. Cell Biol. vol. 2. In press.

Nicklas, R. B., and C. A. Koch. 1969. Chromosome micromanipulation. III. Spindle fiber tension and the reorientation of mal-oriented chromosomes. J. Cell Biol. 43: 40-50.

Nicklas, R. B., and C. A. Staehly. 1967. Chromosome micromanipulation. I. The mechanics of chromosome attachment to the spindle. Chromosoma 21: 1-16.

Oleson, J. J., L. A. Calderella, K. J. Mjos, A. R. Reith, R. S. Thie, and I. Toplin. 1961. The effects of streptonigrin on experimental tumors. Antibiot. Chemother. 11: 158-164.

Östergren, G. 1951. The mechanism of co-orientation in bivalents and multivalents. The theory of orientation by pulling. Hereditas 37: 85-156.

Paweletz, N. 1967. Zur Funktion des "Flemming-Körpers" bei der Teilung tierischer Zellen. Naturwissenschaften 54: 533-535.

Peacock, W. J. 1963. Chromosome duplication and structure as determined by autoradiography. Proc. Nat. Acad. Sci 49: 793-801.

Pickett-Heaps, J. D. 1969. The evolution of the mitotic apparatus: an attempt at comparative ultrastructural cytology in dividing plant cells. Cytobios 1: 257-280.

Pickett-Heaps, J. D. 1971. The autonomy of the centriole: fact or fallacy? Cytobios 3: 205-214.

Pickett-Heaps, J. D., and L. C. Fowke. 1969. Cell division in Oedogonium. I. Mitosis, cytokinesis, and cell elongation. Aust. J. Biol. Sci. 22: 857-894.

Porter, K. R., and R. D. Machado. 1960. Studies on the endoplasmic reticulum. IV. Its form and distribution during mitosis in cells of onion toot tip. J. Biophys. Biochem. Cytol. 7: 167-180.

Puck, T. T. 1964. Phasing, mitotic delay and chromosomal aberrations in mammalian cells. Science 144: 565-566.

Radding, C. M. 1963. Incorporation of H^3 thymidine by K 12 (λ) induced by streptonigrin, p. 22. In S. J. Geerts (ed.) Genetics Today (Proc. XI Int. Congr. Genet.).

Rao, K. V., K. Biemann, and R. B. Woodward. 1963. The structure of streptonigrin. J. Amer. Chem. Soc. 85: 2532-2533.

Rebhun, L. I., and G. Sander. 1967. Ultrastructure and birefringence of the isolated mitotic apparatus of marine eggs. J. Cell Biol. 34: 859-883.

Renaud, F. L., and H. Swift. 1964. The development of basal bodies and flagella in Allomyces arbusculus. J. Cell Biol. 23: 339-354.

Revell, S. H. 1955. A new hypothesis for "chromatid" changes, p. 243-253. In Z. M. Bacq and P. Alexander (eds.) Radiobiology Symposium 1954. Academic Press, New York.

Revell, S. H. 1963. Chromatid aberrations - the generalized theory, p. 41-72. In S. Wolff (ed.) Radiation-Induced Chromosome Aberrations. Columbia Univ. Press, New York.

Reynolds, E. S. 1963. The use of lead citrate at high pH as an electron-opaque stain in electron microscopy. J. Cell Biol. 17: 208-212.

Ringo, D. L. 1967a. Flagellar motion and fine structure of the flagellar apparatus in Chlamydomonas. J. Cell Biol. 33: 543-571.

Ringo, D. L. 1967b. The arrangement of subunits in flagellar fibers. J. Ultrastruct. Res. 17: 266-277.

Ris, H. 1949. The anaphase movement of chromosomes in the spermatocytes of the grasshopper. Biol. Bull. 96: 90-106.

Ris, H. 1955. Cell division, p. 91-125. In B. H. Willier, P. A. Weiss, and V. Hamburger (eds.) Analysis of Development. Saunders, Philadelphia.

Ris, H. 1961. The annual invitation lecture. Ultrastructure and molecular organization of genetic systems. Can. J. Genet. Cytol. 3: 95-120.

Ris, H. 1967. Ultrastructure of the animal chromosome, p. 11-21. In V. V. Koningsberger and L. Bosch (eds.) Regulation of Nucleic Acid and Protein Biosynthesis. Elsevier, New York.

Ris, H., and D. F. Kubai. 1970. Chromosome structure. Annu. Rev. Genet. 4: 263-294.

Robbins, E., and N. K. Gonatas. 1964. The ultrastructure of a mammalian cell during the mitotic cycle. J. Cell Biol. 21: 429-463.

Robbins, E., G. Jentzsch, and A. Micali. 1968. The centriole cycle in synchronized HeLa cells. J. Cell Biol. 36: 329-339.

Roth, L. E. 1964. Motile systems with continuous filaments, p. 527-548. In R. D. Allen and N. Kamiya (eds.) Primitive Motile Systems in Cell Biology. Academic Press, New York.

Roth, L. E. 1967. Electron microscopy of mitosis in amebae. III. Cold and urea treatments: A basis for tests of direct effects of mitotic inhibitors on microtubule formation. J. Cell Biol. 34: 47-60.

Roth, L. E., and E. W. Daniels. 1962. Electron microscopic studies of mitosis in amebae. II. The giant ameba Pelomyxa carolinensis. J. Cell Biol. 12: 57-78.

Roth, L. E., H. J. Wilson, and J. Chakraborty. 1966. Anaphase structure in mitotic cells typified by spindle elongation. J. Ultrastruct. Res. 14: 460-483.

Sauaia, H., and D. Mazia. 1961. As cited by Luykx, 1970.

Schär, B., P. Loustalot, and F. Gross. 1954. Demecolcin (Substanz F), ein neues, aus Colchicum autumnale isoliertes Alkaloid mit starker antimitotischer Wirkung. Klin. Wochenschr. 32: 49-57.

Scheid, W., and H. Traut. 1970. Ultraviolet-microscopical studies on achromatic lesions ("gaps") induced by X-rays in the chromosomes of Vicia faba. Mutation Res. 10: 159-161.

Scheid, W., and H. Traut. 1971. Visualization by scanning electron microscopy of achromatic lesions ("gaps") induced by X-rays in chromosomes of Vicia faba. Mutation Res. 11: 253-255.

Schrader, F. 1936. The kinetochore or spindle fibre locus in Amphiuma tridactylum. Biol. Bull. 70: 484-498.

Schrader, F. 1939. The structure of the kinetochore at meiosis. Chromosoma 1: 230-237.

Schrader, F. 1953. Mitosis, 2nd ed. Columbia Univ. Press, New York. 170 p.

Schroeder, T. E. 1970. The contractile ring. I. Fine structure of dividing mammalian (HeLa) cells and the effects of cytochalasin B. Z. Zellforsch. Mikroskop. Anat. 109: 431-449.

Seaman, G. R. 1960. Large-scale isolation of kinetosomes from the ciliated protozoan Tetrahymena pyriformis. Exp. Cell Res. 21: 292-302.

Sentein, P. 1961. As cited by Biesele, 1962.

Sharp, L. W. 1934. As cited by Schrader, 1936.

Shaw, M. W. 1970. Human chromosome damage by chemical agents. Annu. Rev. Med. 21: 409-432.

Shaw, M. W., and R. S. Krooth. 1964. The chromosomes of the Tasmanian rat-kangaroo (Potorous tridactylis apicalis). Cytogenetics 3: 19-33.

Shimamura, T. 1940. Studies on the effect of the centrifugal force upon nuclear division. Cytologia 11: 186-216.

Sisken, J. E., and E. Wilkes. 1967. The time of synthesis and the conservation of mitosis-related proteins in cultured human amnion cells. J. Cell Biol. 34: 97-110.

Stephens, R. E. 1969. As cited by Nicklas, 1971.

Stubblefield, E. 1968. Centriole replication in a mammalian cell, p. 175-193. In The Proliferation and Spread of Neoplastic Cells. Williams and Wilkins, Baltimore.

Stubblefield, E., and B. R. Brinkley. 1967. Architecture and function of the mammalian centriole, p. 175-218. In K. B. Warren (ed.) Formation and Fate of Cell Organelles. Academic Press, New York.

Stubblefield, E., and W. Wray. 1971 Architecture of the Chinese hamster metaphase chromosome. Chromosoma 32: 262-294.

Taylor, J. H. 1963. DNA synthesis in relation to chromosome reproduction and the reunion of breaks. J. Cell Comp. Physiol. 62 (suppl): 73-86.

Taylor, J. H., P. S. Woods, and W. L. Hughes. 1957. The organization and duplication of chromosomes as revealed by autoradiographic studies using tritium-labeled thymidine. Proc. Nat. Acad. Sci. 43: 122-128.

Uretz, R. B., W. Bloom, and R. E. Zirkle. 1954. Irradiation of parts of individual cells. II. Effects of an ultraviolet microbeam focused on parts of chromosomes. Science 120: 197-199.

Vig, B. K. 1970. Sub-chromatid aberrations in Haworthia attenuata. Can. J. Genet. Cytol. 12: 181-186.

Walen, K. H. 1965. Spatial relationships in the replication of chromosomal DNA. Genetics 51: 915-929.

Walen, K. H., and S. W. Brown. 1962. Chromosomes in a marsupial (Potorous tridactylis) tissue culture. Nature 194: 406.

Watson, M. L. 1958. Staining of tissue sections for electron microscopy with heavy metals. J. Biophys. Biochem. Cytol. 4: 475-478.

Went, H. A. 1960. Dynamic aspects of mitotic apparatus protein. Ann. N. Y. Acad. Sci. 90: 422-429.

Went, H. A. 1966. An indirect method to assay for mitotic centers in sand dollar (Dendraster excentricus) eggs. J. Cell Biol. 30: 555-562.

Wettstein, R., and J. R. Sotelo. 1965. Fine structure of meiotic chromosomes. The elementary components of metaphase chromosomes of Gryllus argentinus. J. Ultrastr. Res. 13: 367-381.

Wilson, H. J. 1968. The fine structure of the kinetochore in meiotic cells of Tradescantia. Planta 78: 379-385.

Wilson, H. J. 1969. Arms and bridges on microtubules in the mitotic apparatus. J. Cell Biol. 40: 854-859.

Wilson, H. J. 1970. Endoplasmic reticulum and microtubule formation in dividing cells of higher plants - a postulate. Planta 94: 184-190.

Wilt, F. H., H. Sakai, and D. Mazia. 1967. Old and new protein in the formation of the mitotic apparatus in cleaving sea urchin eggs. J. Mol. Biol. 27: 1-7.

Wolfe, S. L. 1965. The fine structure of isolated metaphase chromosomes. Exp. Cell Res. 37: 45-53.

Wolfe, S. L. 1969. Molecular organization of chromosomes, p. 3-42. In E. E. Bittar (ed.) The Biological Basis of Medicine, vol. 4. Academic Press, New York.

Wolfe, S. L., and P. G. Martin. 1968. The ultrastructure and strandedness of chromosomes from two species of Vicia. Exp. Cell Res. 50: 140-150.

Wolff, S. (ed.). 1963. Radiation-Induced Chromosome Aberrations. Columbia Univ. Press, New York. 304 p.

Yamanaka, T., and Y. Okada. 1968. Cultivation of fused cells resulting from treatment of cells with HVJ. II. Division of binucleated cells resulting from fusion of two KB cells by HVJ. Exp. Cell Res. 49: 461-469.

Young, C. W., and S. Hodas. 1965. Acute effects of cytotoxic compounds on incorporation of precursors into DNA, RNA, and protein of HeLa monolayers. Biochem. Pharmacol. 14: 205-214.

Zirkin, B. R., and S. L. Wolfe. 1970. The chemical composition of nuclei and chromosomes isolated by the Langmuir trough technique. Chromosoma 32:162-170.

Zubay, G., and P. Doty. 1959. The isolation and properties of deoxyribonucleoprotein particles containing single nucleic acid molecules. J. Mol. Biol. 1: 1-20.

BIOGRAPHICAL SKETCH

Urs-Peter Roos was born August 14, 1938, at Murten, Switzerland. After completing secondary school in Dietikon, Switzerland, in 1953, he began apprenticeship as an engraver and successfully passed the Swiss Federal Examination in 1958. In 1960 he enrolled in the school of the Akademikergemeinschaft in Zurich. He graduated in March, 1963, and obtained the "Schweizerisches Maturitätszeugnis Typus C." He enrolled in the Swiss Federal Institute of Technology (ETH) in Zurich in October, 1963, and graduated from this institution in August, 1967, with the degree of Ingenieur Agronom. In September, 1967, he enrolled in the Graduate School of the University of Florida. He worked as a graduate assistant in the Department of Entomology and Nematology until December, 1968, when he received the degree of Master of Science with a major in Entomology. In September, 1969, he transferred to the Department of Zoology. He worked as a teaching and research assistant and was recipient of a Graduate Fellowship of the College of Arts and Sciences during the time he pursued his work toward the degree of Doctor of Philosophy.

Urs-Peter Roos is married to the former Loan Hiang Ghan and is the father of a son. He is a member of Phi Kappa Phi, Gamma Sigma Delta, Phi Sigma, an associate member of Sigma Xi, and a student member of the American Association for the Advancement of Science and the American Society for Cell Biology.

I certify that I have read this study and that in my opinion it conforms to acceptable standards of scholarly presentation and is fully adequate, in scope and quality, as a dissertation for the degree of Doctor of Philosophy.

F. C. Johnson, Chairman
Associate Professor of Zoology

I certify that I have read this study and that in my opinion it conforms to acceptable standards of scholarly presentation and is fully adequate, in scope and quality, as a dissertation for the degree of Doctor of Philosophy.

H. C. Aldrich, Co-Chairman
Assistant Professor of Botany

I certify that I have read this study and that in my opinion it conforms to acceptable standards of scholarly presentation and is fully adequate, in scope and quality, as a dissertation for the degree of Doctor of Philosophy.

L. H. Larkin
Assistant Professor of Anatomical Sciences

I certify that I have read this study and that in my opinion it conforms to acceptable standards of scholarly presentation and is fully adequate, in scope and quality, as a dissertation for the degree of Doctor of Philosophy.

J. L. Nation
Associate Professor of Entomology

This dissertation was submitted to the Department of Zoology in the College of Arts and Sciences and to the Graduate Council, and was accepted as partial fulfillment of the requirements for the degree of Doctor of Philosophy.

_____

Dean, Graduate School